



HAL
open science

Description et classification 3D des glènes arthrosiques pour une planification préopératoire 3D assistée par ordinateur : l'épaule digitale normale et arthrosique

Marc-Olivier Gauci

► To cite this version:

Marc-Olivier Gauci. Description et classification 3D des glènes arthrosiques pour une planification préopératoire 3D assistée par ordinateur : l'épaule digitale normale et arthrosique. Médecine humaine et pathologie. Université de Bretagne occidentale - Brest, 2019. Français. NNT : 2019BRES0091 . tel-02613833

HAL Id: tel-02613833

<https://theses.hal.science/tel-02613833>

Submitted on 20 May 2020

HAL is a multi-disciplinary open access archive for the deposit and dissemination of scientific research documents, whether they are published or not. The documents may come from teaching and research institutions in France or abroad, or from public or private research centers.

L'archive ouverte pluridisciplinaire **HAL**, est destinée au dépôt et à la diffusion de documents scientifiques de niveau recherche, publiés ou non, émanant des établissements d'enseignement et de recherche français ou étrangers, des laboratoires publics ou privés.

THESE DE DOCTORAT DE

L'UNIVERSITE
DE BRETAGNE OCCIDENTALE
COMUE UNIVERSITE BRETAGNE LOIRE

ECOLE DOCTORALE N° 605
Biologie Santé

Spécialité : Analyse et Traitement de l'Information et de l'Image Médicale

Par **Marc-Olivier GAUCI**

Description et Classification 3D des Glènes Arthrosiques pour une Planification Préopératoire 3D Assistée par Ordinateur

L'EPAULE DIGITALE
NORMALE ET ARTHROSIQUE

Thèse présentée et soutenue à Rennes le 11 décembre 2019
Unité de recherche : Inserm U1101

Rapporteurs avant Soutenance :

Pr George S ATHWAL	Chirurgien Orthopédiste, McFarlane Hand & Upper Limb Centre (HULC), St. Joseph's Health Care London, Ontario, Canada
Pr Luc FAVARD	Professeur d'Université, Chirurgie Orthopédique et Traumatologique, CHU de Tours

Composition du Jury :

Président : **Pr Pascal BOILEAU** Professeur d'Université, Chirurgie Orthopédique et Traumatologique, CHU de Nice

Examineurs :

Pr George S ATHWAL	Chirurgien Orthopédiste, McFarlane Hand & Upper Limb Centre (HULC), St. Joseph's Health Care London, Ontario, Canada
M Jean CHAOUI	President / CEO, Imascap, Plouzané
Pr Luc FAVARD	Professeur d'Université, Chirurgie Orthopédique et Traumatologique, CHU de Tours
Mme Jocelyne TROCCAZ	Directrice de Recherche, CNRS, Equipe GMCAO, Laboratoire TIMC, Grenoble

Directeurs de thèse :

Pr Eric STINDEL	Professeur d'Université, Chirurgie Orthopédique et Traumatologique, CHU de Brest Directeur de Recherche, LaTIM, Inserm, Brest
Dr Gilles WALCH	Chirurgien orthopédiste, Centre Paul Santy et Hôpital Privé Jean Mermoz, Lyon

Table des matières

PREAMBULE	4
CONTEXTE	6
I/ Version glénoïdienne et problématique du plan scapulaire	6
a) Définition de la version glénoïdienne	6
b) Mesures extramédullaires de la version.....	6
c) Mesures intramédullaires de la version.....	10
d) Autres méthodes de mesures de version glénoïdienne	13
II/ Modélisation tridimensionnelle de la surface glénoïdienne	14
a) Modèles sphériques.....	14
b) Modèles planaires.....	15
III/ Inclinaison glénoïdienne et problématique de l'axe transverse	15
a) Mesures bidimensionnelles	15
b) Mesures tridimensionnelles	18
IV/ Subluxation humérale	22
a) Mesures bidimensionnelles	22
b) Mesures tridimensionnelles	24
V/ Supériorité du 3D sur le 2D	26
CONSTITUTION D'UNE BASE DE DONNEES DE SCANNERS D'EPAULES	28
I/ RATIONNEL	28
II/ EPAULES PATHOLOGIQUES	28
a) Constitution de la bibliothèque scientifique	28
b) Paramètres analysés, diagnostic et classification	30
III/ EPAULES NORMALES	32
BIBLIOGRAPHIE	33
Annexes	37
<i>Liste des articles issus du travail de Thèse</i>	40
INTRODUCTIONS	41
OBJECTIFS	42
HYPOTHESES	43
MATERIELS & METHODES	44
RESULTATS	45
CONCLUSIONS	47
PUBLICATIONS	48
Etude I.....	49
Etude II.....	58
Etude III.....	64
Etude IV	65

Etude V	66
Etude VI	76
Etude VII	77
Etude VIII	83
<i>Liste des articles connexes issus de la base de données</i>	93
<i>Conclusion et Perspectives pour les recherches à venir</i>	94

PREAMBULE

L'analyse morphométrique de l'articulation épaule est indispensable à la compréhension de la pathogénèse arthrosique au niveau de l'articulation glénohumérale. Depuis les années 1990, de nombreux travaux ont été menés pour définir l'aspect normale et pathologique de l'extrémité supérieure de l'humérus(1–4) et de la glène(5–7). Ces analyses ont été faites en majorité en 2 dimensions. Avec l'amélioration des techniques de traitement d'image en particulier tomodynamométrique, l'analyse tridimensionnelle est devenue plus accessible et plus rapide en orthopédie. Elle est particulièrement indispensable pour la compréhension de l'articulation glénohumérale puisqu'il s'agit d'une articulation de type sphéroïde, la plus instable de l'organisme, avec 3 degrés de liberté permettant un mouvement de circumduction. Le corollaire de cette analyse tridimensionnelle est la recherche de l'amélioration du diagnostic, donc de la classification des glènes, de la précision des indications chirurgicales à l'aide de nouveaux outils de mesure mais aussi du choix des implants et de leur positionnement. Elle permet la planification préopératoire de la pose des implants voire l'anticipation des résultats théoriques.

L'objectif de cette Thèse centrée sur l'approche tridimensionnelle de l'articulation glénohumérale dans l'omarthrose était de valider l'application d'un logiciel de segmentation automatisée tridimensionnel (Glenosys, Imascap – Plouzané) dans toutes les étapes nécessaires à la prise en charge d'un patient, étapes que nous limiterons au diagnostic, à la décision thérapeutique et au geste technique chirurgical.

Pour ce faire, nous avons choisi plusieurs axes d'approche :

- valider les plans de référence choisis dans le logiciel au travers des mesures générées de version et inclinaison par rapport aux axes de référence 2D habituels.
- améliorer une classification utilisée dans l'arthrose primaire à partir de scanners reformatés dans les plans de références choisis.
- constituer une base de données (bibliothèque scientifique) importante pour mener pour la première fois une analyse de type *big data* sur un nombre important de scanners d'épaule.
- décrire la morphométrie de la glène, de l'humérus et de l'articulation glénohumérale normale et pathologique à partir de la base de données.

- développer et valider une mesure d'aide au diagnostic préopératoire.
- démontrer l'apport de la simulation préopératoire sur logiciel dans la compréhension des limitations de mobilités dues au positionnement et au design des implants.
- déterminer l'efficacité et les limites de l'utilisation des guides issus de la planification préopératoire.

Le format de cette Thèse est celui d'une introduction générale exposant le contexte du projet suivie par la présentation des publications déjà indexées ou soumises issues de ces travaux. Enfin nous concluons en évoquant les principaux axes de recherches qui découleront de ce travail de recherche.

CONTEXTE

I/ Version glénoïdienne et problématique du plan scapulaire

a) Définition de la version glénoïdienne

La version glénoïdienne a d'abord été étudiée comme un des facteurs potentiels de survenue de l'instabilité gléno-humérale(8,9). Le terme de « version » apparaît pour la première fois en 1986 dans l'article de Brewer et al où il remplace le terme de « tilt » glénoïdien(10). Elle est alors mesurée sur des radiographies (roentgonogrammes) axillaires. La même année, Randelli et Gambrioli, toujours sur des épaules instables, publient la première analyse tomodensitométrique et définissent le « tilt antéropostérieur » comme l'angle complémentaire à celui formé par l'intersection entre l'axe du corps de la scapula et la surface glénoïdienne(11). Ils précisent même que le tilt antéropostérieur varie en fonction du niveau de coupe. Du fait d'une importante multiplication des repères géométriques utilisés pour la mesurer, une définition plus générique de la version pourrait être aujourd'hui donnée : une mesure angulaire en 2 dimensions de l'orientation de la glène projetée dans le plan axial. Le plus souvent, cette mesure est exprimée par une valeur positive de rétroversion puisque la glène est le plus souvent rétroversée que ce soit dans la population normale ou pathologique.

b) Mesures extramédullaires de la version

Le scanner a rapidement démontré sa supériorité dans les mesures morphométriques de la glène. En effet, les clichés axillaires (type Bernageau) ne sont pas fiables ni reproductibles. En prenant la ligne scléreuse comme référence sur ces clichés, Nyffeler et al(12) rapporte une surestimation des mesures de version dans plus de 85% des cas (Figure 1). En particulier, la variation de la version peut aller jusqu'à $\pm 15^\circ$.

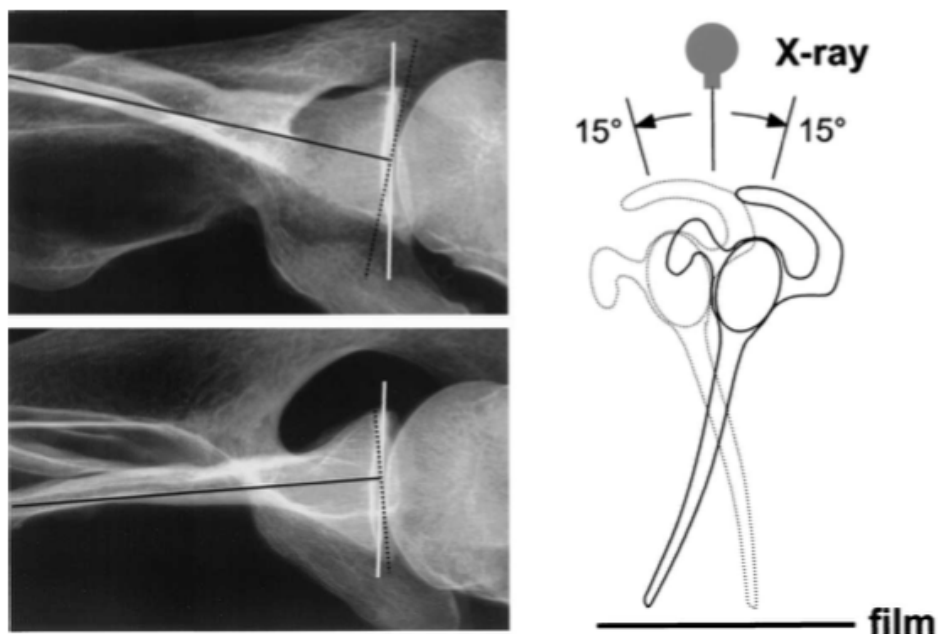


Figure 1 : L'incidence des radiographies axillaires standardisées présente une variation de $\pm 15^\circ$ (courtoisie RW Nyffeler).

Six ans après Randelli et Gambrioli, Friedman et al(13) en 1992 reprend le même axe scapulaire pour mesurer la version et l'applique à une population d'épaules arthrosiques comparée à une population normale. Pour pallier la variation de version en fonction du niveau de coupe, il choisit arbitrairement la première coupe sous la coracoïde. Puis il trace la ligne de référence passant par le point le plus médial de la scapula et le centre de la glène (l'axe scapulaire). La version mesurée moyenne des glènes arthrosiques était de $-11 \pm 8^\circ$ (de -32° à 2°) contre $+2 \pm 5^\circ$ (de -12 à 14°) pour des glènes normales. Cette technique de mesure en 2 dimensions non corrigée a, par la suite, démontré ses limites puisque l'australien Bokor et al(14) en 1999, constate que des rotations mineures de la scapula peuvent altérer la mesure de la version de plus de 10° . Bryce et al(15) confirme ces constatations et démontrent que la version est déjà altérée à partir de 1° de rotation de la scapula dans le plan coronal et sagittal. Afin de limiter les erreurs de référentiel, Kwon et al(16) développe en 2005 un plan basé sur 3 points : le centre de la glène, le point le plus médial de la scapula et le point le plus inférieur de la scapula. Ce plan est appelé « plan anatomique de la scapula ». Cette technique permet d'effectuer des mesures en « 2D corrigé » dans un plan établi en limitant les effets du « gantry angle » dû à la position du patient dans le scanner (figure 2).

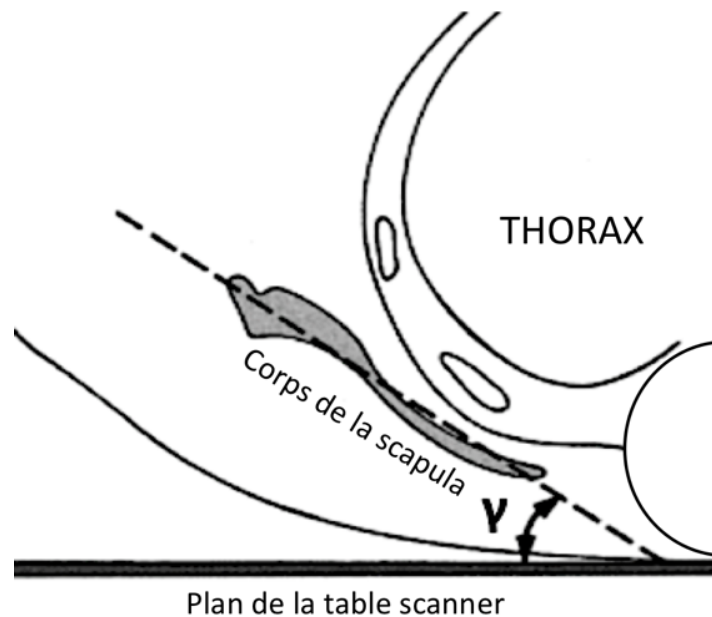


Figure 2 : Schéma représentant le *gantry angle* (γ).

Plusieurs auteurs ont ainsi utilisé ce plan afin d'effectuer des mesures morphométriques de la glène et en particulier de la version^{9,12,13}(16–22)(Figure 3).

L'utilisation du plan anatomique de la scapula présente cependant des limites importantes :

- Elle prend du temps et limite son utilisation dans l'activité chirurgicale quotidienne
- Elle nécessite l'acquisition de la scapula entière puisque ce plan ne peut pas être construit en l'absence des points médial et/ou inférieur.
- Elle se base sur 3 points de la scapula et donc résume la morphologie très complexe de la scapula à 3 points.
- Elle comprend le centre de la glène qui appartient donc à l'objet que l'on souhaite étudier et qui présente une variation dépendant de l'usure de celle-ci.
- Le centre de la glène est difficile à repérer dans les épaules pathologiques car l'arthrose glénohumérale provoque une fusion virtuelle qui rend difficile l'identification de la surface de la glène.
- Le positionnement des points à la main entraîne une variabilité inter et intraobservateur qui nuit à la reproductibilité et à la fiabilité des mesures comme nous l'avons démontré dans une étude récente (non encore publiée encore, Figure 4) sur le picking.

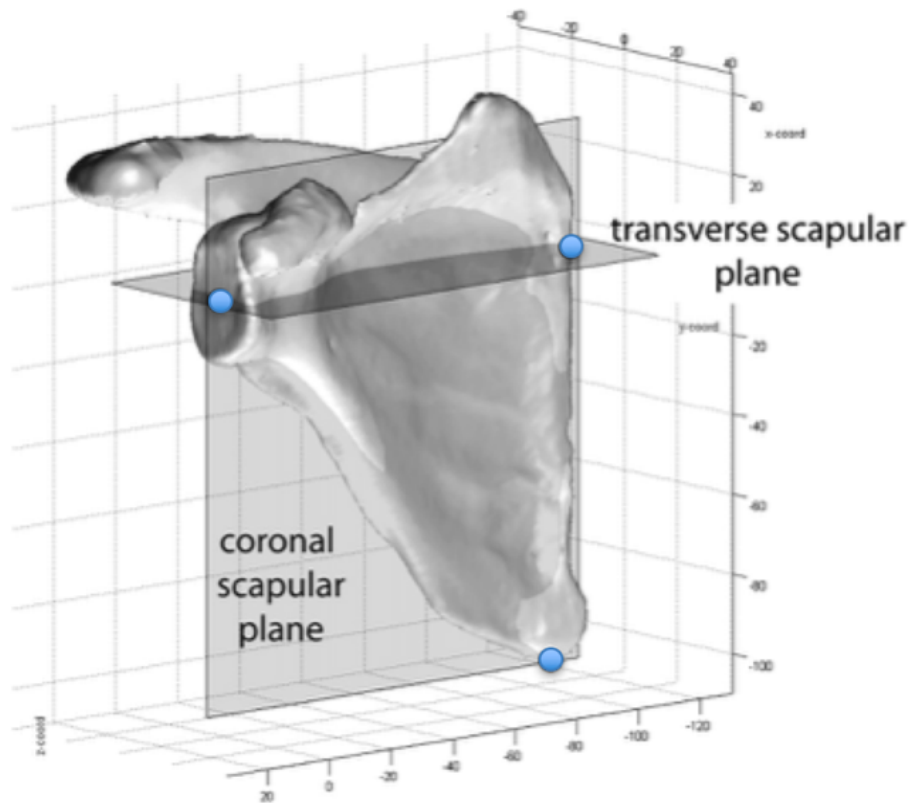


Figure 3 : Plan anatomique de la scapula décrit par Kwon. Il est généré à partir du repérage de 3 points : le centre de la glène, le point le plus médial de la scapula et le point le plus inférieur de la scapula (*courtesy*).

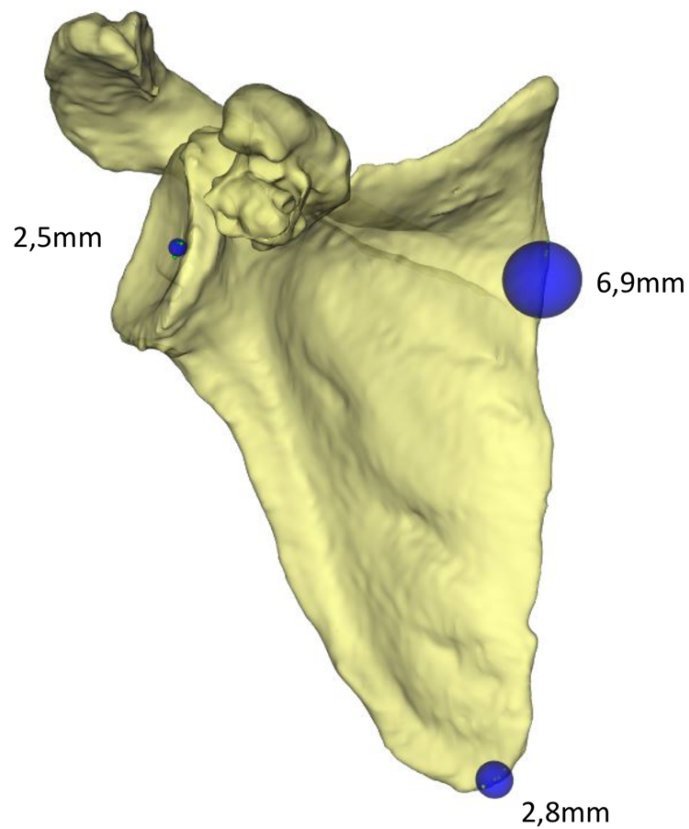


Figure 4 : Exemple de modèle tridimensionnel ayant servi de support au picking des 3 points utilisés pour générer le plan de Kwon par 4 observateurs différents. Le repérage du trigonum est très variable à la fois mal défini anatomiquement et correspondant à une zone large et de surface variable entre les individus

Afin d'éviter ces contraintes, le logiciel Glenosys® (Imascap, Brest, France) propose d'utiliser un algorithme type « Genetic Algorithm » de reconnaissance automatique de modèle « pattern recognition » qui ne nécessite pas d'intervention ou de picking manuels(23). Le logiciel effectue une segmentation¹⁵ automatique de la scapula et reste très précis dans la segmentation glénoïdienne malgré la fusion virtuelle glénohumérale (Figure 5). Il élabore ensuite un plan moyen basé sur l'ensemble des points de la scapula en retirant la glène, l'acromion et la coracoïde : le « Plan du Corps de la Scapula ». Par ailleurs, le logiciel permet d'élaborer un plan moyen de la glène et de déterminer la sphère la plus représentative de la surface concave de la glène ou « *Best Fit Sphere* » (BFS)(24). Il s'agit donc d'un outils automatique qui évite toute variation inter- et intraobservateurs et permet de déterminer un plan moyen de référence scapulaire. C'est cet algorithme qui sera utilisé et développé tout au long de cette thèse.

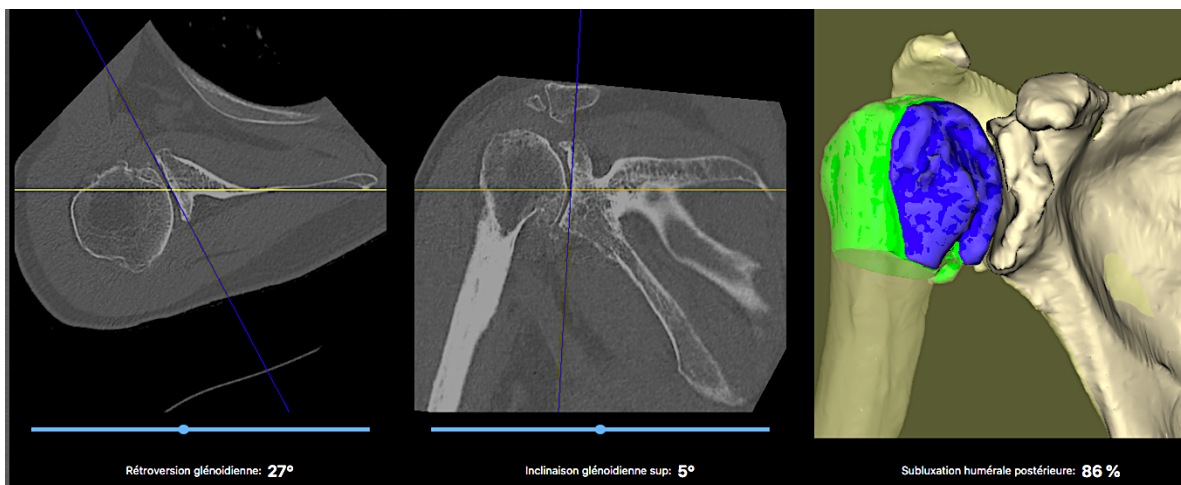


Figure 5 : Segmentation automatique de l'épaule générée par le logiciel Glenosys à partir d'images tomodensitométriques. L'écran affiche les coupes 2D reformattée dans le plan axial et le plan frontal ainsi que la reconstitution 3D.

c) Mesures intramédullaires de la version

Les mesures intramédullaires de la version présentent plusieurs intérêts :

- Elles ne nécessitent pas l'acquisition de toute la scapula
- Elles présentent une application directe en permettant de guider le positionnement de la quille ou du plot central d'un implant glénoïdien et d'assurer ainsi sa meilleure tenue.

- Elle apporte une information morphologique complémentaire au plan de la scapula qui est très importante dans la mesure où la glène évolue de façon indépendante du corps de l'omoplate.
- Enfin certains auteurs promouvant ce référentiel mettent en avant qu'un repère pris dans la voûte glénoïdienne serait moins sensible au *gantry angle* en raison d'un grand axe de la voûte plus court que la longueur de l'omoplate, l'acquisition de toute la scapula ne serait donc pas non plus nécessaire.

Poon modélise la voûte glénoïdienne par un triangle isocèle à sommet médial formé par les surfaces endostées de la voûte(25) (Figure 6). Le contrôle du *gantry angle* est effectué par un *scout* préalable où la surface glénoïdienne est positionnée perpendiculairement à l'axe des coupes natives. Pour mesurer la version, il utilise la bissectrice principale de ce triangle comme référentiel et la ligne antéropostérieure de la glène. Il mesure par cette technique une retroversion moyenne de $19\pm 3^\circ$ dans la population normale. Bien que cette technique présente cependant une approximation dans le contrôle du *gantry angle*, l'utilisation de la partie triangulaire médiale endostée n'est pas soumise aux déformations induites par l'usure lors de l'évolution arthrosique contrairement à la surface glénoïdienne. Elle permet donc d'établir un référentiel stable au cours du temps.

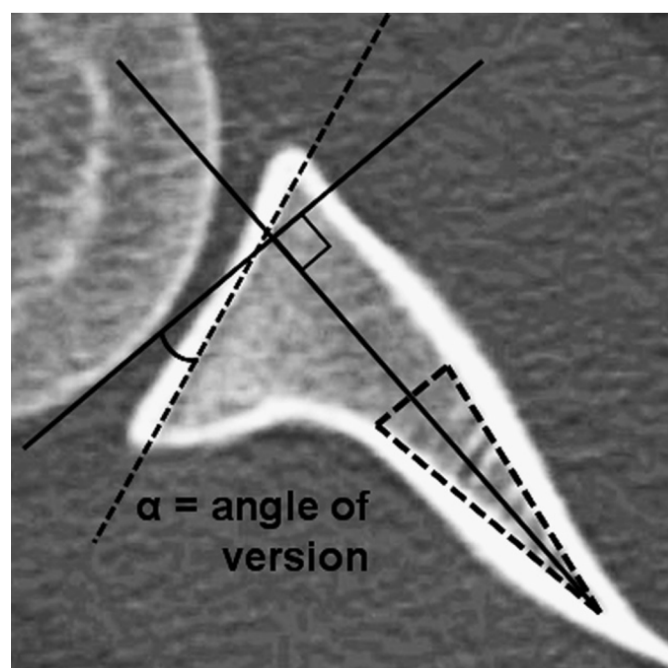


Figure 6 : Technique de mesure de la version à partir de l'axe de la voûte glénoïdienne tel que décrit par Poon et al (courtoisie PC Poon).

De la même façon, et pour permettre une application aisée des mesures scannographiques lors de l'intervention, Andrin et al décrivent le « triangle scapulaire » en utilisant 2 points : le point le plus médial de la voute glénoïdienne et le centre de la glène mais sans contrôle du *gantry angle*(26). C'est l'apport de Bouacida et al qui utilisent cette mesure dans le plan anatomique de la scapula tel que décrit par Kwon. Le modèle décrit est celui de la « carène glénoïdienne ». La rétroversion normale ainsi mesurée est de $12\pm 4^\circ$ (27).

L'apport de la description de la voute glénoïdienne est particulièrement défendu par Iannotti et al qui remarquent que dans la mesure où la glène présente une rétroversion naturelle, un positionnement strictement neutre de l'implant conduirait à implanter celui-ci de façon non-anatomique avec un risque de franchissement du mur postérieur. Il développe ainsi le premier modèle tridimensionnel de la « voute glénoïdienne » (*glenoid vault*). Il démontre que la voute glénoïdienne a une morphologie complexe uniforme définie par les surfaces endostées de la glène et qui peut être déclinée en 5 tailles différentes s'adaptant à la grande majorité de la population moyenne²⁴⁻²⁶(16,20) (Figure 7).

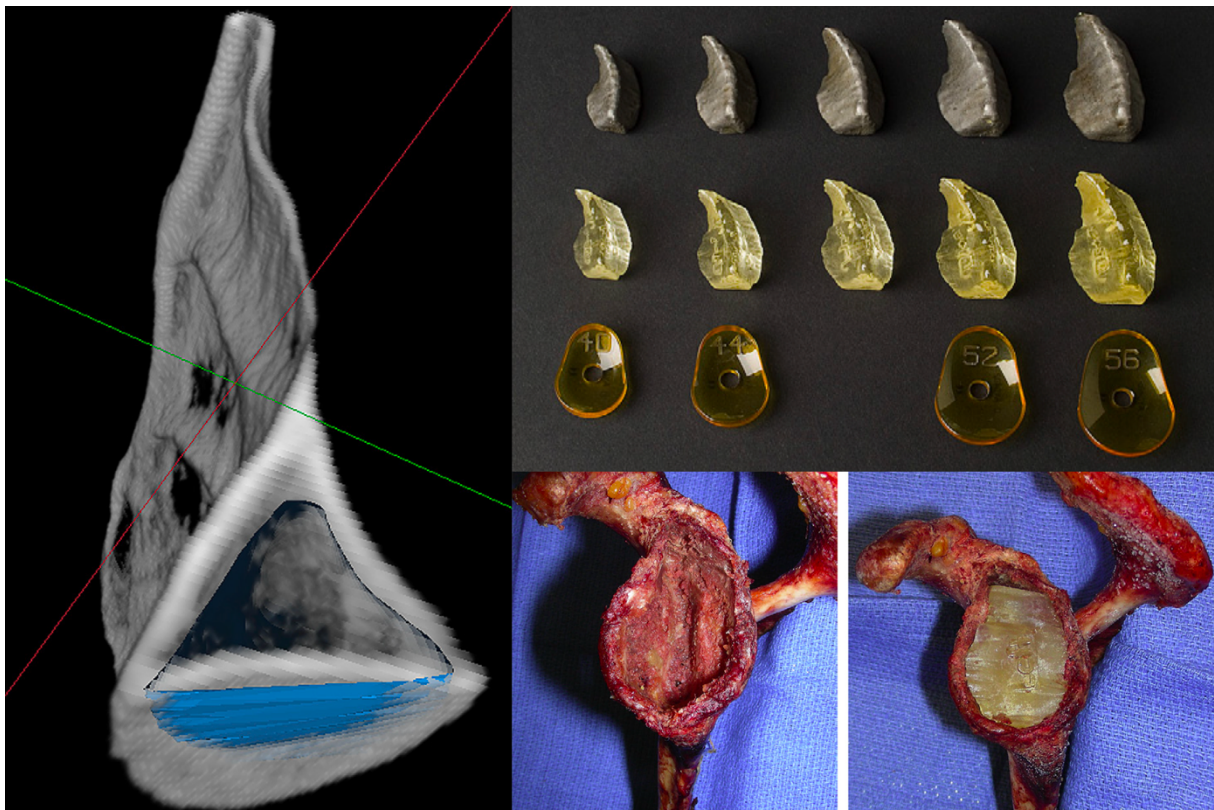


Figure 7 : Modèle de la voute glénoïdienne développé par Iannotti et al. Cinq tailles différentes de voutes glénoïdiennes s'adaptent à la majorité de la population moyenne. Ce modèle peut être généré informatiquement (*figure de gauche*) puis imprimé en 3D (*figure en haut à droite*) pour être validé sur des glènes cadavériques évidées (*figure en bas à droite*) (courtoisie MJ Codsi).

De cette façon, il est possible de retrouver la version de la glène native en superposant le modèle le plus adapté à la voute de la glène dégénérative et en lui autorisant 6 degrés de liberté pour correspondre le mieux à la voute glénoïdienne décrite. Cette technique permet à la fois une description tridimensionnelle de la voute glénoïdienne mais aussi de retrouver la version native d'une glène dégénérative à 2.1° près(21).

d) Autres méthodes de mesures de version glénoïdienne

D'autres repères ont été proposés pour mesurer la version glénoïdienne en s'attachant à rendre celle-ci accessible en peropératoire. En particulier, l'utilisation de la paroi glénoïdienne antérieure a été proposée par Resch (Figure 8) et utilisée par de Wilde et al puis Ganapathi et al(19,28). La valeur moyenne de cette version est de $19\pm 8^\circ$. Cette mesure a été reprise récemment par Moraiti et al(29) et baptisée Glenoid Orientation index (GO index) en spécifiant que cette mesure devait se faire au niveau du plus grand diamètre de la glène. La version moyenne normale obtenue est alors de $26\pm 6^\circ$ avec une forte corrélation aux mesures obtenues par la méthode de Friedman même. Cependant, l'absence de reformatage des scanners dans un plan fixé soumet encore une fois la mesure aux aléas du *gantry angle*.

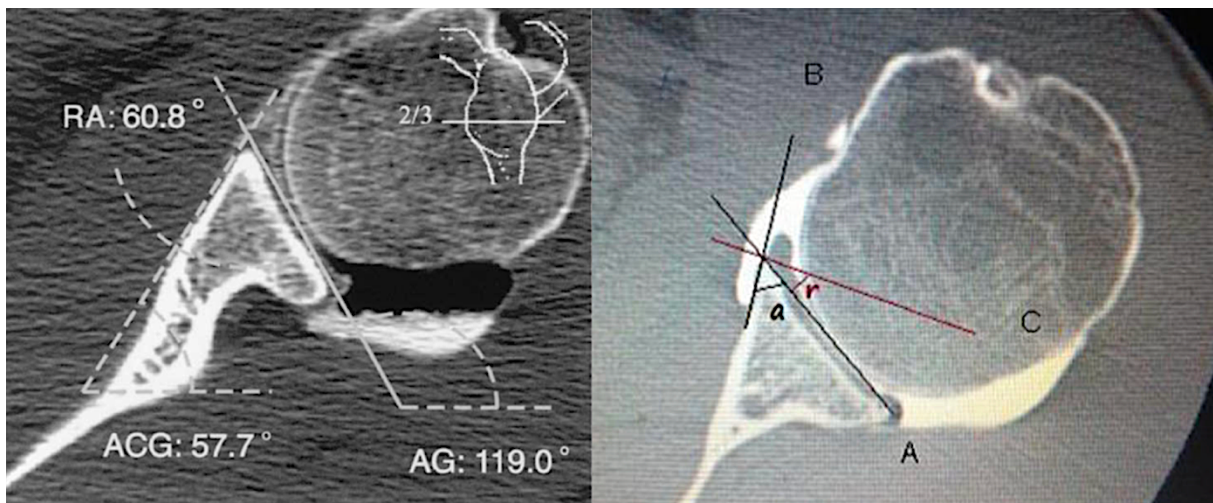


Figure 8 : Présentation de la mesure de l'angle de Resch pour calculer la version glénoïdienne (courtoisie C Moraiti).

II/ Modélisation tridimensionnelle de la surface glénoïdienne

La glène présente une forme hélicoïdale avec une diminution de la rétroversion dans le sens cranio-caudal. Cette variation est estimée entre 5° et 10° dans la littérature²⁹⁻³¹(30-32). La représentation de la surface glénoïdienne est ainsi rendue difficile et les modèles géométriques utilisés sont soit des plans soit des sphères.

a) Modèles sphériques

Lewis et Armstrong utilisent le plan anatomique de la scapula comme référentiel 3D pour la mesure de la version donnée par la *Best Fit Sphere (BFS)*. La version – ainsi que l’inclinaison – sont données par la projection du vecteur centre glène – centre BFS sur le « plan transverse » de la scapula (perpendiculaire au plan anatomique de la scapula passant la droite centre glène - trigonum) (Figure 3 & 9). La version moyenne retrouvée à partir de la sphère est de $-3\pm 3^\circ$. Le rayon de la BFS est en moyenne de $33\pm 4\text{mm}$ (17,33).

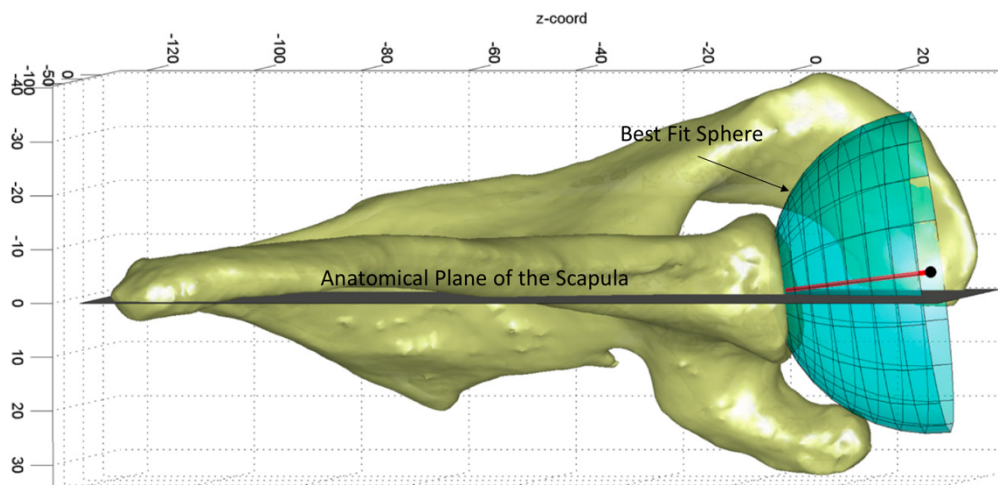


Figure 9 : Modèle de la *Best Fit Sphere* dont les projetés du vecteur centre glène – centre BFS permettent de donner la version et l’inclinaison de la glène((*courtoisie GS Lewis*).

Un an après, Moineau et al démontre la faisabilité de ce même modèle sphérique mais sur des glènes arthrosiques et un plan de la scapula généré automatiquement par Glenosys®. Il calcule une concordance interobservateur de la version supérieure à 0,95 (« quasi parfaite »). Ghafurian et al en utilisant l’axe du *fulcrum* comme repère(34,35) développent aussi un système entièrement automatisé de modélisation sphérique de la glène(36).

b) Modèles planaires

L'utilisation des plans est plus fréquente dans la littérature, en particulier, s'il est possible de déterminer un plan moyen de la glène, plusieurs plans peuvent être identifiés sur la glène en fonction du quadrant auquel on s'intéresse. Ganapathi et al utilisent le « plan de la fosse glénoïdienne » construit à partir de 3 points : 1 au pôle supérieur et 2 au tiers inférieurs, 1 antérieur et 1 postérieur. Il confirme ainsi la fiabilité et le reproductibilité du modèle de la « voûte glénoïdienne » précédemment décrit en particulier pour son applicabilité dans les glènes déformées(19). Plus tard, De Wilde et al compare 5 plans(37) : supérieur, inférieur, postérieur, antérieur et neutre dans le plan anatomique de la scapula. Il retrouve une moindre variabilité de la version pour le plan inférieur. Cela s'explique par une meilleure représentation de la partie la plus circulaire – et la plus inférieure – de la glène par ce plan. Par ailleurs cette analyse permet de constater une rétroversion plus importante de la partie postérieure de la glène chez les femmes que chez les hommes pouvant expliquer une incidence féminine de l'arthrose plus importante.

III/ Inclinaison glénoïdienne et problématique de l'axe transverse

a) Mesures bidimensionnelles

Dès 1959, la problématique de la « pente glénoïdienne » a aussi été abordée par Basmajian et al dans la pathologie de l'instabilité. Il décrit l'existence d'une pente supérieure qui lutte contre la luxation inférieure de l'humérus et permet la sollicitation de la capsule supérieure et le sus-épineux en position neutre et en adduction (Figure 10).

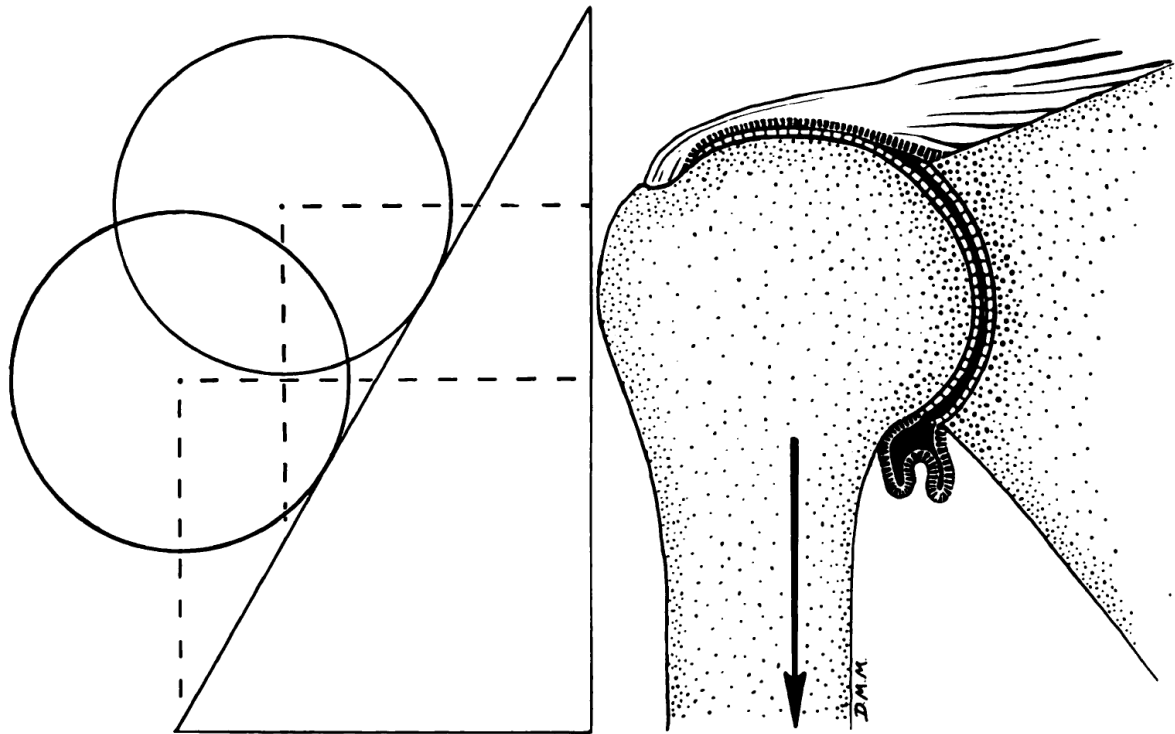


Figure 10 : Schéma de la modélisation de la « pente glénoïdienne » décrite par Basmajian (*courtoisie JV Basmajian*).

Gouaze en 1962, puis d'autres auteurs bien plus tardivement, décrivent une inclinaison inférieure dans certains cas d'instabilité (38–40) et proposent des ostéotomies glénoïdiennes inférieures dans le traitement des instabilités inférieures. Cependant, très peu d'études s'intéressent à la mesure radiographique ou tomodensitométrique jusqu'au début des années 2000 contrairement à la version. Outre la difficulté à établir un référentiel reproductible et fiable en particulier avec la difficulté à contrôler le tilt de la scapula, une autre raison technique peut expliquer l'intérêt plus tardif pour l'inclinaison. En effet, afin de neutraliser l'influence du tilt scapulaire sur la version et de standardiser cette mesure, certains auteurs, comme Bokor en 1999, propose de positionner et de fixer arbitrairement l'inclinaison glénoïdienne à 90° (« plan neutre idéal ») du plan des coupes axiales natives(14). Ce prédicat suppose donc qu'il n'existe pas de variation dans l'inclinaison glénoïdienne. Il est remis en question plus tard par Churchill et al qui accusent cet artifice de donner la fausse impression que toutes les inclinaisons sont identiques contrairement à l'utilisation d'un axe fixe scapulaire. Il propose à cet effet l'utilisation de « l'axe transverse » qu'il définit comme la ligne reliant le centre de la fosse glénoïdienne et le point formé par la jonction entre l'épine et le bord médial de la scapula(41) (Figure 11). Il retrouve une inclinaison glénoïdienne variable et estimée à $4 \pm 3^\circ$ (de -7 à 16°) sur 172 scapula sèches.

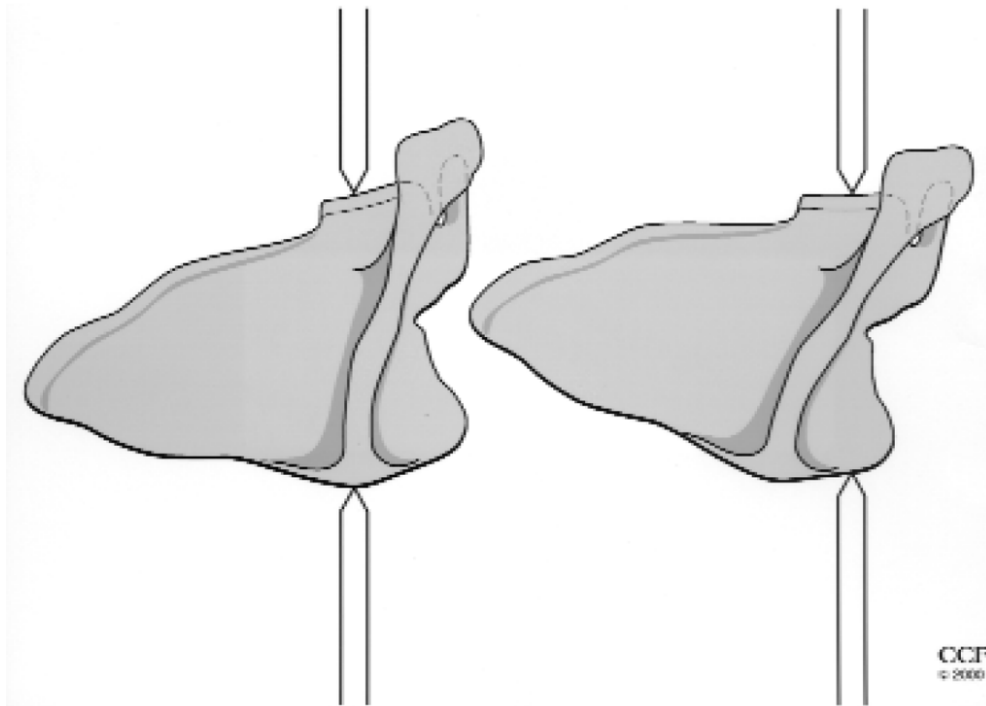


Figure 11 : Comparaison entre 2 positions différentes de scapula. Dans l'image de gauche, les tenons représentent l'axe transverse de la scapula. Dans l'image de droite, la glène est artificiellement positionnée à 90° comme le suggère Bokor et al. Dans ce dernier cas, le tendon du corps n'est plus positionné le long de l'épine de la scapula et correspond à un point non identifié anatomiquement et présentant des variations interindividuelles (courtoisie RS Churchill).

L'intérêt pour l'évaluation de l'inclinaison radiographique renaît avec la suspicion de son association à la pathologie de la coiffe des rotateurs. Hugues et al propose d'utiliser la ligne scléreuse du fond de la fosse du sus-épineux et la ligne craniocaudale glénoïdienne.

Il retrouve une différence significative de 8° entre l'inclinaison glénoïdiennes des épaules normales ($1\pm 5^\circ$) et les épaules souffrant de pathologie de la coiffe ($9\pm 6^\circ$). Reprenant les travaux d'Edelson en 1995 qui décrivait 20 à 30% d'hypoplasie glénoïdienne postéroinférieure, Habermeyer et al ne retrouve pas l'association déjà évoquée avec la pathologie de la coiffe mais pointe le rôle clef de la variation de l'inclinaison dans l'arthrose glénohumérale (il retrouve 4 types d'inclinaison) et surtout la difficulté à établir la mesure de celle-ci en utilisant le bord inférieur du film de la radiographie, ligne supposé parallèle au sol. Alors que de nombreux articles démontre l'importance de l'inclinaison de l'implant glénoïdien(42–47), il faut attendre 2012 pour que soit publiée une étude s'attachant véritablement à étudier la fiabilité des repères radiographiques utilisables pour mesurer l'inclinaison. Maurer et al cherchent à développer une méthode de mesure de l'inclinaison robuste, fiable et reproductible. Il compare 3 référentiels : l'épine, le fond de la fosse du sus-

épineux et le pilier de la scapula et démontre la supériorité de l'utilisation du fond de la fosse du sus-épineux (β -angle), ligne scléreuse clairement identifiable sur les radiographies et les scanners, pour la mesure de l'inclinaison(48) (Figure 12).

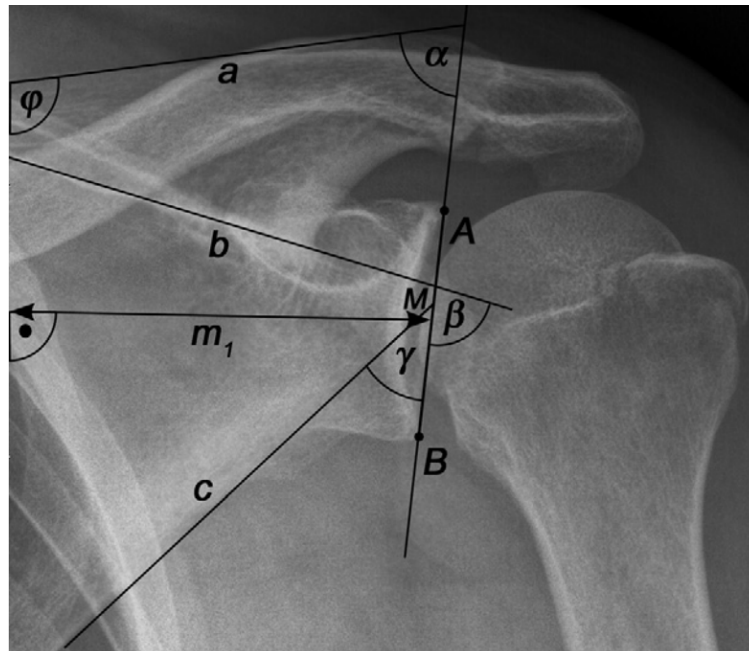


Figure 12 : Définition des différents angles de mesure de l'inclinaison glénoïdienne sur une radiographie à partir de 3 lignes anatomiques identifiables anatomiquement : a) l'épave de la scapula, b) le fond de la fosse du sus-épineux c) le pilier de la scapula. Le β -angle est la méthode radiographique de mesure d'inclinaison glénoïdienne la plus reproductible eu égard aux variations positionnelles du patient lors de l'acquisition (courtoisie A Maurer).

b) Mesures tridimensionnelles

L'analyse tridimensionnelle reprend par la suite le concept du β -angle. En particulier, l'inclinaison rend particulièrement critique la détermination d'un axe ou plan transverse perpendiculaire au plan choisi de la scapula.

Des approximations plus ou moins simplifiées de la ligne du fond de la fosse sont donc proposées de par sa morphologie très complexe, on peut en retenir trois principales :

- Ligne centre glène – trigonum (méthode de Iannotti)(16)
- Fond de la fosse du sus-épineux (méthode Mimics®, Materialise)(49)
- Axe du Y (méthode de Glenosys®, Imascap)(50)

Méthode centre glène – trigonum

Il s'agit de la méthode la plus souvent utilisée. Elle simplifie le fond de la fosse du sus-épineux à une ligne passant par le centre de la glène et le trigonum (Figure 13).

Des griefs sont cependant imputables à cette méthode : 1) le centre de la glène peut être altéré par l'usure de la glène ou la perte de substance osseuse et modifier ce référentiel, 2) le trigonum possède une morphologie très variable qui limite son utilisation comme nous le verrons, 3) il s'agit d'une modélisation simpliste du fond de la fosse du sus-épineux. Ces différentes limites seront étudiées par la suite.

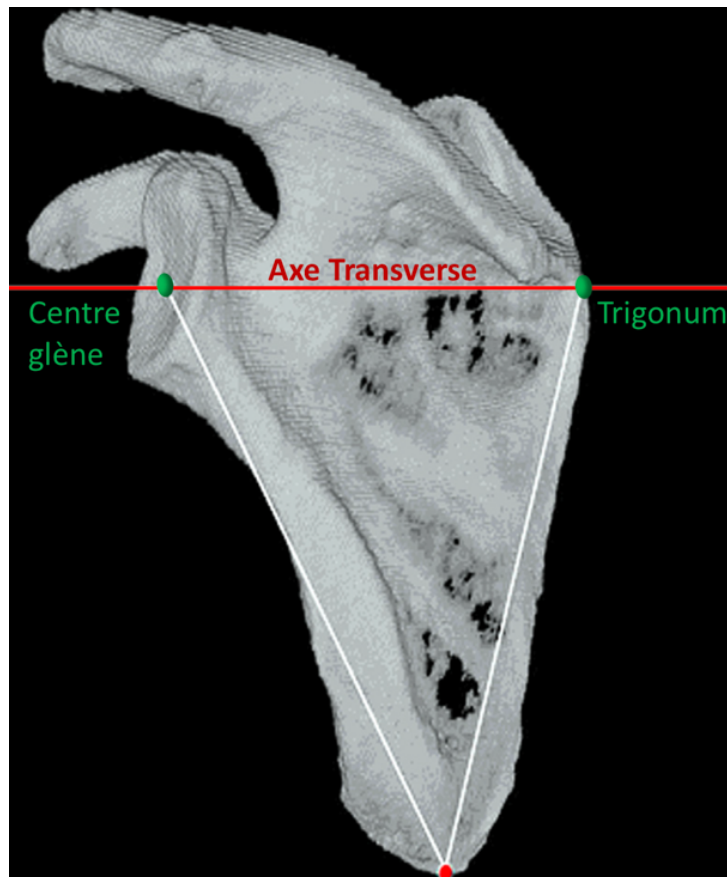


Figure 13 : Méthode centre glène trigonum. L'axe transverse est établi à partir de 2 points : le centre de la glène et le trigonum qui sont repérés manuellement.

Méthode du fond de la fosse du sus-épineux

Elle établit le repère suivant (Figure 14) :

- plan de la scapula (parallèle à \vec{Y}) déterminé par le *picking* manuel du bord axillaire (pilier) de la scapula.
- axe \vec{Z} : parallèle à la ligne du fond de la fosse du sus épineux repéré par un *picking* manuel.
- axe \vec{X} : orthogonal à \vec{Y} et au plan de la scapula.
- axe \vec{Y} : orthogonal à \vec{Z} et \vec{X} .
- origine = l'échancrure spinoglénoïdienne projeté sur l'axe \vec{Z} .

Cette méthode a l'avantage d'exclure la glène (variable étudiée) du référentiel choisi et de ne pas nécessiter la totalité de la scapula. La glène est par ailleurs représentée par une sphère dans ce modèle pour mesurer non plus seulement la version ou l'inclinaison mais l'orientation et la « direction de la version maximale » dans un plan transverse variable selon la morphologie de la glène. C'est donc une véritable analyse spatiale qui est proposée. Cette méthode dans la même analyse donne une variation de 6° avec le plan anatomique de la scapula surtout autour de l'axe \vec{Z} et l'axe \vec{Z} est proche de la ligne centre glène-trigonum. L'inclinaison moyenne retrouvée était de 7°. Cependant, il nécessite un travail de picking chronophage qui n'est pas automatisé.

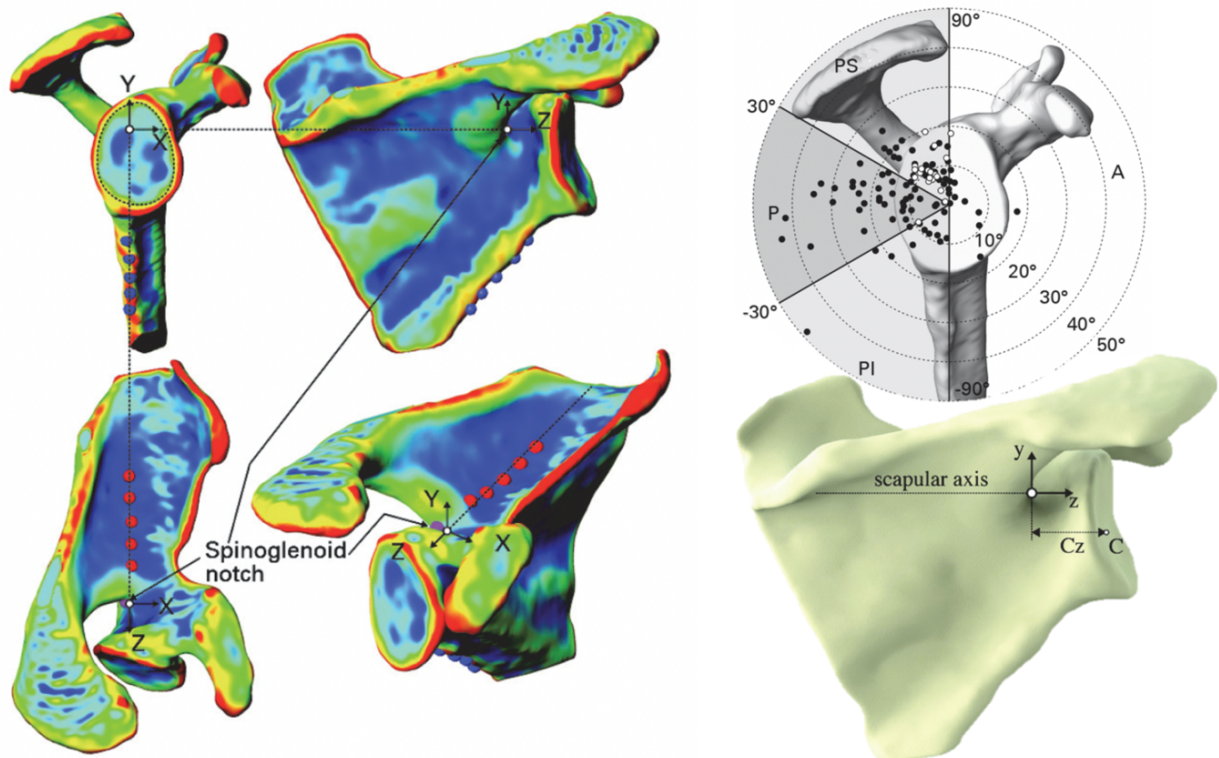


Figure 14 : Méthode du fond de la fosse du sus épineux tel que décrite par Terrier et al(49) (courtoisie A Terrier).

Méthode de l'axe du Y

La méthode de l'axe du Y utilisée par Glenosys® permet le repérage automatique des points constituant l'intersection entre le corps de l'omoplate et l'épine (Figure 15). L'ensemble de ces points constituent une courbe concave vers le bas dont la droite moyenne est l'axe transverse. La validité de cet axe sera étudiée ultérieurement.

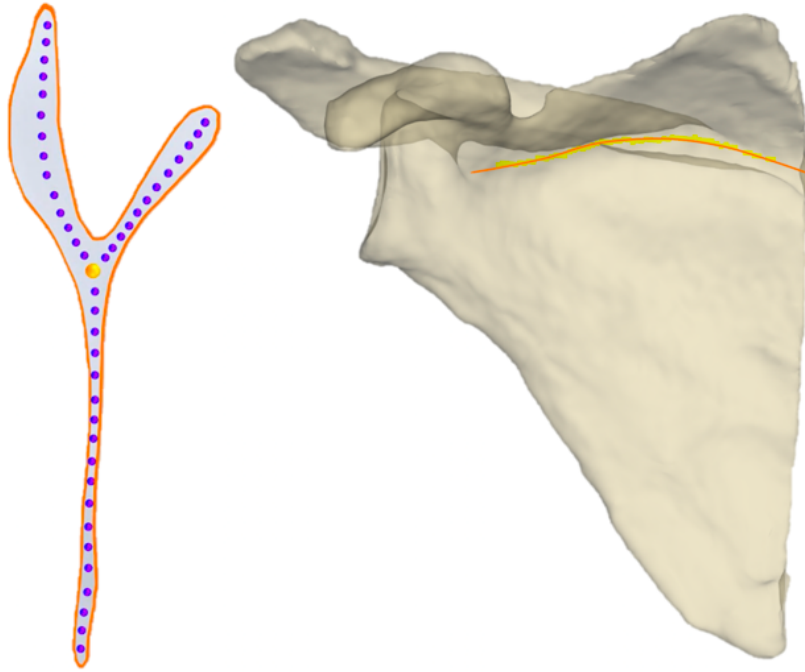


Figure 15 : Méthode de l'axe du Y utilisé dans le logiciel Glenosys. L'ensemble des points constituant l'intersection entre le corps de la scapula et l'épine de permettent de générer une ligne moyenne considéré comme l'axe transverse à l'origine de la mesure de l'inclinaison dans le logiciel.

IV/ Subluxation humérale

a) Mesures bidimensionnelles

Parallèlement à l'évolution des référentiels de mesures glénoïdiens, l'analyse de la subluxation a aussi évolué. Elle a débuté après les constatations par Neer puis Edelson d'érosions glénoïdiennes excentrées à la partie postérieure et inférieure de la glène associées à une subluxation postérieure de la tête humérale(52,56,57) (Figure 16).

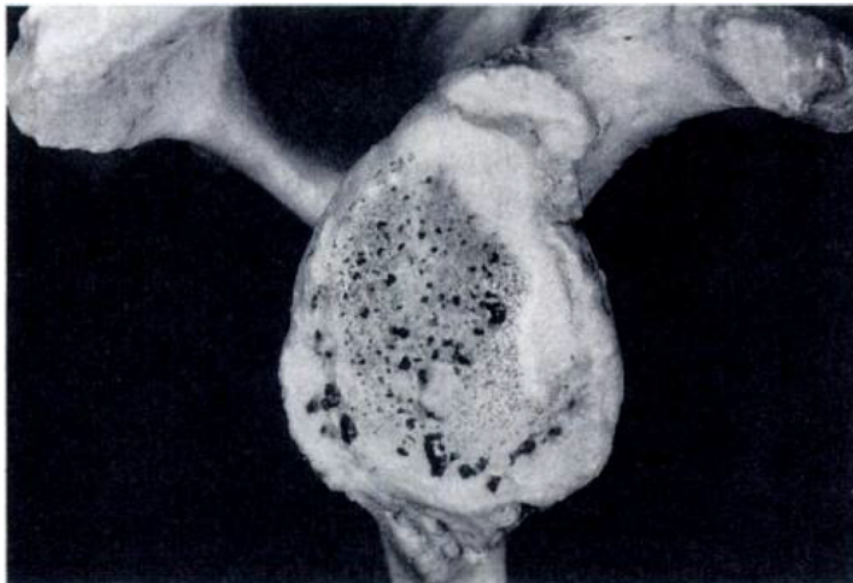


Figure 16 : D'après l'article d'Edelson en 1995 : glène « type II » correspondant aujourd'hui à une glène B2. On remarque la forte usure postérieure et inférieure (*courtoisie JG Edelson*).

Walch le premier a proposé une quantification de cette subluxation(58) (Figure 17) qui explique selon lui cette érosion postérieure constatée. Cette méthode de mesure scannographique, dérivée de la méthode radiographique de Papilion(59), a été largement utilisée par la suite(60–64). Il qualifie cette subluxation postérieure de chronique, d'aggravation progressive. Elle doit être rigoureusement différenciée d'une instabilité postérieure qui est elle dynamique avec des manifestations aiguës et une perte de fonction transitoire ou définitive(65,65). Les origines de cette subluxation restent encore peu connues mais certains auteurs suggèrent qu'elle serait acquise et résulterait d'un décentrage fonctionnel apparaissant lors de l'élévation du bras(66). Walch en 1995 crée une nouvelle classification, qui fait encore autorité aujourd'hui et sur laquelle reposera ce travail, dans laquelle les glènes B sont associées à une subluxation de la tête humérale. Par la suite, la

mesure de la subluxation a suscité un intérêt de plus en plus important avec la découverte de sa forte association aux échecs précoces des implants glénoïdiens(63,67–70) mais aussi au fait que la correction de la version de l'implant glénoïdien peut potentiellement corriger cette subluxation au moins à court terme(71). Là encore, la difficulté sera de choisir la référence de mesure la plus judicieuse et de déterminer les bornes de normalité de la subluxation humérale.

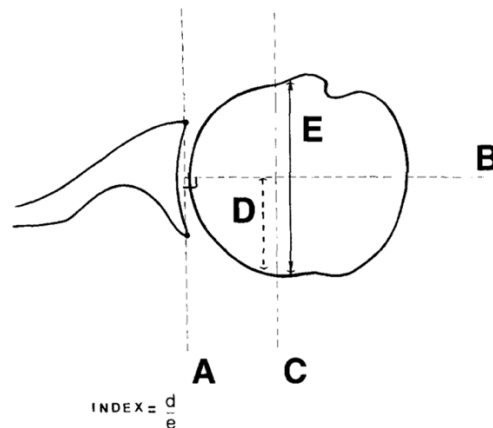


Figure 17 : D'après l'article de Walch et al : index de subluxation de la tête humérale. Il est mesuré par rapport à la médiane du segment représentant la surface glénoïdienne (*courtoisie G Walch*).

La ligne du corps de la scapula pour mesurer la subluxation est apparue comme une alternative plus fiable et plus reproductible (ICC=0,75) que la médiane à la surface glénoïdienne initialement proposée (ICC=0,60)(72) (Figure 18). En utilisant cette méthode, Sabesan et al retrouve une très forte corrélation de la subluxation à la rétroversion glénoïdienne dans les omarthroses primaires ($r^2=0,814$)(73). La limite de subluxation était arbitrairement fixée à 55% par Walch(74) mais Gerber lui préféra 65% pour éviter les cas discutables à l'inclusion des patients(60).

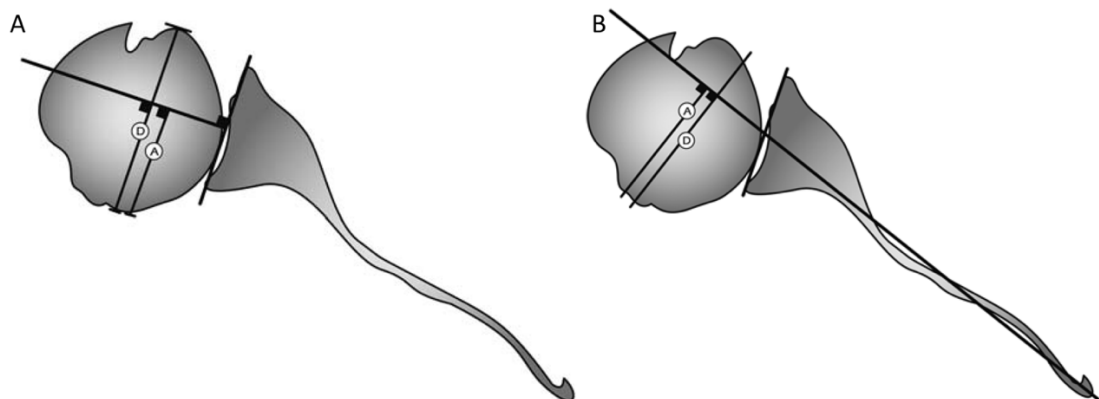


Figure 18 : Deux méthodes de mesures 2D sur scanner de la subluxation (A/D) postérieure de la tête humérale (A) par rapport à la médiane du segment représentant la surface glénoïdienne, (B) par rapport à la ligne moyenne du corps de la scapula (*courtoisie JF Kidder*).

b) Mesures tridimensionnelles

Terrier et al en 2015 transposent les mesures de la subluxation humérale à l'analyse tridimensionnelle(75). Il choisit l'axe du corps de la scapula (selon la méthode du fond de la fosse du sus-épineux) en partant du principe que la tête humérale reste dans certains cas parfaitement centrée sur la surface glénoïdienne tout en n'étant pas alignée avec la scapula et les lignes d'action des muscles intrinsèques de l'épaule. Sur des épaules arthrosiques, il retrouve une bonne corrélation entre la version et la subluxation ($r^2=0,70$) qui sont des mesures projetées sur le plan axiale. Cette corrélation est encore plus forte quand il utilise le plan – oblique – suivant la plus forte subluxation humérale ($r^2=0,864$) (Figure 19). En effet, plus la composante supéro-inférieure est importante plus la subluxation projetée est sous-évaluée. Ces fortes corrélations s'expliquent aussi en partie par le caractère engainant et remodelant de l'arthrose, absent dans l'épaule normale, et qui renforce ce centrage huméral sur la glène dans cette étude.

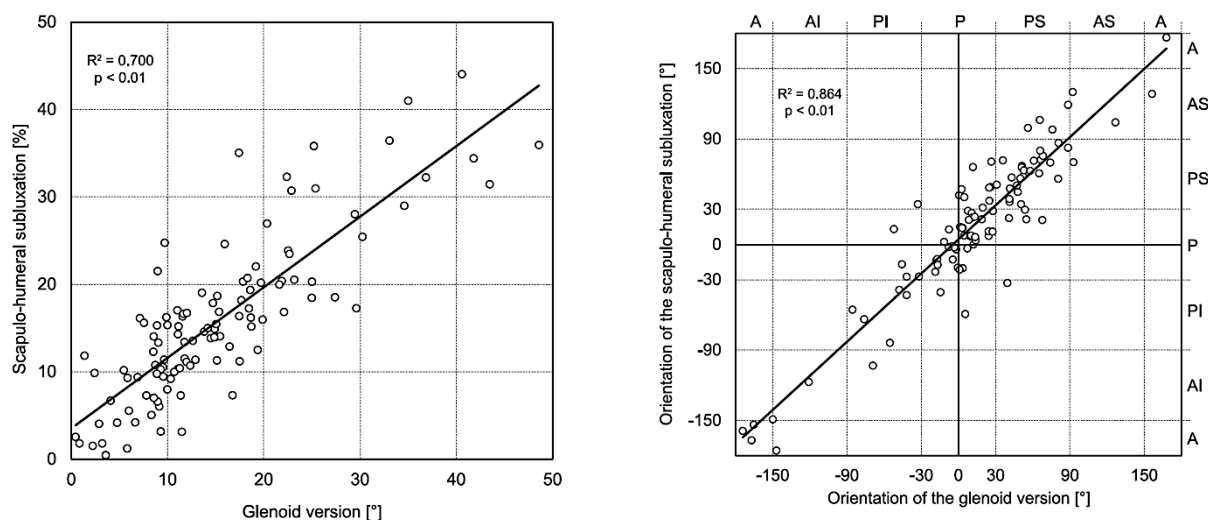


Figure 19 : Corrélation version glénoïdienne/subluxation humérale projetée (figure de gauche) et orientation glénoïdienne/subluxation humérale 3D (figure de droite). Les mesures 3D renforcent la corrélation (courtoisie A Terrier)

La subluxation de la tête humérale doit donc être préférentiellement mesurée par rapport à la scapula et non par rapport à la glène. Cette découverte mènera à la description de la glène B3 en 2016 par Walch(76) (Figure 20). En effet, la première classification de 1995 ne permettait pas de différencier une usure glénoïdienne avec à une tête humérale centrée d'une usure glénoïdienne résultant d'un remodelage secondaire à une subluxation postérieure de la

tête humérale. Dans le premier cas (glène A2), la tête use la glène dans l'axe de la scapula, dans le second cas, la tête humérale est initialement sublaxée en arrière de l'axe de la scapula (glène B1) et use la glène d'abord sur sa partie postérieure (glène biconcave B2 composée d'une néoglène usée et d'une paléoglène native) puis la remodèle entièrement pour former une surface concave avec une forte rétroversion (glène B3).

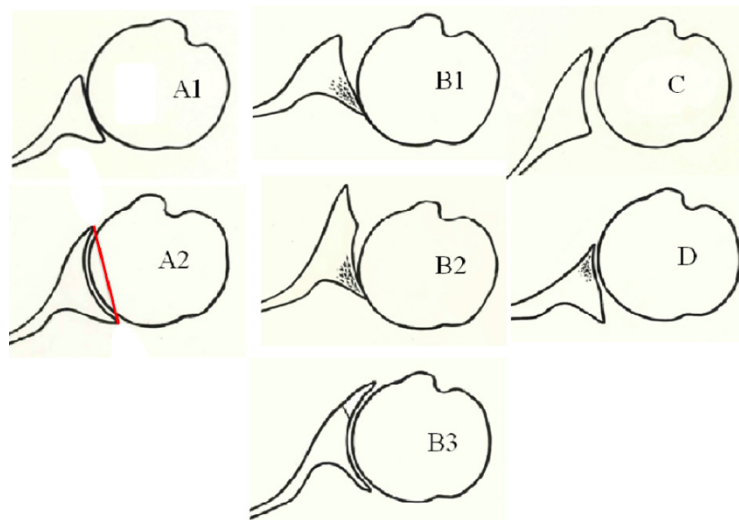


Figure 20 : Classification de Walch modifiée, les glènes A présentent une usure centrée, les B une usure postérieure suivant la sublaxation de la tête humérale, les C sont dysplasiques, les D (rares) présentent une sublaxation antérieure (courtoisie G Walch).

La sublaxation postérieure de l'humérus tient donc une place importante dans l'évolution de l'arthrose primaire glénohumérale sans que l'on connaisse réellement sa place exacte dans l'initiation du phénomène arthrosique. Si comme le prétendent certains auteurs, la version native n'est pas différente entre les arthroses concentriques et sublaxantes(77), la sublaxation postérieure pourrait alors en être le *primum movens* et à ce jour, les artifices techniques ont tous échoué à recentrer la tête humérale sur la glène de façon pérenne.

V/ Supériorité du 3D sur le 2D

Même si l'utilisation d'un modèle tridimensionnel paraît la solution la plus fiable pour représenter l'épaule, sa supériorité dans la pratique quotidienne par rapport au modèle 2D-corrigé n'est, pour l'instant, pas admise par tous. En particulier, là où les modèles 2D corrigés ont fait leur preuve et sont passés dans la pratique quotidienne avec une implication dans le diagnostic et les décisions thérapeutiques, le 3D introduit un tout nouveau point de vue et nécessite de remettre en question les repères habituels.

Le premier modèle tridimensionnel de la scapula a été proposé par Welsch et al en 2003(51). Il y anticipait déjà l'importance d'une analyse 3D préopératoire systématique pour améliorer le diagnostic et la décision thérapeutique et conclut : *"If software programs for 3D visualization become more common, why not combine a good diagnosis with a better therapy?"*.

En effet, les modifications morphologiques de l'épaule ne surviennent pas que dans les plans orthogonaux aux référentiels établis. Hoenecke et al démontre le manque de fiabilité du 2D dans l'étude préopératoire de l'arthrose. D'une part, la position de la scapula doit être normalisée par rapport au « gantry angle » (en moyenne de 35°), d'autre part, l'usure maximale glénoïdienne dans les arthroses primaires est postéroinférieure – comme l'avait déjà constaté sur os secs Edelson dès 1995(52) – et donc sous-estimée si on ne l'analyse que dans le plan axiale même après reformatage(53), cela sera confirmé par la suite(54). De même l'usure est postérosupérieure dans les arthropathies post-rupture de coiffe, il serait donc impropre de parler de glène B2 sur une coupe haute de la glène de ces cas.

Les différences de mesure observées entre le 2D-corrigé et le 3D peuvent cependant être très importantes : Chalmers et al retrouve par exemple une différence de 11% dans ses mesures de subluxation en comparant la méthode 2D-corrigée dans le plan de Kwon (qu'il considère comme le « *gold standard* ») et la méthode 3D Glenosys®(55). Ghafurian et al estime cependant que l'utilisation d'un modèle tridimensionnel de glène, comme la sphère, diminue de 10 à 30% la déviation standard des mesures de version glénoïdienne par rapport au 2D qui sont plus imprécis(36). Les modèles 3D sont donc plus stables cependant, leur choix doit être judicieux et une sphère semble mieux adaptée qu'un plan pour représenter la surface glénoïdienne(17).

La supériorité de l'analyse tridimensionnelle ne se présente donc pas comme une évidence puisque l'ensemble de nos connaissances sur la morphométrie glénohumérale reposaient jusqu'à il y a peu sur des acquis bidimensionnels. Ces modèles bidimensionnels étaient répandus et bien connus. Cependant, l'utilisation de la 3^{ème} dimension fait surgir des limites et des dysfonctionnements dans le système 2D qui bouleversent nos connaissances. Ces constatations et la multitude de référentiels coexistant mettent en avant plusieurs problématiques :

- 1) la **validation** systématique et rigoureuse des logiciels semi-automatiques ou automatiques de mesure et de planification,
- 2) la nécessité de **remettre en question les acquis du 2D** dont les limites sont démontrées même après reformatage,
- 3) l'importance de **préciser le référentiel de mesure et le modèle de représentation** choisis dans chaque étude et publication.

CONSTITUTION D'UNE BASE DE DONNEES DE SCANNERS D'EPAULES (BIBLIOTHEQUE SCIENTIFIQUE)

I/ RATIONNEL

L'étude de la morphométrie de l'épaule nécessitait la constitution d'une base de données représentant l'ensemble des types d'épaule rencontrée dans la population générale. Nous avons donc rassemblé à partir de plusieurs centres, les scanners d'épaule de patients arthrosiques.

Étaient exclus, les arthroscanners, les scanners avec les 2 épaules dans le même champ d'acquisition, les bodyscanners.

Plusieurs contraintes se présentent dans l'élaboration de ce type de base de données :

- Obtenir un **nombre** suffisant de scanners d'épaule
- Rassembler des types d'épaule **rare**s (glènes C, glènes D)
- S'assurer que le **protocole** scanner soit adapté au logiciel
- Obtenir le **consentement** du patient

Protocole scanner adapté :

Le protocole scanner devait respecter celui imposé par le logiciel (cf Annexe 1).

Consentement du patient :

Le patient devait signer un consentement éclairé avant d'effectuer un scanner (cf Annexe 2).

II/ EPAULES PATHOLOGIQUES

a) Constitution de la bibliothèque scientifique

Tous les scanners d'épaules arthrosiques étaient majoritairement recueillis auprès de plusieurs centres et analysés un par un afin de répondre aux contraintes précédemment exposées.

Nous avons exclu dans les suites les scanners d'épaules :

- dont la segmentation n'était pas jugée correcte malgré un protocole scanner respecté (Figure 21)
- dont les plans et les mesures générées étaient évidemment aberrantes

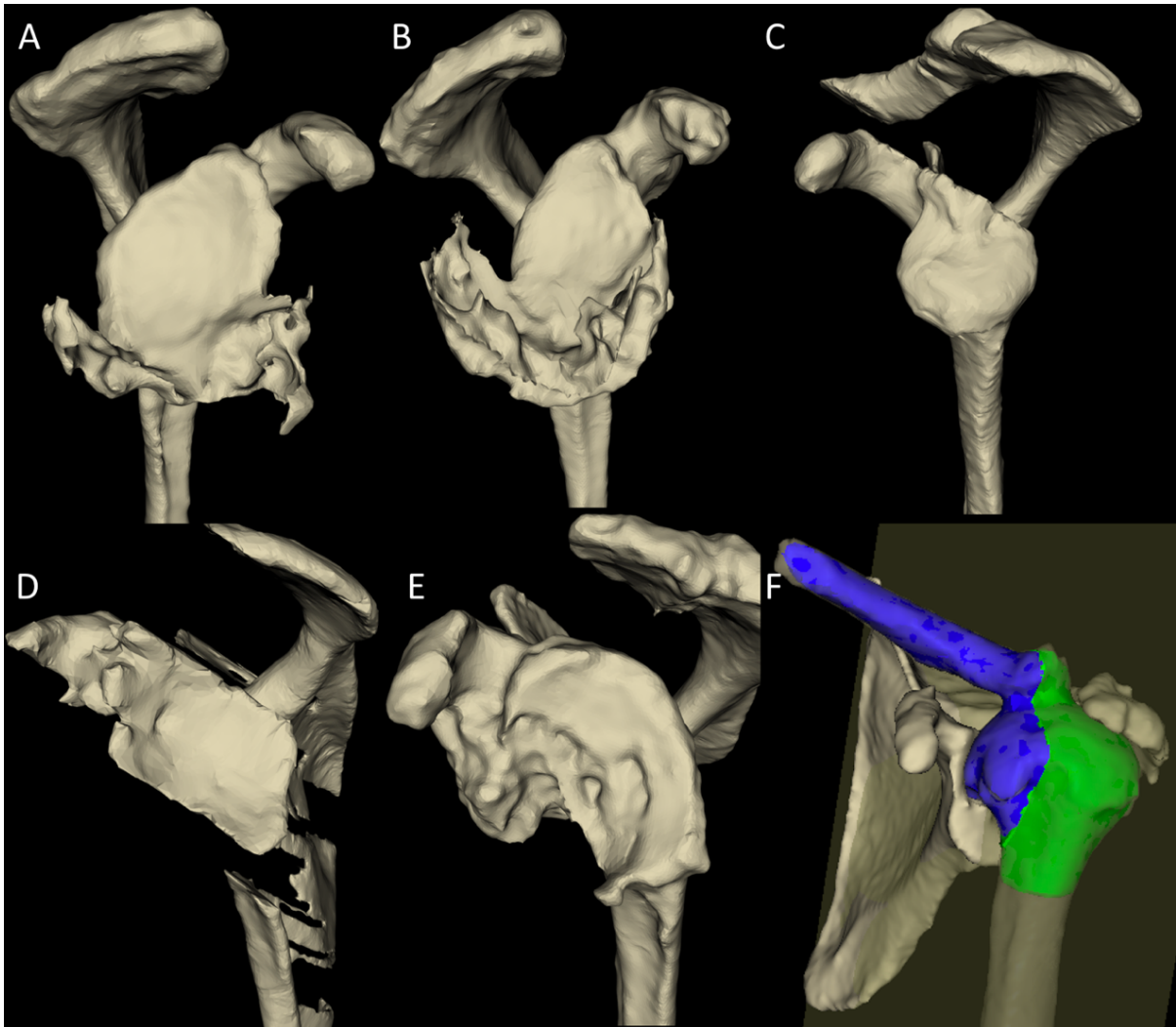


Figure 21 : exemple d'anomalies de segmentation générées par le logiciel (Glenosys v10.4.2). Les erreurs correspondaient à des fusions glénohumérale à l'origine d'un résidu huméral sur la glène (A, B) ou au contraire d'une amputation de la glène (C, D). Des corps étrangers pouvaient être à l'origine d'une mauvaise segmentation du défilé coracoglénoidien (E). Enfin, la clavicule, l'acromion ou la coracoïde pouvaient être fusionnée à la tête humérale si l'ascension humérale était complète (F). Ces scanners ont été exclus de la base de données.

De 2015 à 2017, 1149 épaules pathologiques triées ont finalement été rassemblées dans une bibliothèque scientifiques représentant de façon exhaustive l'ensemble des pathologies arthrosiques de l'épaule se présentant en consultation.

Des difficultés majeures ont dues être maîtrisées durant les processus suivants :

- **l'implémentations** de scanners à partir de plusieurs centres a rendu difficile la centralisation des données.
- **L'archivage** des données sur plusieurs supports ont rendu difficile la mise en commun des données et l'harmonisation des systèmes de consultation.
- **L'anonymisation** a été un point particulièrement difficile a traiter et a nécessité plusieurs allers-retours entre les données-source et les données de sortie du logiciel.
- Le **classement subjectif** des glènes nécessitaient un lancement itératif très chronophage pour chaque cas du logiciel Glenosys. De plus, les différentes versions et améliorations du logiciel se sont succédant en parallèle il était nécessaire à chaque fois d'effectuer un nouvel examen de toute la base de données. Une application de visualisation rapide a été développée pour les dernières versions.

b) Paramètres analysés, diagnostic et classification

Les principaux paramètres analysés étaient :

Démographique :

Age au scanner

Sexe

Latéralité

Morphométrie versant huméral

Rayon de courbure de la BFS (+ RMS error)

Inclinaison

Version (si possible à partir de l'axe biépicondylien huméral distal)

Morphométrie versant glénoïdien

Surface de la glène

Rayon de courbure de la BFS + Root

Mean Square error (RMS)

Version

Inclinaison

RSA Angle (Reverse Shoulder Angle)

CSA (Critical Shoulder Angle)

Orientation

Direction

Relations glénohumérales

Orientation humérale

Direction humérale

Subluxation

Les épaules étaient classées en fonction du diagnostic en utilisant d'une part l'histoire clinique issue des dossiers médicaux et d'autre part l'interprétation du scanner.

Plusieurs diagnostics étaient possibles :

Arthrose primaire (PGHOA)

Rupture massive de coiffe (MRCT)

Arthrose secondaire à une rupture de coiffe (CTA)

Arthrose post traumatique (PTA)

Arthrose post instabilité (PIA)

Arthrose sur ostéonécrose (AON)

Arthrose sur arthrite rhumatoïde (RA)

Les épaules atteintes de PGHOA, MRCT et CTA étaient classées par 2 chirurgiens (GW & MOG) suivant la classification de Walch-modifiée(58,76) et de Favard(78,79).

III/ EPAULES NORMALES

En parallèle une base de données de 122 épaules normales étaient constituées à partir de scanners effectués sur des individus à épaules saines. Elle était en grande partie issue de scanners effectués chez des patients accueillis au Service d'Accueil des Urgences entre 2017 et 2018.

Étaient inclus dans cette base de données les patients polytraumatisés sans urgence vitale, des patients scannés pour un accident vasculaire cérébral ou un contrôle de traumatisme crânien, des patients présentant une fracture ou une disjonction acromioclaviculaire traumatique sur l'épaule controlatérale.

Cette base de données était utilisée d'une part pour effectuer une analyse de l'épaule 3D normale, d'autre part pour comparer les données morphométriques des épaules pathologiques à celles des épaules normales.

BIBLIOGRAPHIE

1. Amadi HO, Hansen UN, Wallace AL, Bull AMJ. A scapular coordinate frame for clinical and kinematic analyses. *J Biomech.* 19 juill 2008;41(10):2144-9.
2. Boileau P, Walch G. The Three-Dimensional Geometry of the Proximal Humerus. *J Bone Joint Surg Br.* 1 sept 1997;79-B(5):857-65.
3. Hertel R, Knothe U, Ballmer FT. Geometry of the proximal humerus and implications for prosthetic design. *J Shoulder Elbow Surg.* août 2002;11(4):331-8.
4. Robertson DD, Yuan J, Bigliani LU, Flatow EL, Yamaguchi K. Three-dimensional analysis of the proximal part of the humerus: relevance to arthroplasty. *J Bone Joint Surg Am.* nov 2000;82(11):1594-602.
5. Couteau B, Mansat P, Darmana R, Mansat M, Egan J. Morphological and mechanical analysis of the glenoid by 3D geometric reconstruction using computed tomography. *Clin Biomech (Bristol, Avon).* 2000;15 Suppl 1:S8-12.
6. Couteau B, Mansat P, Estivalèzes E, Darmana R, Mansat M, Egan J. Finite element analysis of the mechanical behavior of a scapula implanted with a glenoid prosthesis. *Clin Biomech (Bristol, Avon).* août 2001;16(7):566-75.
7. Rouleau DM, Kidder JF, Pons-Villanueva J, Dynamidis S, Defranco M, Walch G. Glenoid version: how to measure it? Validity of different methods in two-dimensional computed tomography scans. *J Shoulder Elbow Surg.* déc 2010;19(8):1230-7.
8. Cyprien JM, Vasey HM, Burdet A, Bonvin JC, Kritsikis N, Vuagnat P. Humeral retrotorsion and glenohumeral relationship in the normal shoulder and in recurrent anterior dislocation (scapulometry). *Clin Orthop Relat Res.* mai 1983;(175):8-17.
9. Saha AK. Dynamic stability of the glenohumeral joint. *Acta Orthop Scand.* 1971;42(6):491-505.
10. Brewer BJ, Wubben RC, Carrera GF. Excessive retroversion of the glenoid cavity. A cause of non-traumatic posterior instability of the shoulder. *J Bone Joint Surg Am.* juin 1986;68(5):724-31.
11. Randelli M, Gambrioli PL. Glenohumeral osteometry by computed tomography in normal and unstable shoulders. *Clin Orthop Relat Res.* juill 1986;(208):151-6.
12. Nyffeler RW, Jost B, Pfirrmann CWA, Gerber C. Measurement of glenoid version: conventional radiographs versus computed tomography scans. *Journal of Shoulder and Elbow Surgery.* 1 sept 2003;12(5):493-6.
13. Friedman RJ, Hawthorne KB, Genes BM. The use of computerized tomography in the measurement of glenoid version. *J Bone Joint Surg Am.* août 1992;74(7):1032-7.
14. Bokor DJ, O'Sullivan MD, Hazan GJ. Variability of measurement of glenoid version on computed tomography scan. *J Shoulder Elbow Surg.* déc 1999;8(6):595-8.
15. Bryce CD, Davison AC, Lewis GS, Wang L, Flemming DJ, Armstrong AD. Two-dimensional glenoid version measurements vary with coronal and sagittal scapular rotation. *J Bone Joint Surg Am.* mars 2010;92(3):692-9.
16. Kwon YW, Powell KA, Yum JK, Brems JJ, Iannotti JP. Use of three-dimensional computed tomography for the analysis of the glenoid anatomy. *J Shoulder Elbow Surg.* févr 2005;14(1):85-90.
17. Lewis GS, Armstrong AD. Glenoid spherical orientation and version. *J Shoulder Elbow Surg.* janv 2011;20(1):3-11.
18. Budge MD, Lewis GS, Schaefer E, Coquia S, Flemming DJ, Armstrong AD. Comparison of standard two-dimensional and three-dimensional corrected glenoid version measurements. *J Shoulder Elbow Surg.* juin 2011;20(4):577-83.
19. Ganapathi A, McCarron JA, Chen X, Iannotti JP. Predicting normal glenoid version from the pathologic scapula: a comparison of 4 methods in 2- and 3-dimensional models. *J Shoulder Elbow Surg.* mars 2011;20(2):234-44.
20. Codsí MJ, Bennetts C, Gordiev K, Boeck DM, Kwon Y, Brems J, et al. Normal glenoid vault

- anatomy and validation of a novel glenoid implant shape. *Journal of Shoulder and Elbow Surgery*. 1 mai 2008;17(3):471-8.
21. Scalise JJ, Codsí MJ, Bryan J, Iannotti JP. The three-dimensional glenoid vault model can estimate normal glenoid version in osteoarthritis. *Journal of Shoulder and Elbow Surgery*. 1 mai 2008;17(3):487-91.
 22. Scalise JJ, Iannotti JP. Bone grafting severe glenoid defects in revision shoulder arthroplasty. *Clin Orthop Relat Res*. janv 2008;466(1):139-45.
 23. Chaoui J, Hamitouche C, Stindel E, Roux C. Recognition-based segmentation and registration method for image guided shoulder surgery. *Conf Proc IEEE Eng Med Biol Soc*. 2011;2011:6212-5.
 24. Moineau G, Levigne C, Boileau P, Young A, Walch G. Three-dimensional measurement method of arthritic glenoid cavity morphology: Feasibility and reproducibility. *Orthopaedics & Traumatology: Surgery & Research*. oct 2012;98(6, Supplement):S139-45.
 25. Poon PC, Ting FSH. A 2-dimensional glenoid vault method for measuring glenoid version on computed tomography. *J Shoulder Elbow Surg*. mars 2012;21(3):329-35.
 26. Andrin J, Macaron C, Pottecher P, Martz P, Baulot E, Trouilloud P, et al. Determination of a new computed tomography method for measuring the glenoid version and comparing with a reference method. Radio-anatomical and retrospective study. *Int Orthop*. mars 2016;40(3):525-9.
 27. Bouacida S, Gauci M-O, Coulet B, Lazerges C, Cyteval C, Boileau P, et al. Interest in the glenoid hull method for analyzing humeral subluxation in primary glenohumeral osteoarthritis. *J Shoulder Elbow Surg*. 31 mars 2017;
 28. De Wilde LF, Berghs BM, VandeVyver F, Schepens A, Verdonk RC. Glenohumeral relationship in the transverse plane of the body. *J Shoulder Elbow Surg*. juin 2003;12(3):260-7.
 29. Moraiti C, Klouche S, Werthel JD, Bauer T, Hardy P. Description and reproducibility assessment of a new computerised tomography scan index to measure the glenoid orientation in relation to the anterior glenoid surface. *Int Orthop*. 2017;41(5):1017-22.
 30. Monk AP, Berry E, Limb D, Soames RW. Laser morphometric analysis of the glenoid fossa of the scapula. *Clin Anat*. sept 2001;14(5):320-3.
 31. Schlemmer B, Dosch JC, Gicquel P, Boutemy P, Wolfram R, Kempf JF, et al. [Computed tomographic analysis of humeral retrotorsion and glenoid retroversion]. *Rev Chir Orthop Reparatrice Appar Mot*. oct 2002;88(6):553-60.
 32. Inui H, Sugamoto K, Miyamoto T, Machida A, Hashimoto J, Nobuhara K. Evaluation of three-dimensional glenoid structure using MRI. *J Anat*. sept 2001;199(Pt 3):323-8.
 33. Kelkar R, Wang VM, Flatow EL, Newton PM, Ateshian GA, Bigliani LU, et al. Glenohumeral mechanics: a study of articular geometry, contact, and kinematics. *J Shoulder Elbow Surg*. févr 2001;10(1):73-84.
 34. Braunstein V, Korner M, Brunner U, Mutschler W, Biberthaler P, Wiedemann E. The fulcrum axis: a new method for determining glenoid version. *J Shoulder Elbow Surg*. oct 2008;17(5):819-24.
 35. Braunstein V, Kirchhoff C, Ockert B, Sprecher CM, Korner M, Mutschler W, et al. Use of the fulcrum axis improves the accuracy of true anteroposterior radiographs of the shoulder. *J Bone Joint Surg Br*. août 2009;91(8):1049-53.
 36. Ghafurian S, Galdi B, Bastian S, Tan V, Li K. Computerized 3D morphological analysis of glenoid orientation. *J Orthop Res*. avr 2016;34(4):692-8.
 37. De Wilde LF, Verstraeten T, Speeckaert W, Karelse A. Reliability of the glenoid plane. *J Shoulder Elbow Surg*. avr 2010;19(3):414-22.
 38. Freedman L, Munro RR. Abduction of the arm in the scapular plane: scapular and glenohumeral movements. A roentgenographic study. *J Bone Joint Surg Am*. déc 1966;48(8):1503-10.
 39. Mallon WJ, Brown HR, Vogler JB, Martinez S. Radiographic and geometric anatomy of the scapula. *Clin Orthop Relat Res*. avr 1992;(277):142-54.
 40. Gouaze A, Castaing J, Soutoul JH, Chantepie G. [On the orientation of the scapula and of its glenoid cavity]. *Arch Anat Pathol (Paris)*. sept 1962;10:175-81.
 41. Churchill RS, Brems JJ, Kotschi H. Glenoid size, inclination, and version: an anatomic study. *J Shoulder Elbow Surg*. août 2001;10(4):327-32.

42. Terrier A, Merlini F, Pioletti DP, Farron A. Total shoulder arthroplasty: downward inclination of the glenoid component to balance supraspinatus deficiency. *J Shoulder Elbow Surg.* juin 2009;18(3):360-5.
43. Bishop JL, Kline SK, Aalderink KJ, Zael R, Bey MJ. Glenoid inclination: in vivo measures in rotator cuff tear patients and associations with superior glenohumeral joint translation. *J Shoulder Elbow Surg.* avr 2009;18(2):231-6.
44. Hopkins AR, Hansen UN, Amis AA, Emery R. The effects of glenoid component alignment variations on cement mantle stresses in total shoulder arthroplasty. *J Shoulder Elbow Surg.* déc 2004;13(6):668-75.
45. Konrad GG, Markmiller M, Jolly JT, Ruter AE, Sudkamp NP, McMahon PJ, et al. Decreasing glenoid inclination improves function in shoulders with simulated massive rotator cuff tears. *Clin Biomech (Bristol, Avon).* nov 2006;21(9):942-9.
46. Oosterom R, Rozing PM, Bersee HEN. Effect of glenoid component inclination on its fixation and humeral head subluxation in total shoulder arthroplasty. *Clin Biomech (Bristol, Avon).* déc 2004;19(10):1000-8.
47. Strauss EJ, Roche C, Flurin P-H, Wright T, Zuckerman JD. The glenoid in shoulder arthroplasty. *J Shoulder Elbow Surg.* oct 2009;18(5):819-33.
48. Maurer A, Fucentese SF, Pfirrmann CWA, Wirth SH, Djahangiri A, Jost B, et al. Assessment of glenoid inclination on routine clinical radiographs and computed tomography examinations of the shoulder. *J Shoulder Elbow Surg.* août 2012;21(8):1096-103.
49. Terrier A, Ston J, Larrea X, Farron A. Measurements of three-dimensional glenoid erosion when planning the prosthetic replacement of osteoarthritic shoulders. *Bone Joint J.* avr 2014;96-B(4):513-8.
50. Boileau P, Cheval D, Gauci M-O, Holzer N, Chaoui J, Walch G. Automated Three-Dimensional Measurement of Glenoid Version and Inclination in Arthritic Shoulders. *J Bone Joint Surg Am.* 3 janv 2018;100(1):57-65.
51. Welsch G, Mamisch TC, Kikinis R, Schmidt R, Lang P, Forst R, et al. CT-based preoperative analysis of scapula morphology and glenohumeral joint geometry. *Comput Aided Surg.* 2003;8(5):264-8.
52. Edelson JG. Patterns of degenerative change in the glenohumeral joint. *J Bone Joint Surg Br.* mars 1995;77(2):288-92.
53. Hoenecke HR, Hermida JC, Flores-Hernandez C, D'Lima DD. Accuracy of CT-based measurements of glenoid version for total shoulder arthroplasty. *J Shoulder Elbow Surg.* mars 2010;19(2):166-71.
54. Knowles NK, Ferreira LM, Athwal GS. Premorbid retroversion is significantly greater in type B2 glenoids. *Journal of Shoulder and Elbow Surgery.* 1 juill 2016;25(7):1064-8.
55. Chalmers PN, Salazar D, Chamberlain A, Keener JD. Radiographic characterization of the B2 glenoid: the effect of computed tomographic axis orientation. *J Shoulder Elbow Surg.* 31 août 2016;
56. Neer CS, Morrison DS. Glenoid bone-grafting in total shoulder arthroplasty. *J Bone Joint Surg Am.* sept 1988;70(8):1154-62.
57. Neer CS. Replacement arthroplasty for glenohumeral osteoarthritis. *J Bone Joint Surg Am.* janv 1974;56(1):1-13.
58. Walch G, Badet R, Boulahia A, Houry A. Morphologic study of the Glenoid in primary glenohumeral osteoarthritis. *The Journal of Arthroplasty.* 1 sept 1999;14(6):756-60.
59. Papilion JA, Shall LM. Fluoroscopic evaluation for subtle shoulder instability. *Am J Sports Med.* oct 1992;20(5):548-52.
60. Gerber C, Costouros JG, Sukthankar A, Fucentese SF. Static posterior humeral head subluxation and total shoulder arthroplasty. *Journal of Shoulder and Elbow Surgery.* 1 juill 2009;18(4):505-10.
61. Habermeyer P, Magosch P, Luz V, Lichtenberg S. Three-dimensional glenoid deformity in patients with osteoarthritis: a radiographic analysis. *J Bone Joint Surg Am.* juin 2006;88(6):1301-7.
62. Walch G, Boulahia A, Boileau P, Kempf JF. Primary glenohumeral osteoarthritis: clinical and

- radiographic classification. The Aequalis Group. *Acta Orthop Belg.* 1998;64 Suppl 2:46-52.
63. Iannotti JP, Norris TR. Influence of preoperative factors on outcome of shoulder arthroplasty for glenohumeral osteoarthritis. *J Bone Joint Surg Am.* févr 2003;85-A(2):251-8.
64. Badet R, Boileau P, Noel E, Walch G. Arthrography and computed arthrotomography study of seventy patients with primary glenohumeral osteoarthritis. *Rev Rhum Engl Ed.* oct 1995;62(9):555-62.
65. Domos P, Checchia CS, Walch G. Walch B0 glenoid: pre-osteoarthritic posterior subluxation of the humeral head. *J Shoulder Elbow Surg.* janv 2018;27(1):181-8.
66. Hsu JE, Gee AO, Lucas RM, Somerson JS, Warme WJ, Matsen FA. Management of intraoperative posterior decentering in shoulder arthroplasty using anteriorly eccentric humeral head components. *Journal of Shoulder and Elbow Surgery.* 1 déc 2016;25(12):1980-8.
67. Boileau P, Avidor C, Krishnan SG, Walch G, Kempf J-F, Molé D. Cemented polyethylene versus uncemented metal-backed glenoid components in total shoulder arthroplasty: A prospective, double-blind, randomized study. *Journal of Shoulder and Elbow Surgery.* juill 2002;11(4):351-9.
68. Gauci MO, Bonneville N, Moineau G, Baba M, Walch G, Boileau P. Anatomical total shoulder arthroplasty in young patients with osteoarthritis. *Bone Joint J.* 1 avr 2018;100-B(4):485-92.
69. Walch G, Young AA, Boileau P, Loew M, Gazielly D, Molé D. Patterns of loosening of polyethylene keeled glenoid components after shoulder arthroplasty for primary osteoarthritis: results of a multicenter study with more than five years of follow-up. *J Bone Joint Surg Am.* 18 janv 2012;94(2):145-50.
70. Haines JF, Trail IA, Nuttall D, Birch A, Barrow A. The results of arthroplasty in osteoarthritis of the shoulder. *The Journal of Bone and Joint Surgery British volume.* 1 avr 2006;88-B(4):496-501.
71. Nyffeler RW, Sheikh R, Atkinson TS, Jacob HAC, Favre P, Gerber C. Effects of glenoid component version on humeral head displacement and joint reaction forces: an experimental study. *J Shoulder Elbow Surg.* oct 2006;15(5):625-9.
72. Kidder JF, Rouleau DM, Pons-Villanueva J, Dynamidis S, DeFranco MJ, Walch G. Humeral Head Posterior Subluxation on CT Scan: Validation and Comparison of 2 Methods of Measurement: Techniques in Shoulder and Elbow Surgery. sept 2010;11(3):72-6.
73. Sabesan VJ, Callanan M, Youderian A, Iannotti JP. 3D CT assessment of the relationship between humeral head alignment and glenoid retroversion in glenohumeral osteoarthritis. *J Bone Joint Surg Am.* 16 avr 2014;96(8):e64.
74. Mizuno N, Denard PJ, Raiss P, Walch G. Reverse total shoulder arthroplasty for primary glenohumeral osteoarthritis in patients with a biconcave glenoid. *J Bone Joint Surg Am.* 17 juill 2013;95(14):1297-304.
75. Terrier A, Ston J, Farron A. Importance of a three-dimensional measure of humeral head subluxation in osteoarthritic shoulders. *J Shoulder Elbow Surg.* févr 2015;24(2):295-301.
76. Bercik MJ, Kruse II K, Yalozis M, Gauci M-O, Chaoui J, Walch G. A modification to the Walch classification of the glenoid in primary glenohumeral osteoarthritis using three-dimensional imaging. *Journal of Shoulder and Elbow Surgery.* oct 2016;25(10):1601-6.
77. Ricchetti ET, Hendel MD, Collins DN, Iannotti JP. Is premorbid glenoid anatomy altered in patients with glenohumeral osteoarthritis? *Clin Orthop Relat Res.* sept 2013;471(9):2932-9.
78. Sirveaux F, Favard L, Oudet D, Huquet D, Walch G, Mole D. Grammont inverted total shoulder arthroplasty in the treatment of glenohumeral osteoarthritis with massive rupture of the cuff. *The Journal of Bone and Joint Surgery British volume.* 1 avr 2004;86-B(3):388-95.
79. Huguet D, Favard L, Lautman S. Epidemiology, imaging, and classification of glenohumeral osteoarthritis with massive and non reparable rotator cuff tear. In: 2000 shoulder prosthesis: two to ten year follow-up. Sauramps Medical. Montpellier, France: Walch G, Boileau P (eds); 2001. p. pp 233 to 240.

Annexes

Annexe 1 : Feuille de consentement du patient

[Formulaire patient à faire signer préalablement à l'utilisation du logiciel BluePrint™ et à conserver par le professionnel de santé]

Formulaire d'information et de consentement patient

Nom du patient : _____

Prénom du patient : _____

Je suis informé(e) de ce que, en vue de l'intervention chirurgicale qui sera pratiquée par le Dr _____ (ci-après « le Docteur »), le _____, le Docteur utilise un logiciel de planification de procédures orthopédiques sur lequel il saisit des données me concernant.

Les données saisies via ce logiciel sont hébergées auprès d'un hébergeur agréé afin d'assurer le niveau de confidentialité et de sécurité adapté à la nature des données me concernant traitées via ce logiciel.

Ce logiciel permet également au Docteur de commander et faire fabriquer auprès de la société Tornier, un outil d'implantation personnalisé qu'il utilisera lors de l'intervention chirurgicale.

Aux fins de commande, fabrication et livraison de cet outil personnalisé, le Docteur communique à la société Tornier :

- . un code clé unique généré par le logiciel ;
- . un certain nombre de données me concernant.

Pour générer le code clé unique, le Docteur collecte mon prénom, nom de famille, date de naissance. Seul le Docteur sera en mesure de relier ces informations permettant mon identification aux autres données de santé collectées. Le code clé unique généré est anonyme.

Les autres données collectées me concernant sont mon sexe, diagnostic, type de glène, la date et lieu de l'opération envisagée, des copies d'écrans CT scans, mesures et anatomie.

Aucune donnée permettant mon identification directe telle que mon identité ou mon numéro de sécurité sociale n'est communiquée à la société Tornier.

La société Tornier, qui est enregistrée au Registre du commerce de Grenoble sous le numéro 070501275 et est située 161 rue Lavoisier, 38330 Montbonnot-Saint-Martin, FRANCE traitera ces données aux fins de fabrication et livraison de l'outil personnalisé qui lui est commandé par le Docteur, conformément à mon consentement exprimé ci-dessous.

Ces données étant strictement nécessaires aux fins identifiées ci-dessus, Tornier ne sera pas en mesure de fabriquer et livrer l'outil personnalisé si elle n'obtient pas communication de ces données, ou si je choisis de retirer mon consentement à leur traitement, préalablement à la date de mon intervention chirurgicale.

Ces données sont destinées aux membres autorisés des services de gestion des commandes/facturation, fabrication des outils, logistique et transport de la société Tornier.

Elles sont traitées et conservées par la société Tornier jusqu'à la date de l'intervention chirurgicale envisagée.

Après cette date, elles sont archivées sur une base sécurisée pendant 10 ans, conformément aux dispositions légales applicables.

Elles pourront également être traitées sous forme anonyme et agrégée à des fins d'utilisation sous forme statistique, de référence, de recherche, d'analyse de données et d'amélioration du logiciel.

Je dispose d'un droit d'accéder aux données me concernant et d'en demander la rectification, lorsqu'elles sont inexactes, ainsi que de m'opposer à leur hébergement auprès d'un hébergeur agréé pour des motifs légitimes.

Je dispose également du droit de demander la limitation du traitement de mes données, ainsi que du droit de transmettre des directives concernant le sort de mes données après ma mort. Je suis également en droit de demander une copie de mes données personnelles traitées dans les conditions décrites ci-dessus sous un format structuré, couramment utilisé et lisible par machine. Je peux exercer ces droits en adressant ma demande directement au Docteur ou auprès du médecin Hébergeur COREYE :

- . Par écrit à l'adresse suivante : 61, avenue de l'Harmonie - 59262 Sainghin-en-Mélantois, FRANCE
- . Par courriel à l'adresse : support@coreye.fr
- . Par téléphone en contactant le support au : 03.28.520.525

Les réclamations relatives à l'utilisation de mes données personnelles peuvent être adressées à la Commission Nationale de l'Informatique et des Libertés, 3 Place de Fontenoy - TSA 80715 - 75334 PARIS CEDEX 07 - FRANCE

Je consens expressément au traitement de mes données dans les conditions, par les personnes et aux fins décrites ci-dessus.

Fait à _____, le _____

[Signature du patient]

Annexe 2 : Protocole d'acquisition scanner

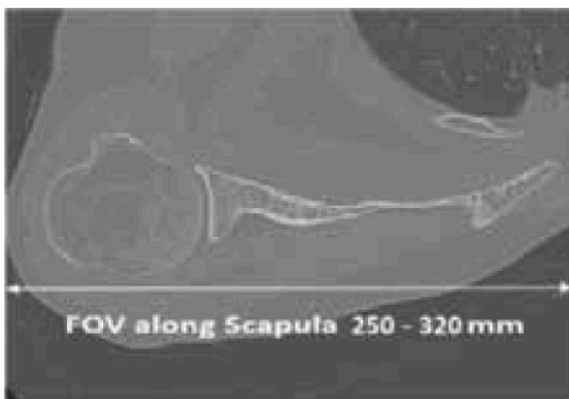
» Paramètres recommandés

Paramètre	Recommandé
Modalité - (0008,0060)	CT
Kernel / Algorithm - (0018,1210)	Bone or Bone+
kVp - (0018,0060)	120 or 140 kVp
mAs - (0018,1152)	Manuel 240 mA NE PAS utiliser auto-mA
Intervalle des coupes - (0018,0088)	1.2 mm
Temps d'exposition - (0018,1150)	1000 ms

Note: Utiliser le réglage manual-mA à 240mA permettra d'avoir des images compatibles avec le logiciel BLUEPRINT™ 3D PLANNING.

» Détails pour le paramètre « Display Field Of View » (DFOV):

Paramètre	Recommandé
DFOV (vue axiale)	Inclure l'omoplate en entier Entre 25 cm et 32 cm
DFOV (vue frontale)	Inclure l'omoplate en entier Supérieur à 10 cm
Taille de la matrice	512 x 512



Liste des articles issus du travail de Thèse

Etude I

Boileau P, Cheval C, **Gauci MO**, Holzer N, Chaoui J, Walch G. "Automated Three-Dimensional Measurement of Glenoid Version and Inclination in Arthritic Shoulders." *The Journal of Bone and Joint Surgery. American Volume* 100, no. 1 (January 3, 2018): 57–65.
<https://doi.org/10.2106/JBJS.16.01122>.

Etude II

Bercik, MJ, Kruse II K, Yalozis M, **Gauci MO**, Chaoui J, Walch G. "A Modification to the Walch Classification of the Glenoid in Primary Glenohumeral Osteoarthritis Using Three-Dimensional Imaging." *Journal of Shoulder and Elbow Surgery* 25, no. 10 (October 2016): 1601–6. <https://doi.org/10.1016/j.jse.2016.03.010>.

Etude III

Gauci MO, Deransart P, Chaoui J, Urvoy M, Athwal GS, Sanchez-Sotelo J, Boileau P, Walch G. "Three-Dimensional Geometry of the Normal Shoulder: a Software Analysis" (*submitted to JSES*)

Etude IV

Gauci MO, Urvoy M, Athwal GS, Sanchez-Sotelo J, Chaoui J, Boileau P, Walch G. Three-Dimensional Geometry of the Glenohumeral Joint in Primary Glenohumeral Osteoarthritis (*submitted to JBJS Am*)

Etude V

Boileau P, **Gauci MO**, Wagner ER, Clowez G, Chaoui J, Chelli M, Walch G. "The Reverse Shoulder Arthroplasty Angle: A New Measurement of Glenoid Inclination for Reverse Shoulder Arthroplasty." *Journal of Shoulder and Elbow Surgery*, March 29, 2019.
<https://doi.org/10.1016/j.jse.2018.11.074>.

Etude VI

Gauci MO, Chaoui J, Berhouet, Jacquot A, Baba M, Walch G, Boileau P. "Can Surgeons Optimize Range Of Motion And Reduce Scapulohumeral Impingements In Reverse Shoulder Arthroplasty: a Computational Study" (*Submit to JJAOS*)

Etude VII

Gauci MO, Boileau P, Baba M, Chaoui J, Walch G. "Patient-Specific Glenoid Guides Provide Accuracy and Reproducibility in Total Shoulder Arthroplasty." *Bone Joint J* 98-B, no. 8 (August 1, 2016): 1080–85. <https://doi.org/10.1302/0301-620X.98B8.37257>.

Etude VIII

Jacquot A, **Gauci MO**, Chaoui J, Baba M, Deransart P, Boileau P, Mole D, Walch G. "Proper Benefit of a Three Dimensional Pre-Operative Planning Software for Glenoid Component Positioning in Total Shoulder Arthroplasty." *International Orthopaedics*, July 2, 2018.
<https://doi.org/10.1007/s00264-018-4037-1>.

INTRODUCTIONS

Etude I

Preoperative shoulder arthroplasty planning with 2D or 3D manual or semi-automatic methods is time consuming and depends on the various observers. We developed a 3D-fully automatic surgeon operated software which provide complete 3D reconstruction of the shoulder and fully automated measurements of the glenoid.

Etude II

Several authors have reported varying level of inter- and intra-observer reliability in Walch classification for primary glenohumeral osteoarthritis. We developed a “modified” classification to increase inter- and intra-observer variability.

Etude III

Normal glenohumeral joint morphology and glenohumeral relationships have not been assessed using specifically the 3D-scapular body plane generated by a fully-automatic software.

Etude IV

Primary glenohumeral osteoarthritis threshold in the modified-Walch glenoid classification has been establish subjectively. To date the collection of important CT-scan databases and the use of automatic 3D segmentation softwares may help to better refine the limits of each subtypes.

Etude V

Glenoid inclination definition is highly discussable. In reverse shoulder arthroplasty positioning of the baseplate depend on the anatomy of the inferior glenoid and the global inclination underestimates its superior tilt.

Etude VI

Reverse shoulder arthroplasty positioning and designs have progressed a lot from the 2000's. To date 3D automatic software allows simulating the prosthetic motion and reducing the scapulohumeral impingements.

Etude VII

Positioning of the prosthetic implant is a critical factor for early loosening especially on the glenoid side. Patient specific instrumentations after 3D planning are available and have already proven their accuracy in glenoid implantation in cadavers.

Etude VIII

Respective implications of 3D planning and patient specific guides are not known in the improvement of implant positioning accuracy.

OBJECTIFS

Etude I

To use our fully automated method to measure 3D glenoid version and inclination in osteoarthritic shoulders, and to assess validity and reliability in comparison with previously described methods.

Etude II

To present several modifications to the original Walch classification system to enable more accurate and reliable description of glenoid morphology.

Etude III

- 1) To determine the 3D-geometry of the normal glenohumeral joint with reference to a scapular body plane defined through autosegmentation independent of the glenoid.
- 2) To evaluate the spatial correlation between humeral head position and glenoid orientation.

Etude IV

To perform a three-dimensional description of the GHJ in PGHOA and to establish the morphometric differences and thresholds that exist between normal shoulders and primary glenohumeral osteoarthritis (PGHOA), and amongst the various types of the Walch classification when possible

Etude V

To describe and validate a new method for measuring the inclination relevant to the reverse prosthesis in the inferior half of the glenoid for use in both plain radiography and 2D and 3D computed tomography to avoid superior tilt in reverse shoulder arthroplasty.

Etude VI

To compare the range of motion in reverse shoulder arthroplasty between different humeral implant designs (Inlay-155° vs Onlay-145°) and a glenoid implant that could be lateralized or not (RSA vs BIO-RSA) using a 3D automatic software that represents the evolution of our daily practice.

Etude VII

To determine the mean error in version and inclination and mean deviation of the position of the entry point of the guide wire in relation to the planned parameters in patients operated for total shoulder arthroplasty.

Etude VIII

To evaluate the proper role of the patient-specific guide in improving the surgeon's accuracy by comparing the accuracy of glenoid implant position 1) with isolated 3D-preoperative planning (Glenosys-Imascap) using a freehand implantation method and with the use of a patient-specific guide for glenoid implantation.

HYPOTHESES

Etude I

The automated measurements of osteoarthritic shoulders with this novel software would be valid and comparable with those obtained with previously described manual or semi-automated methods

Etude II

These modifications to the Walch classification system, when using 3D glenoid reconstructions, will lead to improved interobserver and intraobserver agreement.

Etude III

The humeral head position is correlated with the glenoid orientation and direction.

Etude IV

There are clear morphometric discriminants between the various glenoid types, and that specific numeric limit values may allow identifying each glenoid type.

Etude V

1) The RSA angle would reliably and accurately measure the inclination relevant to the reverse prosthesis on plain radiographs and CT scans and
2) preoperative measurement of glenoid inclination over the entire glenoid surface (TSA angle or b angle) would underestimate the potential superior inclination of the RSA baseplate and, therefore, the amount of correction required for implantation in neutral inclination.

Etude VI

Our hypothesis was that the glenoid lateralization allowed a better ROM and that the Onlay design increased the risk of early acromial abutment.

Etude VII

Preoperative planning and patient specific guide provide an accurate and reproducible positioning and orientation of the glenoid component in anatomical TSA.

Etude VIII

Patient specific instrumentation improves the positioning and the orientation of the glenoid implant compared with freehand implantation.

MATERIELS & METHODES

Etude I

From 60 CT-scans of shoulders with primary glenohumeral osteoarthritis, we generated the glenoid measurements of the version and inclination with an automated, surgeon-operated 3D-software. Those measures were compared with five previously described manual methods achieved by 2 independent surgeons (inter- and intraobserver analysis).

Etude II

We modified the Walch classification especially by adding the B3-type (retroversion $\geq 15^\circ$ and/or subluxation $\geq 70^\circ$) and the D-type (anteversion $\geq 5^\circ$) glenoids. Using 3D CT-scan glenoid reconstructions, 3 evaluators used the original Walch classification and the modified-Walch classification to classify 129 glenoids on 4 separate occasions. Reliabilities were assessed by calculating κ coefficients.

Etude III

From 122 strictly normal glenohumeral joints, we performed 3D-segmentation and measurements with a fully automatic software. Geometric measurements included: version, inclination, direction, orientation, best-fit sphere radius, humeral subluxation, critical shoulder angle and reverse shoulder angle, glenoid area and glenohumeral distance.

Etude IV

From 707 shoulders with primary glenohumeral osteoarthritis and 122 normal shoulders we described and compared the pathologic 3D glenoid and humeral morphometrics and the glenohumeral relationships from measures provided by a 3D automatic software. When possible we also determined thresholds to differentiate each glenoid types.

Etude V

From 47 shoulders suffering from cuff tear arthropathy or massive rotator cuff tear, we made an inter- and intra-observer analysis of the measurements of the “reverse shoulder angle” (RSA-angle) and “total shoulder angle” (TSA-angle) on AP X-rays, reformatted 2D CT-scans and with a 3D automatic software.

Etude VI

From 31 shoulders suffering from cuff tear arthropathy (Favard-E1), we simulated 4 different planning with or without glenoid implant lateralization (*RSA* or *BIO-RSA*) and an *Inlay* or *Onlay* humerus implant. The range of motion and the impingement zones were reported.

Etude VII

From 17 total shoulder arthroplasty performed with a patient-specific guide printed after a 3D preoperative planning, we compared the planned and the actual pre- and post-operative version, inclination and endpoint of the glenoid implant.

Etude VIII

From 17 total shoulder arthroplasty performed with a single preoperative planning, the position of the glenoid component was compared to the planned position. Then, the results were compared to those obtained in Study VII that used of the patient specific guides.

RESULTATS

Etude I

The differences between the automatic software and the handmade methods varied from 1.8 to 2.5° for version (*almost perfect* agreement) and 0.2 for inclination (*very good* agreement) and were not significant. No differences were found in the inter- and intraobservers analysis.

Etude II

Inter- and intra-observer improved between the use of the original Walch classification and the modified-Walch classification (0.391 to 0.703 and 0.605 to 0.882). The observers never agreed on a B1 glenoid entirely.

Etude III

Glenoid version and inclination were $-6\pm 4^\circ$ and $7^\circ\pm 5$ respectively on average. Males and females were found to have significantly different values for inclination (6° vs 9° , $p=0.02$), but not for version. Humeral subluxation was $59\pm 7\%$ with a linear correlation with glenoid retroversion ($r=-0.70$, $p=0.0001$) regardless of age. There was a significant and linear correlation between glenoid and humeral orientation and direction ($r=0.72$ and $r=0.70$, $p<0.001$).

Etude IV

In primary glenohumeral osteoarthritis, 90% of the glenoids and 85% of the humeral head were directed posteriorly. Joint narrowing under 3mm was a marker of A-type glenoids. Humeral subluxation $>70\%$ was the most discriminating parameter between the normal GHJ and a B1-type. The root mean square error of the glenoid-BFS helped to identify B2-types. B3 had a greater retroversion ($>13^\circ$) and subluxation ($> 71\%$) than A2-types. The C glenoid retroversion inferior limit of glenoid retroversion was 21° , whereas normal glenoids never presented a retroversion greater than 16° .

Etude V

The mean RSA angle was $25\pm 8^\circ$ on AP X-Rays, $20\pm 6^\circ$ on reformatted 2D CT-scans, and $21\pm 5^\circ$ via 3D software. The mean TSA angle was on average $10\pm 5^\circ$ lower than the mean RSA angle ($p<0.001$) regardless of the method of measurement. In Favard type E1 glenoids with central concentric erosion, the difference between the 2 angles was $12\pm 4^\circ$ ($p<0.001$).

Etude VI

Lateralization provided better results in all motion. Onlay implants allowed better rotations, extension and adduction with delayed impingements with the pilar. The greater tuberosity conflicts with the acromion were associated with the lowest abduction independently from the lateralization, and the Inlay design was the most performing in abduction motion.

Etude VII

The mean error in the accuracy of the entry point was -0.1 ± 1.4 mm in the horizontal plane, and 0.8 ± 1.3 mm in the vertical plane. The mean error in the orientation of the glenoid component was $3.4\pm 5.1^\circ$ for version and $1.8\pm 5.3^\circ$ for inclination.

Etude VIII

The use of the planning alone allowed an accuracy of 2.9 ± 1.4 mm vs 2.1 ± 0.9 mm with a guide ($p=0.05$). Guide provided more accuracy in glenoids with severe retroversion ($>10^\circ$). The differences were not significant in version and inclination.

CONCLUSIONS

Etude I

Automated measurement of 3D glenoid inclination and version on standard CT-images of osteoarthritic shoulders is valid, with excellent correlation to previously proposed 2D and 3D manual or semi-automated methods. The automated method eliminates inter- and intraobserver discrepancies.

Etude II

When 3-dimensional glenoid reconstructions and the modified Walch classification described herein are used, improved interobserver and intraobserver reliabilities are obtained.

Etude III

The 3D-geometry of the glenoid and humeral head remains consistent in normal shoulders; interindividual variations, regardless of the size, are relative to the scapular plane. There exists a strong correlation between the position of the humeral head and the glenoid orientation and direction.

Etude IV

Morphometric differences and thresholds can be identified from three-dimensional measurements obtained with an automatic preoperative planning software in shoulders suffering from PGHOA. This method and the provided results can be of substantial interest to develop automatic diagnostic assistance algorithms.

Etude V

RSA angle is representative of the inferior glenoid tilt while the TSA angle underestimates its superior orientation. The RSA angle needs to be corrected to achieve neutral inclination of the baseplate. E1-glenoids are at risk for baseplate superior tilt if RSA angle is not corrected.

Etude VI

Glenoid lateralization delays the glenohumeral impingement in RSA and gives the best rotations, adduction and extension when associated with neutral inclination and humeral 145° inclination. GT abutment has to be avoided in abduction and the Inlay design provides the best abduction.

Etude VII

Pre-operative planning with automatic software and the use of PSGs provides accurate and reproducible positioning and orientation of the glenoid component in anatomical TSA.

Etude VIII

3D pre-operative planning allowed accurate glenoid component positioning with a freehand method. Patient-specific guides slightly improved the position of the central point, especially for severely retroverted glenoids, but not the orientation of the component.

PUBLICATIONS

Automated Three-Dimensional Measurement of Glenoid Version and Inclination in Arthritic Shoulders

Pascal Boileau, MD, PhD, Damien Cheval, MD, Marc-Olivier Gauci, MD, MSc, Nicolas Holzer, MD, PhD, Jean Chaoui, PhD, and Gilles Walch, MD

Investigation performed at iULS (Institut Universitaire Locomoteur & du Sport), Hôpital Pasteur 2, University of Nice Sophia-Antipolis, Nice, and Centre Orthopédique Santy, Hôpital Privé Jean Mermoz, Lyon, France

Background: Preoperative computed tomography (CT) measurements of glenoid version and inclination are recommended for planning glenoid implantation in shoulder arthroplasty. However, current manual or semi-automated 2-dimensional (2D) and 3-dimensional (3D) methods are user-dependent and time-consuming. We assessed whether the use of a 3D automated method is accurate and reliable to measure glenoid version and inclination in osteoarthritic shoulders.

Methods: CT scans of osteoarthritic shoulders of 60 patients scheduled for shoulder arthroplasty were obtained. Automated, surgeon-operated, image analysis software (Glenosys; Imascap) was developed to measure glenoid version and inclination. The anatomic scapular reference planes were defined as the mean of the peripheral points of the scapular body as well as the plane perpendicular to it, passing along the supraspinatus fossa line. Measurements were compared with those obtained using previously described manual or semi-automated methods, including the Friedman version angle on 2D CTs, Friedman method on 3D multiplanar reconstructions (corrected Friedman method), Ganapathi-Iannotti and Lewis-Armstrong methods on 3D volumetric reconstructions (for glenoid version), and Maurer method (for glenoid inclination). The mean differences (and standard deviation) and the concordance correlation coefficients (CCCs) were calculated. Two orthopaedic surgeons independently examined the images for the interobserver analysis, with one of them measuring them twice more for the intraobserver analysis; interobserver and intraobserver reliability was calculated using the intraclass correlation coefficients (ICCs).

Results: The mean difference in the Glenosys glenoid version measurement was $2.0^{\circ} \pm 4.5^{\circ}$ (CCC = 0.93) compared with the Friedman method, $2.5^{\circ} \pm 3.2^{\circ}$ (CCC = 0.95) compared with the corrected Friedman method, $1.5^{\circ} \pm 4.5^{\circ}$ (CCC = 0.94) compared with the Ganapathi-Iannotti method, and $1.8^{\circ} \pm 3.8^{\circ}$ (CCC = 0.95) compared with the Lewis-Armstrong method. There was a mean difference of $0.2^{\circ} \pm 4.7^{\circ}$ (CCC = 0.78) between the inclination measurements made with the Glenosys and Maurer methods. The difference between the overall average 2D and 3D measurements was not significant ($p = 0.45$).

Conclusions: Use of fully automated software for 3D measurement of glenoid version and inclination in arthritic shoulders is reliable and accurate, showing excellent correlation with previously described manual or semi-automated methods.

Clinical Relevance: The use of automated surgeon-operated image analysis software to evaluate 3D glenoid anatomy eliminates interobserver and intraobserver discrepancies, improves the accuracy of preoperative planning for shoulder replacement, and offers a potential gain of time for the surgeon.

The success of total shoulder arthroplasty depends on the ability of the surgeon to identify the severity of glenoid bone loss and determine the appropriate location and orientation for the glenoid implant¹. Glenoid version and in-

clination need to be corrected at the time of prosthetic glenoid implantation. Malpositioning of the glenoid component (i.e., with excessive retroversion and/or inclination) in shoulder arthroplasty has been shown to predispose to prosthetic

Disclosure: No external funds were received in support of this study. On the **Disclosure of Potential Conflicts of Interest** forms, which are provided with the online version of the article, one or more of the authors checked "yes" to indicate that the author had a relevant financial relationship in the biomedical arena outside the submitted work (including Imascap, of which J. Chaoui is CEO) and "yes" to indicate that the author had other relationships or activities that could be perceived to influence, or have the potential to influence, what was written in this work (P. Boileau, G. Walch, and J. Chaoui are involved in the development of the 3-dimensional software [Glenosys; Imascap] that was used in the present study and are shareholders of Imascap) (<http://links.lww.com/JBJS/E547>).

TABLE I Recommended CT-Scan Parameters

CT-Scan Parameters	Recommended Values
Slice thickness	<1.0 mm
No. of slices	>200
Field of view	Whole scapula
X,Y resolution	<0.5 mm
Matrix size	512 × 512
kV	140
mA	>300

instability and early component loosening or failure²⁻⁴. Assessment of glenoid version and inclination in arthritic shoulders is therefore of paramount importance for preoperative planning of glenoid implantation^{5,6}.

Computed tomography (CT) images have become the gold standard to assess retroversion and inclination and to calculate the potential correction needed. The first proposed methods for assessing glenoid version and inclination used 2-dimensional (2D) CT images⁷⁻¹⁴. Several studies have recently shown that 3-dimensional (3D) reconstructions for measurements of glenoid version and inclination were more accurate than standard 2D-CT slices^{15,16}. Although 3D methods avoid measurement inaccuracies attributed to uncorrected 2D images, these techniques need manual or semi-automated reformatting and processing in order to obtain 3D reconstruction of the scapula. Additionally, most of the current methods rely on the individual surgeon and engineers, which potentially introduces uncontrolled variability.

To overcome these problems, we developed automated surgeon-operated image analysis software (Glenosys; Imascap), which provides complete 3D reconstruction of the scapula and humerus and fully automated measurements of 3D glenoid orientation.

The purpose of this study was to use our fully automated method to measure 3D glenoid version and inclination in osteoarthritic shoulders, and to assess validity and reliability in comparison with previously described methods. We

hypothesized that the automated measurements of osteoarthritic shoulders with this novel software would be valid and comparable with those obtained with previously described manual or semi-automated methods.

Materials and Methods

This study was approved by the Institutional Review Board of the Ethical Committee of Hôpital Privé Jean Mermoz, Lyon, France (No. 2016-03).

Sample Size

An a priori power analysis was performed to determine the sample size needed for a paired-means comparison. Type-1 and type-2 errors were set at 0.05 and 0.20, respectively. We considered a mean difference (and standard deviation) of $5^\circ \pm 13^\circ$ between measurements to be acceptable¹⁷. Using MedCalc software (version 12.7), we calculated that the minimum required sample size to allow comparison was 55 patients.

Study Cohort

A CT scan of the shoulder was obtained for 63 patients with glenohumeral osteoarthritis scheduled for shoulder replacement by the 2 senior authors (G.W. and P.B.). Three patients with inadequate CT scans (low-resolution images and/or a truncated scapula) were excluded from the study, leaving 60 patients. The mean patient age was 66 ± 8 years (range, 54 to 76 years). There were 28 men and 32 women. Osteoarthritis was identified on radiographs and on the basis of clinical findings of a painful and restricted range of motion. Patients with previous shoulder surgery, rheumatoid arthritis, a history of glenohumeral trauma, shoulder instability, rotator cuff tears, or infection were excluded. The preoperative CT studies were performed at the discretion of each surgeon as part of his normal preoperative evaluation. According to the classification described by Walch et al.⁵, there were 17 A1, 16 A2, 8 B1, 9 B2, and 10 C glenoids.

CT Image Acquisition

With the patient positioned supine on the CT table, a scan that included the entire scapula was made of each shoulder with

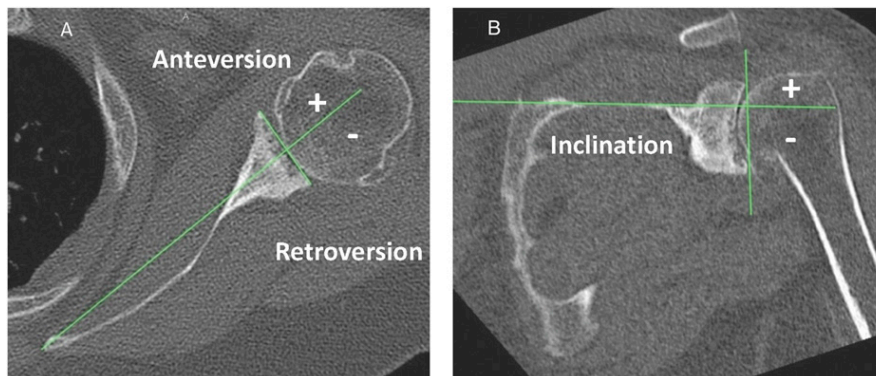


Fig. 1

Two-dimensional measurements of glenoid version on corrected axial slices (according to the modified method of Friedman et al.^{8,20}) (Fig. 1-A) and of glenoid inclination on corrected sagittal slices (according to the method described by Maurer et al.²⁴) (Fig. 1-B).

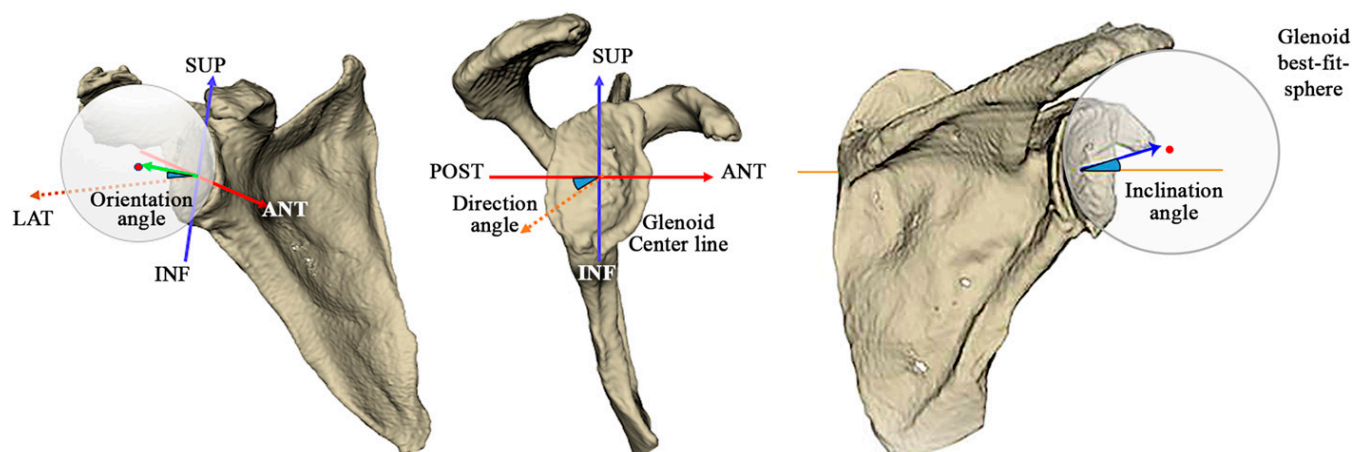


Fig. 2

Methods to measure 3D glenoid version and inclination in an arthritic shoulder with fully automated Glenosys software. SUP = superior, LAT = lateral, INF = inferior, ANT = anterior, and POST = posterior.

a Siemens Somatom CT scanner (Siemens Healthcare). All scans were made with the same acquisition parameters (Table I).

3D Volumetric Reconstruction and Segmentation of the Scapula
Analysis was performed by comparing 2D or 3D measurements obtained with manual segmentation (tracing) with those

obtained with automated segmentation and measurements with our system.

In order to apply the manual measurements, the scapulae were segmented with a semi-automated method using Amira version-5.0 software (Visualization Sciences Group). For each slice, a bone mask was generated using an intensity-based

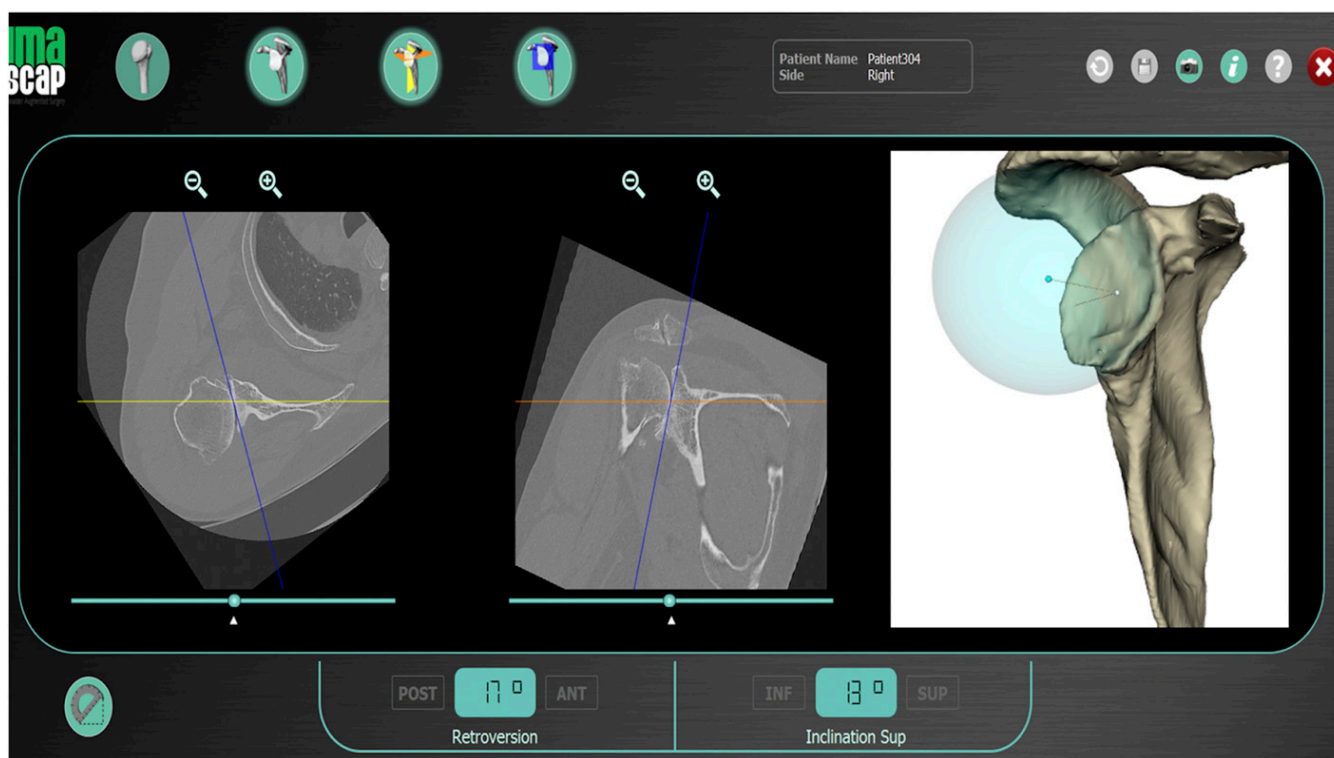


Fig. 3

Screen shot made during preoperative planning for shoulder replacement in an arthritic shoulder with automated 3D measurement of glenoid version and inclination (17° of retroversion and 13° of superior inclination in this case). The 2D axial CT cuts are generated from the 3D images and reformatted perpendicular to the scapular plane, whereas the 2D coronal CT cuts are reformatted parallel to the scapular plane.

TABLE II Glenoid Version and Inclination in Arthritic Shoulders (N = 60) Measured with Glenosys and Previous Methods

	Mean (°)	Standard Deviation (°)	Standard Error (°)	95% Confidence Interval (°)	Minimum (°)	Maximum (°)
Version						
Glenosys	-9.75	12.81	1.65	-13.060, -6.44	-54.0	39.0
Friedman	-7.29	12.81	1.65	-10.60, -3.98	-59.4	44.1
Corrected Friedman	-7.21	12.77	1.61	-10.42, -3.99	-58.7	49.8
Ganapathi-Iannotti	-8.44	14.90	1.88	-12.19, -4.68	-72.8	44.5
Lewis-Armstrong	-7.69	13.47	1.70	-11.08, -4.29	-64.5	40.8
Inclination						
Glenosys	7.28	7.38	0.95	5.38, 9.19	-10.0	22.0
Maurer	7.68	6.61	0.83	6.02, 9.35	-12.1	23.2

thresholding. Manual corrections, if needed, were applied on selected pathologically affected regions prior to 3D reconstruction of the scapula. Three-dimensional segmentation using Glenosys software is fully automated and has been found to be valid and reliable, allowing measurement of angles to be made; the mean error for segmentation using Glenosys software was 0.4 ± 0.09 mm^{18,19}.

2D Measurement of Glenoid Version: Friedman Method

The Friedman version angle²⁰ was measured manually in the 60 scapulae using OsiriX software, version 5.6 32-bit (Pixmeo). The anatomic axis of the scapula (Friedman line) was defined as the line passing through the most medial point of the scapula to the middle of the glenoid fossa on the first axial image inferior to the coracoid process. A second straight line was drawn from the anterior to the posterior edge of the glenoid fossa (intermediate joint line). The glenoid version corresponds to the angle between this joint line and the Friedman line. A positive value was interpreted as anteversion, whereas a negative angle was interpreted as retroversion (Fig. 1).

In the presence of posterior glenoid erosion (a B2 glenoid), 3 different reference lines of the glenoid joint surface can be determined corresponding to the paleoglenoid (native glenoid surface), the neoglenoid (new posterior erosion facet), and the intermediate glenoid (line from anterior to posterior edge)²¹. The intermediate glenoid line takes into account irregularities secondary to posterior erosion. It has been shown that the intermediate line is more reliable for assessing version of glenoids with posterior erosion (B2 glenoids)²¹. The intermediate line also approximates the surface that can be obtained with minimal bone loss after conservative reaming of the glenoid surface²².

3D Measurement of Glenoid Version

CT scans of the scapulae were acquired, and 3D multiplanar reconstruction was performed using the same OsiriX software⁸. The scapular anatomic plane was determined as previously described¹⁰, by manually selecting 3 landmarks on the scapular body: the glenoid center, the intersection of the scapular spine and the medial border, and the most inferior point of the scapular body. Glenoid version was then measured manually

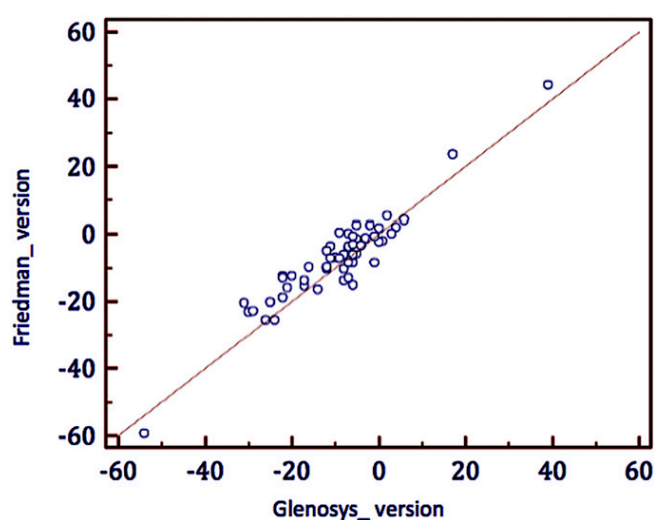


Fig. 4

Fig. 4 Correlation between Glenosys and Friedman version measurements.

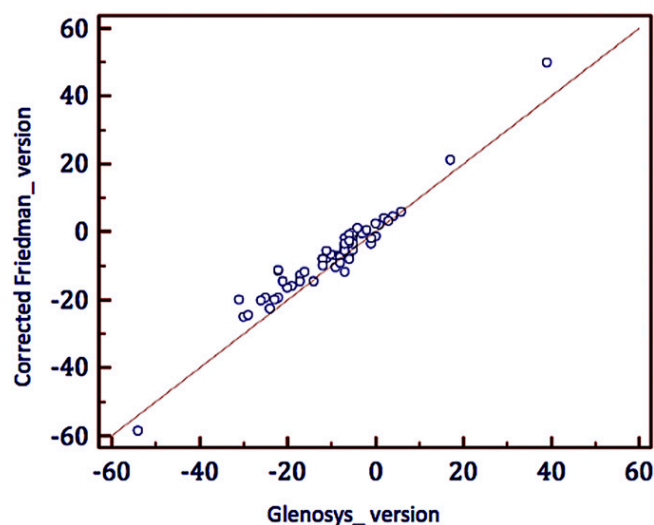


Fig. 5

Fig. 5 Correlation between Glenosys and corrected Friedman version measurements.

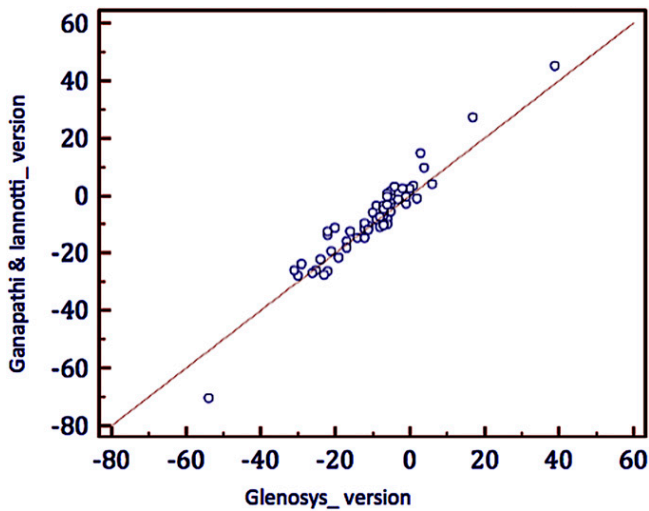


Fig. 6

Fig. 6 Correlation between Glenosys and Ganapathi-Iannotti version measurements.

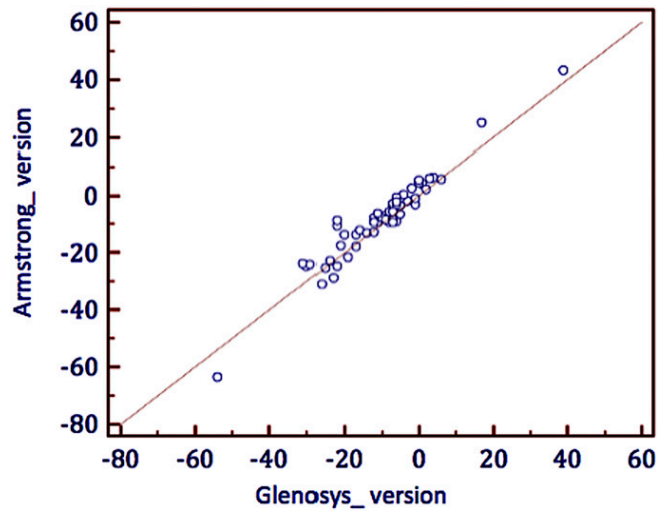


Fig. 7

Fig. 7 Correlation between Glenosys and Lewis-Armstrong version measurements.

with the Friedman method, the Ganapathi-Iannotti method, and the Lewis-Armstrong method^{8,15,16,20}.

Corrected Friedman Method: Manual 3D Version Measurement with 3D Multiplanar Reconstruction

The original CT scan data were reconstructed using OsiriX software to align the coronal and sagittal planes with the superior-inferior axis of the glenoid and the scapular body, respectively. The reconstructed images correct for variation in scapular positioning relative to the original CT axial cuts, which has been shown to cause measurement error^{9,23}. The Friedman angle was measured on the reformatted images in the transverse plane parallel to the supraspinatus fossa line and passing under the tip of the coracoid process.

Ganapathi-Iannotti Method: Manual 3D Version Measurement with 3D Volumetric Reconstruction

We used the glenoid fossa method described by Ganapathi et al.¹⁶ to determine the glenoid plane using 3 points: the superior pole of the glenoid and 2 points anterior and posterior on the inferior third of the glenoid. The scapular plane was defined, as previously described^{15,16}, by 3 points: 1 at the center of the glenoid, a second at the medial border of the scapula where the scapular spine intersects the scapular body, and the third at the inferior tip of the scapula. The glenoid version angle was determined as the angle between the plane of the glenoid fossa and the plane of the scapula.

Lewis-Armstrong Method: Manual 3D Version Measurement with 3D Volumetric Reconstruction

The Lewis-Armstrong method utilizes a best-fit sphere of the humeral head. The radial line connecting the sphere center and the glenoid fossa center point was determined. The glenoid version angle was the angle between the radial line and the scapular plane¹⁵. The scapular plane for this method was the same as in the corrected Friedman method.

Measurement of Glenoid Inclination: Maurer Method

Glenoid inclination was measured using 3D multiplanar reconstruction. According to Maurer et al.²⁴, the inclination angle is defined as the angle between the supraspinatus fossa and glenoid face. The axis passing through the supraspinatus fossa is an accurate landmark with which to assess glenoid inclination (Fig. 1). A positive value is interpreted as superior inclination, whereas a negative value indicates inferior inclination.

3D Measurements of Version and Inclination Using Glenosys Fully Automated Method

The Glenosys software allows automated segmentation of the humerus and scapula, definition of scapular planes, and determination of glenoid version and inclination. The automated method for 3D reconstruction of the scapula defines a reference

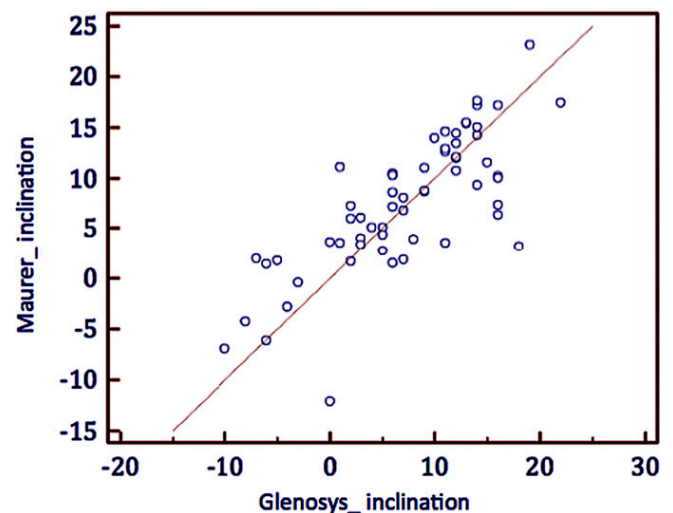


Fig. 8

Correlation between Glenosys and Maurer inclination measurements.

TABLE III Intraobserver and Interobserver Reliability		
	ICC	
	Intraobserver	Interobserver
Version		
Glenosys	1 (automated)	1 (automated)
Friedman	0.984	—
Corrected Friedman	0.982	—
Ganapathi-Iannotti	0.977	0.975
Lewis-Armstrong	0.970	0.970
Inclination		
Glenosys	1 (automated)	1 (automated)
Maurer	0.884	0.895

scapular plane based on all 3D points of the scapular body (the scapular body plane). We have applied skeletonization (a mathematical morphological operation) to extract the central

path of a 3D shape and topology of the scapula. This method preserves the topology of the scapula (i.e., its shape) and provides all of the points within the scapula. Thousands of points were used to find the best-fit plane to the scapular blade including the glenoid area. Only the glenoid articular surface, the coracoid process, and the acromion were excluded from the computation. The curvature of the scapular blade is a common limitation of all previous methods that impacts the orientation plane. The use of a cloud of points of the scapular body reduced the impact of curvature variation.

The same process was applied to define a best-fit sphere of the glenoid surface, using a 3D watershed-based method applied on the 3D scapular model (Fig. 2). This method treats the glenoid as a “catchment basin” and separates it from other anatomic parts. When there was a biconcave glenoid, the spherical fit was an averaged estimation of the best-fit sphere on both neoglenoid and paleoglenoid surfaces. The software excludes osteophytes from axis and version measurements. However, it still provides global 3D representation of the glenoid orientation.

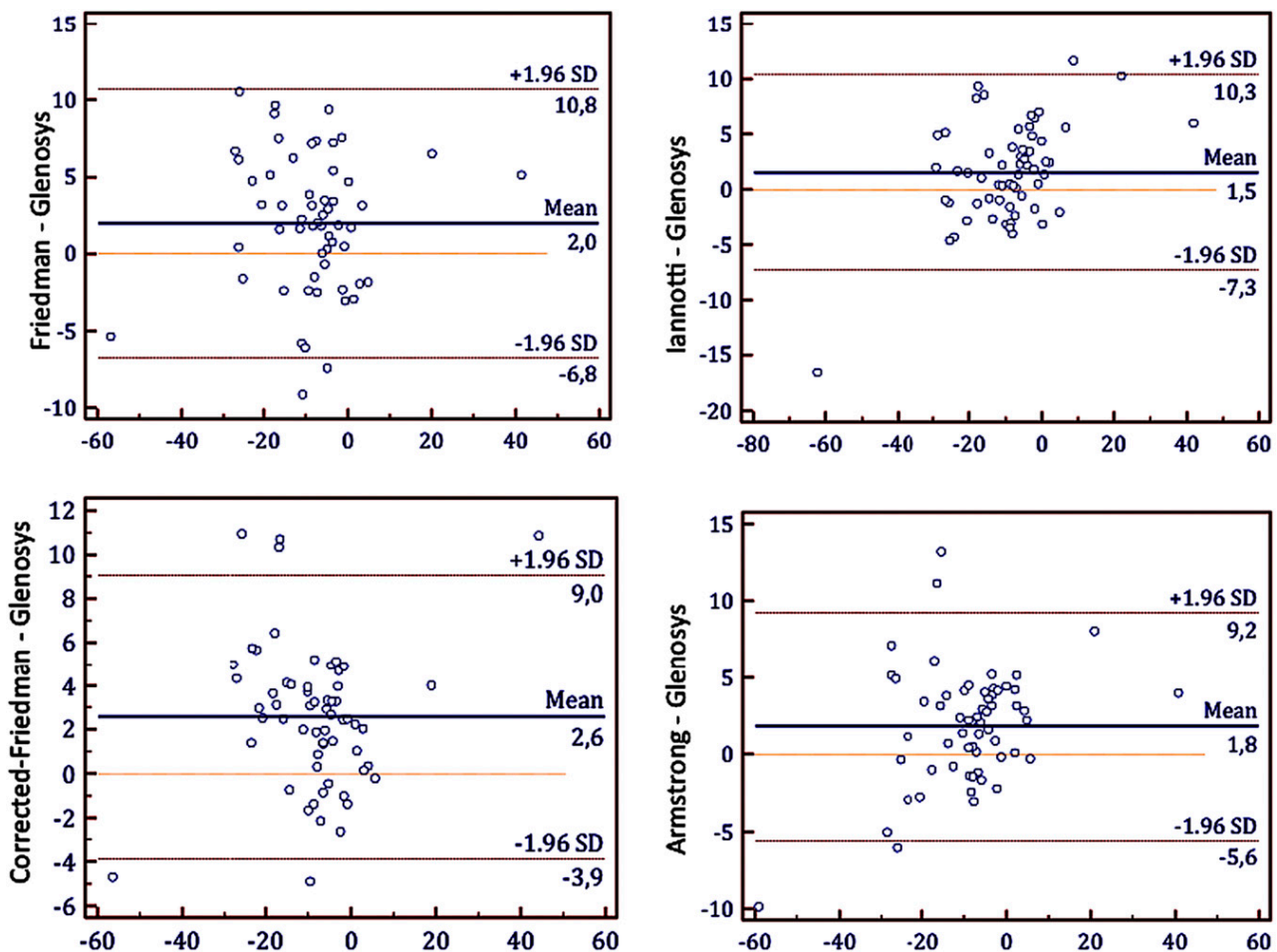


Fig. 9 Analysis with the Bland and Altman method of concordance between the measurements of glenoid version with Glenosys software and those with the other methods. SD = standard deviation.

**TABLE IV Concordance Coefficient Correlation (CCC) Between
Glenosys and Previous Methods**

	CCC	95% Confidence Interval
Version		
Friedman	0.93	0.89, 0.96
Corrected Friedman	0.95	0.92, 0.97
Ganapathi-Iannotti	0.94	0.91, 0.96
Lewis-Armstrong	0.95	0.92, 0.97
Inclination		
Maurer	0.78	0.65, 0.86

The version angle was automatically computed as the angulation between the scapular plane and the glenoid best-fit-sphere centerline projected on the transverse scapular plane. The glenoid centerline was defined as the line connecting the glenoid center and the best-fit-sphere center, where the glenoid center is the centroid of the clouds of points defining the glenoid surface. As the method uses all of the points of the scapula and glenoid, there was no need to manually define any point on the 3D model (Fig. 3).

The inclination was measured on the basis of the transverse line that runs through the supraspinatus fossa between the trigonum scapulae and the middle of the glenoid vault. This line is also detected automatically. To calculate this axis, the program reslices the scapula in the sagittal plane and identifies the intersection point of the 3 branches of the Y shape formed by the coracoid, scapular spine, and scapular body. Then the computer adjusts a best-fit line to these intersection points in order to define the transverse axis. This axis perfectly fits the intersection curve between the scapular spine and the scapular blade. The inclination angle is defined as the angle between the transverse line and the glenoid centerline projected on the scapular plane.

Statistical Analysis

The reproducibility of measurements was verified by determining the intraclass correlation coefficients (ICCs) for 2D and 3D

methods²⁵. The CT images for each subject were presented individually to 2 experienced orthopaedic shoulder surgeons, who measured each image with the 4 manual methods (while blinded to each other's results) for the interobserver analysis. One of the observers also performed the measurements twice more at 1-week intervals for the intraobserver analysis. As the measurements of glenoid version and inclination using Glenosys software are fully automated, no interobserver or intraobserver analysis was needed.

Comparison of Glenosys measurements and those obtained with each manual technique was performed using the concordance coefficient correlation (CCC) with values of ≥ 0.81 indicating almost perfect agreement²⁶. A graphic analysis with the Bland-Altman plot was also used, and the reliability coefficient was then calculated²⁷. Repeated-measures analysis of variance (ANOVA) was used to detect significant differences between the measured angles.

Statistical analysis was performed using MedCalc software (version 12.7). The results were calculated in terms of means (and standard deviations) and percentages. The level of significance was set at 0.05 ($p < 0.05$).

Results

Glenoid Version and Inclination

The mean values for glenoid version and inclination are summarized in Table II. Glenoid version measured with the Glenosys method did not differ significantly from that measured with any of the 4 manual methods, and glenoid inclination measured with the Glenosys method did not differ significantly from that measured with the Maurer method (Figs. 4 through 8). The difference between the overall average 2D and 3D measurements was not significant ($p = 0.45$).

Intraobserver and Interobserver Reliability

Table III shows the intraobserver and interobserver reliability of the methods with which the Glenosys method was compared. The interobserver analysis was performed for the Ganapathi-Iannotti and Lewis-Armstrong methods. Interobserver error analysis revealed no statistical differences between the 2 observers (Fig. 9). All the methods had excellent intraobserver reliability.

TABLE V Analysis of Concordance with Bland and Altman Method*

Methods	Mean Difference (°)	95% CI (°)	SD (°)	Reliability Coefficient (1.96 SD) (°)
Version				
Friedman	2.0	0.8, 3.2	4.5	—
Corrected Friedman	2.5	1.7, 3.4	3.2	—
Ganapathi-Iannotti	1.5	0.3, 2.7	4.5	8.8
Lewis-Armstrong	1.8	0.8, 2.8	3.8	7.4
Inclination	0.2	-1, 1.5	4.7	9.25

*SD = standard deviation, and CI = confidence interval.

Concordance of Measurements with the Fully Automated Software

Concordance of measurements made with the Glensys software and other methods demonstrated almost perfect agreement for glenoid version and very good agreement for inclination (Table IV).

Analysis of concordance with the Bland and Altman method²⁷ demonstrated reliability of the Glensys measurements of glenoid version and inclination compared with the measurements made with the other methods (Table V).

Discussion

Assessment of glenoid version and inclination in arthritic shoulders is of paramount importance for preoperative planning of prosthetic glenoid implantation. In 2 previous in vitro studies, we demonstrated excellent reliability and reproducibility of glenoid measurements made with novel fully automated software in non-arthritic cadaveric scapulae^{18,19}. The purpose of the present study was to measure 3D glenoid version and inclination in osteoarthritic shoulders with this automated method and to compare these measurements with those obtained with previously described manual 2D and 3D methods. In this way, we sought to investigate the clinical potential for replacing manual segmentation, landmarking, and version and inclination measurement with an automated technique.

The analysis of the data confirmed our hypothesis that the use of fully automated 3D imaging software to measure glenoid version and inclination in arthritic shoulders is valid and accurate when compared with previously described manual or semi-automated methods. Our results for glenoid retroversion and inclination of the arthritic shoulder were also similar to those published in the literature^{8,11,12,20,23,28}. The fully automated method is at least as accurate as the previously proposed manual or semi-automated methods. The reliability and reproducibility of glenoid measurements with this fully automated software, previously demonstrated in in vitro studies of non-arthritic scapulae^{18,19}, were confirmed in the present in vivo study of arthritic shoulders. The automated method eliminates interobserver and intraobserver discrepancies, takes into account osteophytes, and is a useful tool in preoperative planning for shoulder replacement²⁹. Preoperative planning with automated software allows surgeons to anticipate the intraoperative technical challenges of shoulder arthroplasty, to anticipate the type of implant to be used (standard, augmented, or reverse glenoid implant), and ultimately to improve the accuracy of the placement and thus the long-term survival of the glenoid implant.

Using standardized CT studies of the arthritic shoulder, our software allows rapid and automated segmentation of the scapula, determination of the reference planes, and 3D measurements of version and inclination of the pathologically altered glenoid surface^{18,19}. The 3D fully automated Glensys software offers several potential advantages: (1) it

is time-saving for the surgeon since there is no need for preliminary manual segmentation of the scapula (third-party intervention) to define the coordinate system prior to making measurements and no need to correct the position of the scapula to be aligned in the coronal, sagittal, and axial planes; (2) it is independent of the surgeon's experience to select reference points, determine scapular and glenoid planes, or determine the best-fit sphere; (3) the preoperative planning can be done independently by the surgeon; and (4) the software is free.

The reliability of the reference planes defined with the automated method can be questioned^{18,19,29}. With traditional 2D and 3D methods, the coronal and transverse scapular planes are based on manual positioning of 3 points (glenoid center, most inferior point, and intersection between the spine and the medial border of the scapula), whereas the glenoid plane is determined by positioning 3 points on the glenoid rim or by applying the best-fit sphere^{8,10-12,15,16,30}. With the automated software, calculation of the reference planes is based on thousands of 3D points on the scapular body, and the glenoid plane is determined through automated application of the best-fit sphere on the glenoid surface. The present study shows that such robust methodology is at least equivalent to the previously published 2D and 3D methods^{1,29}.

There are several limitations of this study. The manual methodology used in the 2D and 3D manual methods may have introduced inaccuracy. However, the observers registered the specific reference points according to recommendations of the developers of the 3D manual methods. To validate these 3D manual methods, we performed a reproducibility analysis of the registration procedure and the intraobserver and interobserver reproducibility for this process was very high (R1/4 = 0.99 and 0.99, respectively). Although our new automated method differs from other 2D or 3D computer planning methods, it is potentially useful for defining reliable measurements because there is no sensitivity to anatomic landmark definition. Finally, although it is accepted that excessive uncorrected retroversion and inclination are detrimental to the biomechanics and survivorship of anatomic shoulder arthroplasty implants, there is a lot that we do not know about scapular and glenoid position and glenohumeral kinematics that is not accounted for in this study. Nevertheless, the use of the automated software for preoperative planning could avoid major errors in implant placement and orientation in shoulder arthroplasty, especially for tier-2 and 3 surgeons who have less surgical experience and a lower volume.

In conclusion, automated measurement of 3D glenoid inclination and version on standard CT images of osteoarthritic shoulders is valid, with excellent correlation to previously proposed 2D and 3D manual or semi-automated methods. The automated method eliminates surgeon interobserver and intraobserver discrepancies and facilitates and improves the accuracy of preoperative planning for shoulder replacement. The automated 3D software is accurate, reliable,

time-saving, and independent of the surgeon's experience to select specific landmarks or determine reference planes. With knowledge of the 3D inclination and retroversion of arthritic shoulders, the surgeon can anticipate reorientation and positioning of the glenoid component in shoulder arthroplasty ("trial without error"). ■

Pascal Boileau, MD, PhD¹
Damien Cheval, MD²
Marc-Olivier Gauci, MD, MSc¹
Nicolas Holzer, MD, PhD³
Jean Chaoui, PhD⁴
Gilles Walch, MD⁵

¹IULS (Institut Universitaire Locomoteur & du Sport), Hôpital Pasteur 2, University of Nice Sophia-Antipolis, Nice, France

²Department of Orthopaedic Surgery, Centre Hospitalier Intercommunal de Cornouaille, Quimper, France

³Division of Orthopaedics and Trauma Surgery, Department of Surgery, Geneva University Hospitals, Geneva, Switzerland

⁴Telecom Bretagne and Imascap, Brest, France

⁵Centre Orthopédique Santy, Hôpital Privé Jean Mermoz, Lyon, France

E-mail address for P. Boileau: boileau.p@chu-nice.fr

ORCID iD for P. Boileau: [0000-0003-0140-9505](https://orcid.org/0000-0003-0140-9505)

References

- Walch G, Mesiha M, Boileau P, Edwards TB, Lévine C, Moineau G, Young A. Three-dimensional assessment of the dimensions of the osteoarthritic glenoid. *Bone Joint J.* 2013 Oct;95-B(10):1377-82.
- Farron A, Terrier A, Büchler P. Risks of loosening of a prosthetic glenoid implanted in retroversion. *J Shoulder Elbow Surg.* 2006 Jul-Aug;15(4):521-6.
- Shapiro TA, McGarry MH, Gupta R, Lee YS, Lee TQ. Biomechanical effects of glenoid retroversion in total shoulder arthroplasty. *J Shoulder Elbow Surg.* 2007 May-Jun;16(3)(Suppl):S90-5.
- Büchler P, Ramaniraka NA, Rakotomanana LR, Iannotti JP, Farron A. A finite element model of the shoulder: application to the comparison of normal and osteoarthritic joints. *Clin Biomech (Bristol, Avon).* 2002 Nov-Dec;17(9-10):630-9.
- Walch G, Badet R, Boulahia A, Khoury A. Morphologic study of the glenoid in primary glenohumeral osteoarthritis. *J Arthroplasty.* 1999 Sep;14(6):756-60.
- Scalise JJ, Codsi MJ, Brems JJ, Iannotti JP. Inter-rater reliability of an arthritic glenoid morphology classification system. *J Shoulder Elbow Surg.* 2008 Jul-Aug;17(4):575-7. Epub 2008 Apr 28.
- Friedman RJ, Hawthorne KB, Genez BM. The use of computerized tomography in the measurement of glenoid version. *J Bone Joint Surg Am.* 1992 Aug;74(7):1032-7.
- Budge MD, Lewis GS, Schaefer E, Coquia S, Flemming DJ, Armstrong AD. Comparison of standard two-dimensional and three-dimensional corrected glenoid version measurements. *J Shoulder Elbow Surg.* 2011 Jun;20(4):577-83. Epub 2011 Feb 16.
- Bokor DJ, O'Sullivan MD, Hazan GJ. Variability of measurement of glenoid version on computed tomography scan. *J Shoulder Elbow Surg.* 1999 Nov-Dec;8(6):595-8.
- Kwon YW, Powell KA, Yum JK, Brems JJ, Iannotti JP. Use of three-dimensional computed tomography for the analysis of the glenoid anatomy. *J Shoulder Elbow Surg.* 2005 Jan-Feb;14(1):85-90.
- Hoenecke HR Jr, Hermida JC, Flores-Hernandez C, D'Lima DD. Accuracy of CT-based measurements of glenoid version for total shoulder arthroplasty. *J Shoulder Elbow Surg.* 2010 Mar;19(2):166-71. Epub 2009 Dec 2.
- Churchill RS, Brems JJ, Kotschi H. Glenoid size, inclination, and version: an anatomic study. *J Shoulder Elbow Surg.* 2001 Jul-Aug;10(4):327-32.
- Nyffeler RW, Jost B, Pfirrmann CWA, Gerber C. Measurement of glenoid version: conventional radiographs versus computed tomography scans. *J Shoulder Elbow Surg.* 2003 Sep-Oct;12(5):493-6.
- Randelli M, Gambrioli PL. Glenohumeral osteometry by computed tomography in normal and unstable shoulders. *Clin Orthop Relat Res.* 1986 Jul;(208):151-6.
- Lewis GS, Armstrong AD. Glenoid spherical orientation and version. *J Shoulder Elbow Surg.* 2011 Jan;20(1):3-11. Epub 2010 Oct 8.
- Ganapathi A, McCarron JA, Chen X, Iannotti JP. Predicting normal glenoid version from the pathologic scapula: a comparison of 4 methods in 2- and 3-dimensional models. *J Shoulder Elbow Surg.* 2011 Mar;20(2):234-44. Epub 2010 Oct 12.
- Hoenecke HR Jr, Tibor LM, D'Lima DD. Glenoid morphology rather than version predicts humeral subluxation: a different perspective on the glenoid in total shoulder arthroplasty. *J Shoulder Elbow Surg.* 2012 Sep;21(9):1136-41. Epub 2011 Nov 12.
- Moineau G, Levigne C, Boileau P, Young A, Walch G. French Society for Shoulder & Elbow (SOFEC). Three-dimensional measurement method of arthritic glenoid cavity morphology: feasibility and reproducibility. *Orthop Traumatol Surg Res.* 2012 Oct;98(6)(Suppl):S139-45. Epub 2012 Sep 7.
- Walch G, Vezeridis PS, Boileau P, Deransart P, Chaoui J. Three-dimensional planning and use of patient-specific guides improve glenoid component position: an in vitro study. *J Shoulder Elbow Surg.* 2015 Feb;24(2):302-9. Epub 2014 Aug 31.
- Friedman RJ. Glenohumeral translation after total shoulder arthroplasty. *J Shoulder Elbow Surg.* 1992 Nov;1(6):312-6. Epub 2009 Feb 19.
- Rouleau DM, Kidder JF, Pons-Villanueva J, Dynamidis S, Defranco M, Walch G. Glenoid version: how to measure it? Validity of different methods in two-dimensional computed tomography scans. *J Shoulder Elbow Surg.* 2010 Dec;19(8):1230-7. Epub 2010 May 10.
- Denard PJ, Walch G. Current concepts in the surgical management of primary glenohumeral arthritis with a biconcave glenoid. *J Shoulder Elbow Surg.* 2013 Nov;22(11):1589-98. Epub 2013 Sep 3.
- Bryce CD, Davison AC, Lewis GS, Wang L, Flemming DJ, Armstrong AD. Two-dimensional glenoid version measurements vary with coronal and sagittal scapular rotation. *J Bone Joint Surg Am.* 2010 Mar;92(3):692-9.
- Maurer A, Fucentese SF, Pfirrmann CWA, Wirth SH, Djahangiri A, Jost B, Gerber C. Assessment of glenoid inclination on routine clinical radiographs and computed tomography examinations of the shoulder. *J Shoulder Elbow Surg.* 2012 Aug;21(8):1096-103. Epub 2011 Oct 29.
- Shrout PE, Fleiss JL. Intraclass correlations: uses in assessing rater reliability. *Psychol Bull.* 1979 Mar;86(2):420-8.
- Lin LIK. A concordance correlation coefficient to evaluate reproducibility. *Biometrics.* 1989 Mar;45(1):255-68.
- Bland JM, Altman DG. Statistical methods for assessing agreement between two methods of clinical measurement. *Lancet.* 1986 Feb 8;1(8476):307-10.
- Merrill A, Guzman K, Miller SL. Gender differences in glenoid anatomy: an anatomic study. *Surg Radiol Anat.* 2009 Mar;31(3):183-9. Epub 2008 Oct 21.
- Gauci MO, Boileau P, Baba M, Chaoui J, Walch G. Patient-specific glenoid guides provide accuracy and reproducibility in total shoulder arthroplasty. *Bone Joint J.* 2016 Aug;98-B(8):1080-5.
- Scalise JJ, Codsi MJ, Bryan J, Iannotti JP. The three-dimensional glenoid vault model can estimate normal glenoid version in osteoarthritis. *J Shoulder Elbow Surg.* 2008 May-Jun;17(3):487-91. Epub 2008 Feb 20.



A modification to the Walch classification of the glenoid in primary glenohumeral osteoarthritis using three-dimensional imaging



Michael J. Bercik, MD^{a,*}, Kevin Kruse II, MD^b, Matthew Yalizis, MBBS, FRACS^c,
Marc-Olivier Gauci, MD, MSc^d, Jean Chaoui, PhD^e, Gilles Walch, MD^f

^aLancaster Orthopedic Group, Lancaster, PA, USA

^bTexas Orthopaedic Associates, Dallas, TX, USA

^cSydney Shoulder and Elbow Specialists, Ramsgate, NSW, Australia

^dDepartment of Orthopaedic and Sport Surgery, University Institute of Locomotion and Sports, Pasteur 2 Hospital, Nice, France

^eTelecom Bretagne, Plouzané, France

^fCentre Orthopédique Santy, Lyon, France

Background: Since Walch and colleagues originally classified glenoid morphology in the setting of glenohumeral osteoarthritis, several authors have reported varying levels of interobserver and intraobserver reliability. We propose several modifications to the Walch classification that we hypothesize will increase interobserver and intraobserver reliability.

Methods: We propose the addition of the B3 and D glenoids and a more precise definition of the A2 glenoid. The B3 glenoid is monoconcave and worn preferentially in its posterior aspect, leading to pathologic retroversion of at least 15° or subluxation of 70%, or both. The D glenoid is defined by glenoid anteversion or anterior humeral head subluxation. The A2 glenoid has a line connecting the anterior and posterior native glenoid rims that transects the humeral head. Using 3-dimensional computed tomography glenoid reconstructions, 3 evaluators used the original Walch classification and the modified Walch classification to classify 129 nonconsecutive glenoids on 4 separate occasions. Reliabilities were assessed by calculating κ coefficients.

Results: Interobserver reliabilities improved from an average of 0.391 (indicating fair agreement) using the original classification to an average of 0.703 (substantial agreement) using the modified classification. Intraobserver reliabilities improved from an average of 0.605 (moderate agreement) to an average of 0.882 (nearly perfect agreement).

Conclusion: When 3-dimensional glenoid reconstructions and the modified Walch classification described herein are used, improved interobserver and intraobserver reliabilities are obtained.

Level of evidence: Basic Science Study; Development or Validation of Classification System
© 2016 Journal of Shoulder and Elbow Surgery Board of Trustees. All rights reserved.

Keywords: Shoulder; arthroplasty; reverse arthroplasty; Walch classification; glenoid; idiopathic arthritis

The Ethical Committee and Institutional Review Board at Hôpital Privé Jean Mermoz and the Centre Orthopédique Santy approved this study (Ref. Study 2015-16).

*Reprint requests: Michael J. Bercik, MD, Lancaster Orthopedic Group, 231 Granite Run Dr, Lancaster, PA 17601, USA.

E-mail address: michaelbercik@gmail.com (M.J. Bercik).

Walch et al¹⁹ previously developed a classification system to describe glenoid morphology in cases of primary glenohumeral osteoarthritis. Since that classification system was first presented, several authors have commented on the interobserver and intraobserver reliability of the classification, with varying results.^{10,15,17} Most critical were Scalise et al,¹⁷ who reported only fair agreement for interobserver and intraobserver assessments.

The original classification and subsequent reviews were limited in several ways. First, they used traditional 2-dimensional (2D) computed tomography (CT) scans, which have since been found to portray glenoid version less reliably than 3D reconstructions that analyze the scapula as a free body.^{1,3,12,18} These 3D reconstructions provide corrected axial 2D images that are strictly in the plane of the scapula, regardless of patient orientation, allowing for more accurate assessments of version and subluxation.

Second, glenoid morphologies not described in the original classification have since been identified and characterized.

Finally, a translational error from the original report that defines the C glenoid as one with 25° of retroversion “regardless of erosion,” has caused some misuse of that categorization; a more precise definition of the C glenoid would be one of 25° of retroversion “not caused by erosion.” This has caused erroneous labelling of B2 glenoids as C glenoids despite the presence of biconcavity or the absence of dysplasia, or both.

The goal of this report is to present several modifications to the original Walch classification system to enable more accurate and reliable description of glenoid morphology. We hypothesize that these modifications to the Walch classification system, when using 3D glenoid reconstructions, will lead to improved interobserver and intraobserver agreement.

Materials and methods

The original classification includes 5 categories of glenoid patterns: (1) A1—centered humeral head, minor erosion; (2) A2—centered humeral head, major central glenoid erosion; (3) B1—posterior subluxated head, no bony erosion; (4) B2—posterior subluxated head, posterior erosion with biconcavity of the glenoid; and (5) C—dysplastic glenoid with at least 25° of retroversion regardless of erosion (Fig. 1).¹⁹

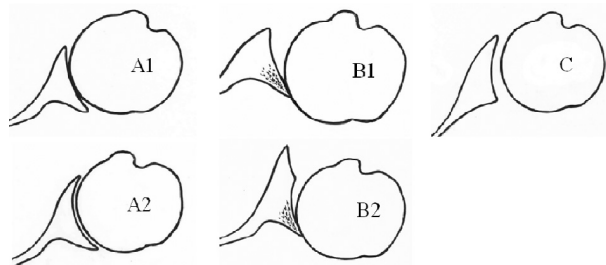


Figure 1 A schematic representation shows the original Walch classification.

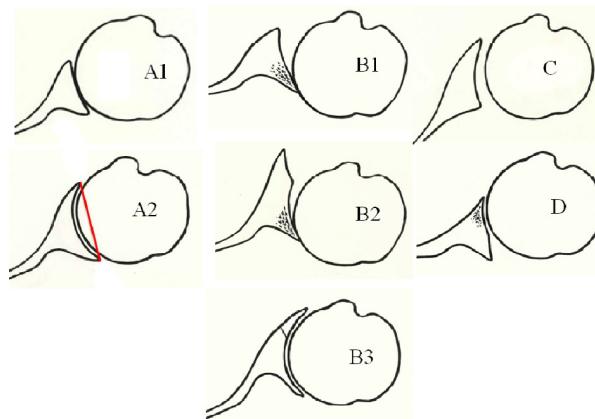


Figure 2 A schematic representation shows the modified classification presented here. Note that a line drawn from the anterior to posterior native glenoid rim transects the humeral head in the A2 glenoid but not in the A1 glenoid.

We propose several modifications to this original classification system (Fig. 2). Specifically, we suggest the addition of the “B3” and “D” glenoids and a more precise definition of the A2 glenoid. We define the B3 glenoid as monoconcave and posteriorly worn, with at least 15° of retroversion or at least 70% posterior humeral head subluxation, or both. The B3 glenoid with posterior subluxation without significant retroversion differs from the B1 by the presence of posterior wear. We define the D glenoid as one with any level of glenoid anteversion or with humeral head subluxation of less than 40% (ie, anterior subluxation).

Lastly, the definition of the A2 glenoid “cupula” is also updated to describe glenoids in which a line drawn from the anterior to posterior rims of the native glenoid transects the humeral head. This is in contrast to the A1 glenoid, in which a line drawn from the anterior to posterior rim of the native glenoid does not transect the humeral head. The definitions of the B1, B2, and C glenoid are unchanged, although we clarify here the C glenoid to be a dysplastic glenoid with at least 25° of retroversion “not caused by erosion.”

The new threshold values for defining the B3 glenoid and D glenoid were determined based on the current literature. We selected 15° or more of retroversion to define the B3 glenoid because studies have shown that eccentric reaming in glenoids with that amount of retroversion does not allow for proper implantation of an anatomic glenoid without perforating the glenoid walls.^{2,6,8,13,14} Posterior subluxation has been described and reported to be a contributor to early glenoid loosening.⁵ We observed that anterior subluxation did not occur in normal shoulders, and thus felt the type D glenoid was also an appropriate addition to the classification. The threshold for anterior subluxation has also been reported.⁵ Consideration was given to defining both D1 and D2 glenoids based on monoconcavity vs. biconcavity, but given the small number of cases, the final decision was made to combine all anteverted or anteriorly subluxated glenoids into one category.

We selected 129 shoulders with primary osteoarthritis scheduled for anatomic or reverse arthroplasty for evaluation. Inclusion criteria were (1) primary osteoarthritis, (2) no previous surgery, (3) inclusion of the entire scapula on the CT scan, which is necessary for conversion to 3D reconstructions, and (4) slice thickness <0.6 mm and slice increments between 0.312 and 0.625 mm, which are requirements of the protocol to obtain the appropriate CT scans.

Exclusion criteria included (1) diagnoses other than primary osteoarthritis (eg, avascular osteonecrosis, rheumatoid arthritis), (2) previous surgery, and (3) shoulders with CT scans that did not meet the described requirements. Of the most common types—A1, A2, B2 and B3—an approximately equal number were obtained. Then, the maximum number of the remaining glenoids that met the inclusion and exclusion criteria was added. The CT scans were blinded and randomized before distribution to 3 evaluators.

The Glenosys software system (Imascap, Brest, France) was used to convert CT scans to 3D reconstructions. This software performs automatic segmentation and full morphologic analysis of the anatomic structure of the bone, creating a 3D model of the scapula and proximal humerus. After reformatting in the plane of the scapula, a 2D series of images is created with computer-calculated estimates of glenoid version and humeral head subluxation. This is performed without any need to manually define points on the model (Fig. 3).

With this system, glenoid version is calculated according to the method described by Friedman et al.⁴ This method of measuring glenoid version has been shown to be more reliable than other methods that are related to the glenoid surface.¹⁶ Humeral head posterior subluxation is measured according to the scapula method, in which the scapular axis is drawn from the medial border of the scapular body to the middle of the glenoid, and the head subluxation is measured relative to that line.¹¹ The Glenosys automation has been described and validated.^{13,20,22} The evaluators could scan the entirety of the glenoid when making their decisions.

Three different evaluators used the Glenosys software system to examine 2D axial CT images reformatted perpendicular to the plane of the scapula first using the original classification. After a 1-week interval, the same evaluators repeated the exercise, but incorporated

the updated A2, B3, and D glenoid criteria. Repeat examinations using the original classification and the modified classification were performed 1 and 2 weeks later, respectively, for a total of 4 categorizations per evaluator. The repeat evaluations permitted an assessment of intraobserver reliability. The 3 evaluators were 3 fellowship-trained shoulder surgeons. Before starting the first series of assessments, the 3 evaluators (M.B., K.K., and M.Y.) and the senior author met to discuss the definitions of the original and modified classification systems. Written detailed explanations were provided to each evaluator to ensure any variabilities were not due to misunderstandings of the classifications.

Statistical analysis was performed using MedCalc Statistical Software 15.11.3 (MedCalc Software bvba, Ostend, Belgium). We calculated κ coefficients for interobserver and intraobserver reliabilities. Two data sets were used: set I—classification with original Walch classification (ie, A1, A2, B1, B2, and C); and set II—classification with modified Walch classification (ie, A1, updated A2, B1, B2, B3, C and D). Conventionally, a κ of 0 to 0.2 indicates slight agreement; 0.21 to 0.4 indicates fair agreement; 0.41 to 0.6 indicates moderate agreement; 0.61 to 0.80 indicates substantial agreement; and ≥ 0.81 indicates nearly perfect agreement.

Results

In set I (ie, the original Walch classification), the interobserver κ value between observer 1 and 2 was 0.446 (moderate agreement), 0.383 (fair agreement) between observer 1 and 3, and 0.345 (fair agreement) between observer 2 and 3. In set II (ie, the modified Walch classification), the interobserver κ value

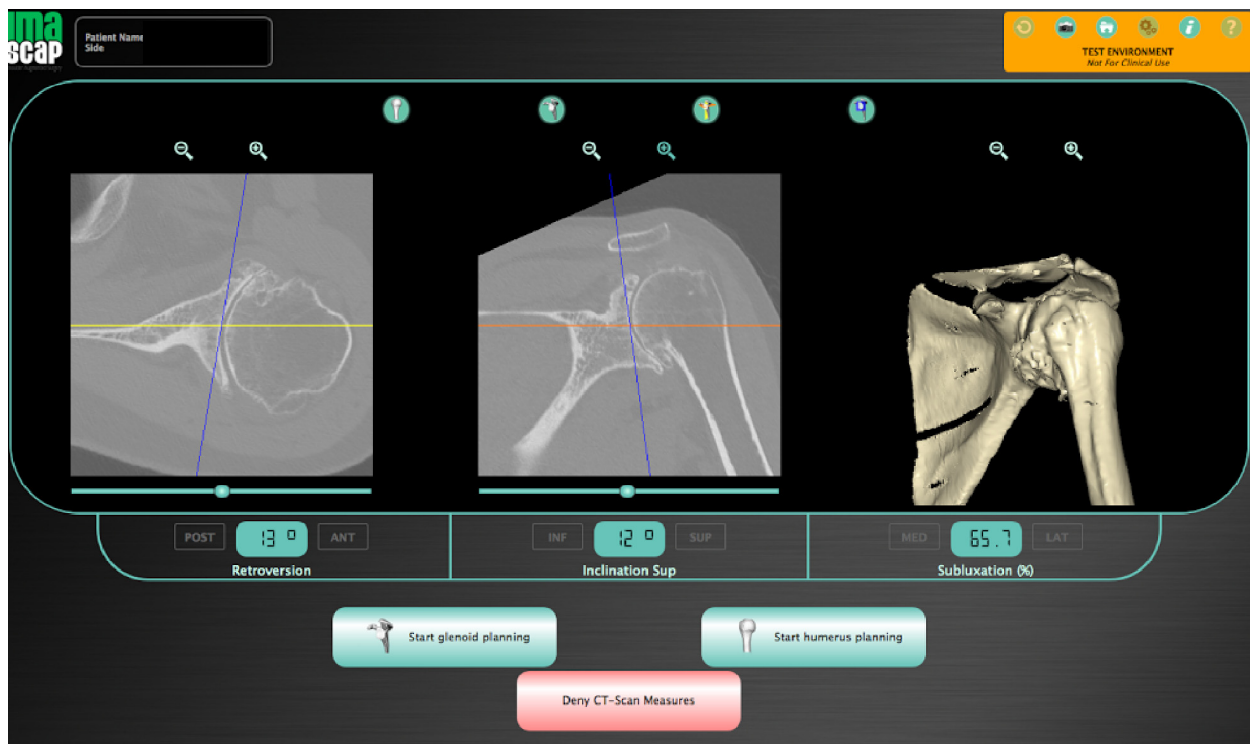


Figure 3 Screenshot of the Glenosys software system (Imascap, Brest, France) demonstrates its ability to provide version and subluxation estimates.

Table I Interobserver reliability

Data set		Observer 1:2	Observer 1:3	Observer 2:3	Average
I	Original Walch classification, κ Agreement	0.446 Moderate	0.383 Fair	0.345 Fair	0.391 Fair
II	Modified Walch classification, κ Agreement	0.776 Substantial	0.662 Substantial	0.671 Substantial	0.703 Substantial

Table II Intraobserver reliability

Data set		Observer 1	Observer 2	Observer 3	Average
I	Original Walch classification, κ Agreement	0.624 Substantial	0.629 Substantial	0.558 Moderate	0.604 Moderate
II	Modified Walch classification, κ Agreement	0.884 Nearly perfect	0.861 Nearly perfect	0.9 Nearly perfect	0.881666667 Nearly perfect

between observer 1 and 2 was 0.776 (substantial agreement), 0.662 (substantial agreement) between observer 1 and 3, and 0.671 (substantial agreement) between observer 2 and 3. The average interobserver κ value was 0.391 (fair agreement) in set I and was 0.703 (substantial agreement) set II (Table I).

The intraobserver κ values for the 3 observers in set I were 0.624, 0.629 and 0.558, with an average value of 0.604. This average value indicates an overall moderate level of agreement. The intraobserver κ values in set II were 0.884, 0.861, and 0.9, with an average value of 0.882. This suggests a nearly perfect average intraobserver agreement (Table II).

In the original classification, there were 32 instances of 129 in which all 3 observers agreed in all assessments. Specifically, they agreed on 16 B2 glenoids, 11 A2 glenoids, 3 B1 glenoids, and 2 C glenoids. With the modified classification system, there were 70 instances of 129 in which all 3 observers agreed in all assessments. They agreed on 21 B3 glenoids, 20 B2 glenoids, 13 A2 glenoids, 12 D glenoids, 3 A1 glenoids, and 1 C glenoid. The observers never agreed on a B1 glenoid entirely in the modified classification systems. A full summary of all evaluations is provided in the Appendix.

Discussion

Walch et al¹⁹ introduced their description of the morphology of arthritic glenoids in 1999. It has since become the most common classification used to describe glenoids in the setting of shoulder replacement. Although a classification system should ideally have good reproducibility among orthopedic surgeons, mixed results have been reported when independently evaluating the Walch classification for interobserver and intraobserver agreement.^{10,15,17} Furthermore, as experience with shoulder replacements has grown, undescribed glenoid morphologies have since been identified that occur with regular frequencies.

Our data reveal improvement in both the intraobserver and interobserver reliability of the Walch classification with the

mentioned modifications when using 3D reconstructions. Of note, in this study we did not compare the reliability of the classifications when using 2D CT scans vs. 3D reconstructions because 3D reconstructions have already been determined to be more reliable.^{1,3,12,18} When using the original classification, our observers had an average interobserver agreement of 0.446, which is “moderate.” This is slightly worse than the results reported by Kidder et al¹⁰ and Nowak et al,¹⁵ who reported interobserver reliabilities of 0.600 and 0.508, respectively, but improved over Scalise et al¹⁷ who reported interobserver reliability of only 0.37. When using the modified Walch classification, our observers had an average κ value of 0.776, which is “substantial” and the best reported thus far.

When our study looked at intraobserver reliability, there was a similar improvement when going from the original Walch classification to the modified one. Again, our results were worse than those of Kidder et al¹⁰ and Nowak et al¹⁵ at 0.604 compared with 0.87 and 0.611, but were better than those reported by Scalise et al¹⁷ at 0.34. After incorporation of the modified criteria, our observers demonstrated an average intraobserver reliability of 0.882. Again, these suggest “substantial” agreement and are the best-reported values among current studies.

The most commonly identified “new” morphology is the B3 concave glenoid with posterior bony wear and severe pathologic retroversion or posterior subluxation, or both. This represents the arthritic glenoid with severe pathologic retroversion and posterior wear without biconcavity that is not caused by dysplasia. We believe the formation of the B3 glenoid occurs via 1 of 2 mechanisms. The B2 glenoid may convert into a B3 as increased erosion completely destroys the paleoglenoid. Alternatively, persistent posterior subluxation may preferentially erode the posterior glenoid, leading to significant retroversion without an interval biconcave period. The development of anterior osteophytes also contributes to the retroverted appearance of the B3 in either situation. This is a problematic morphology to classify using the original Walch classification. Upon review of the reports by Kidder et al,¹⁰ Nowak et al¹⁵ and Scalise et al,¹⁷ it was most likely

inappropriately characterized as a C due to the severe retroversion or as an A2 due to the lack of a biconcave appearance. The modifications to the classification help avoid these potential areas of disagreement.

Accurately and reliably classifying glenoids has important clinical implications. An appreciation for excessive retroversion and posterior bone loss, for example, is necessary because these factors can portend suboptimal outcomes. After monitoring a series of 66 shoulders radiographically and clinically for at least 2 years, Ho et al⁷ showed that preoperative retroversion and postoperative retroversion correlated with increased lucency around the glenoid central peg and higher Lazarus grades of component loosening. Although the clinical importance of osteolysis is still up for debate, Walch et al²¹ reported revision rates of 16.3% in patients who received shoulder arthroplasties in the setting of a biconcave glenoid. Others have determined that higher degrees of retroversion may lead to increased peg perforation.^{2,6,8,14} Having an easily reproducible method of classification aids the surgeon in preoperative planning to recognize potentially troublesome morphologies. Furthermore, a reliable classification system also aids research because a common language among surgeons facilitates the appropriate interpretation of results and comparisons between studies.

The addition of the B3 glenoid to the classification allows the surgeon to differentiate between cases with and without excessive retroversion and humeral head posterior subluxation in a way not possible with the original classification. The future will tell if this is important, as 3D technology provides improved measurements of glenoid version and humeral head subluxation and these values can be correlated to radiographic loosening and clinical outcomes. In our opinion, the D glenoids cannot be treated with standard arthroplasty because they are at greater risk of prosthetic anterior instability. We were unable to find any publications related to anteverted glenoids at the time this report was written, and much research needs to be performed to validate these theories. The improvement of the classification system presented here allows for more accurate comparisons between studies so that this research can be done.

One potential weakness of this report pertains to the reproducibility of these results, because 3D reconstructions are required but have yet to become commonplace and available to all surgeons. We believe, however, that 3D reconstructions will become the standard of care going forward because the benefits of 3D reconstruction are not simply academic but may lead to better clinical results.^{9,22}

Another potential weakness of the study is that the glenoids were evaluated 4 times in 4 weeks. There was concern initially that this could lead to the evaluators remembering certain glenoids and affecting the intrarater results. Although possible, the large number of glenoids included made recall difficult and minimized this bias.

Also, because all classifications were discussed before the study, awareness of the modified classification system could have biased evaluation of the original system. This was done

because discussing the modified system after the first evaluation of the original classification may have diminished the intraobserver reliability of that classification.

Finally, having an unequal amount of each glenoid type potentially skews the results, thereby affecting the validation scores obtained. Lastly, although equal numbers of all classifications would be ideal, this was not the case because some types (eg, the type C and type D) are much less frequent than others. Had we used the maximum number of our least frequent glenoid type as a cutoff, we would have had fewer numbers of comparisons overall. We felt that having a higher number was preferable to have better statistical power of our evaluations.

Conclusion

When 3D reconstructions of the scapula and the modified Walch classification described here are used, improved interobserver and intraobserver reliabilities are obtained. The surgeon should be aware of this classification during his or her preoperative planning because clinical and radiologic results may vary according to the glenoid classification. Further research needs to be completed to determine the specific treatment regimens required for each category and to compare the results of anatomic and reverse shoulder arthroplasty for each type of glenoid.

Disclaimer

Gilles Walch receives personal fees in the form of royalties from Tornier and has equity in Imascap. Neither Tornier nor Imascap provided funding specific to this study. The other authors, their immediate families, and any research foundations with which they are affiliated have not received any financial payments or other benefits from any commercial entity related to the subject of this article.

Supplementary data

Supplementary data to this article can be found online at [doi:10.1016/j.jse.2016.03.010](https://doi.org/10.1016/j.jse.2016.03.010).

References

1. Budge MD, Lewis GS, Schaefer E, Coquia S, Flemming DJ, Armstrong AD. Comparison of standard two-dimensional and three-dimensional corrected glenoid version measurements. *J Shoulder Elbow Surg* 2011;20:577-83. <http://dx.doi.org/10.1016/j.jse.2010.11.003>
2. Clavert P, Millett PJ, Warner JJ. Glenoid resurfacing: what are the limits to asymmetric reaming for posterior erosion? *J Shoulder Elbow Surg* 2007;16:843-8. <http://dx.doi.org/10.1016/j.jse.2007.03.015>
3. Daggett M, Werner B, Gauci MO, Chaoui J, Walch G. Comparison of glenoid inclination angle using different clinical imaging modalities. *J*

- Shoulder Elbow Surg 2016;25:180-5. <http://dx.doi.org/10.1016/j.jse.2015.07.001>
4. Friedman RJ, Hawthorne KB, Genez BM. The use of computerized tomography in the measurement of glenoid version. *J Bone Joint Surg Am* 1992;74:1032-7.
 5. Gerber C, Costouros JG, Sukthankar A, Fucentese SF. Static posterior humeral head subluxation and total shoulder arthroplasty. *J Shoulder Elbow Surg* 2009;18:505-10. <http://dx.doi.org/10.1016/j.jse.2009.03.003>
 6. Gillespie R, Lyons R, Lazarus M. Eccentric reaming in total shoulder arthroplasty: a cadaveric study. *Orthopedics* 2009;31:21. <http://dx.doi.org/10.3928/01477447-20090101-07>
 7. Ho JC, Sabesan VJ, Iannotti JP. Glenoid component retroversion is associated with osteolysis. *J Bone Joint Surg Am* 2013;95:e82. <http://dx.doi.org/10.2106/JBJS.L.00336>
 8. Iannotti JP, Greeson C, Downing D, Sabesan V, Bryan JA. Effect of glenoid deformity on glenoid component placement in primary shoulder arthroplasty. *J Shoulder Elbow Surg* 2012;21:48-55. <http://dx.doi.org/10.1016/j.jse.2011.02.011>
 9. Iannotti JP, Weiner S, Rodriguez E, Subhas N, Patterson TE, Jun BJ, et al. Three-dimensional imaging and templating improve glenoid implant positioning. *J Bone Joint Surg Am* 2015;97:651-8. <http://dx.doi.org/10.2106/JBJS.N.00493>
 10. Kidder JF, Rouleau DM, Defranco MJ, Pons-Villanueva J, Dynamidis S. Revisited: Walch classification of the glenoid in glenohumeral osteoarthritis. *Shoulder Elbow* 2011;4:11-5. <http://dx.doi.org/10.1111/j.1758-5740.2011.00151.x>
 11. Kidder JF, Rouleau DM, Pons-Villanueva J, Dynamidis S, Defranco MJ, Walch G. Humeral head posterior subluxation on CT scan: validation and comparison of 2 methods of measurement. *Tech Shoulder Elbow Surg* 2010;11:72-6. <http://dx.doi.org/10.1097/BTE.0b013e3181e5d742>
 12. Kwon YW, Powell KA, Yum JK, Brems JJ, Iannotti JP. Use of three-dimensional computed tomography for the analysis of the glenoid anatomy. *J Shoulder Elbow Surg* 2005;14:85-90. <http://dx.doi.org/10.1016/j.jse.2004.04.011>
 13. Moineau G, Levigne C, Boileau P, Young A, Walch G. Three-dimensional measurement method of arthritic glenoid cavity morphology: feasibility and reproducibility. *Orthop Traumatol Surg Res* 2012;98(6S):S139-45. <http://dx.doi.org/10.1016/j.otsr.2012.06.007>
 14. Nowak DD, Bahu MJ, Gardner TR, Dyrszka MD, Levine WN, Bigliani LU, et al. Simulation of surgical glenoid resurfacing using three-dimensional computed tomography of the arthritic glenohumeral joint: the amount of glenoid retroversion that can be corrected. *J Shoulder Elbow Surg* 2009;18:680-8. <http://dx.doi.org/10.1016/j.jse.2009.03.019>
 15. Nowak DD, Gardner TR, Bigliani LU, Levine WN, Ahmad CS. Interobserver and intraobserver reliability of the Walch classification in primary glenohumeral arthritis. *J Shoulder Elbow Surg* 2010;19:180-3. <http://dx.doi.org/10.1016/j.jse.2009.08.003>
 16. Rouleau DM, Kidder JF, Pons-Villanueva J, Dynamidis S, Defranco M, Walch G. Glenoid version: how to measure it? Validity of different methods in two-dimensional computed tomography scans. *J Shoulder Elbow Surg* 2010;19:1230-7. <http://dx.doi.org/10.1016/j.jse.2010.01.027>
 17. Scalise JJ, Codsí MJ, Brems JJ, Iannotti JP. Inter-rater reliability of an arthritic glenoid morphology classification system. *J Shoulder Elbow Surg* 2008;17:575-7. <http://dx.doi.org/10.1016/j.jse.2007.12.006>
 18. Scalise JJ, Codsí MJ, Bryan J, Brems JJ, Iannotti JP. The influence of three-dimensional computed tomography images of the shoulder in preoperative planning for total shoulder arthroplasty. *J Bone Joint Surg Am* 2008;90:2438-45. <http://dx.doi.org/10.2106/JBJS.G.01341>
 19. Walch G, Badet R, Boulahia A, Khoury A. Morphologic study of the glenoid in primary glenohumeral osteoarthritis. *J Arthroplasty* 1999;14:756-60.
 20. Walch G, Mesiha M, Boileau P, Edwards TB, Lévine C, Moineau G, et al. Three-dimensional assessment of the dimensions of the osteoarthritic glenoid. *Bone Joint J* 2013;95B:1377-82. <http://dx.doi.org/10.1302/0301-620X.95B10.32012>
 21. Walch G, Moraga C, Young A, Castellanos-Rosas J. Results of anatomic nonconstrained prosthesis in primary osteoarthritis with biconcave glenoid. *J Shoulder Elbow Surg* 2012;21:1526-33. <http://dx.doi.org/10.1016/j.jse.2011.11.030>
 22. Walch G, Vezeridis PS, Boileau P, Deransart P, Chaoui J. Three-dimensional planning and use of patient-specific guides improve glenoid component position: an in vitro study. *J Shoulder Elbow Surg* 2015;24:302-9. <http://dx.doi.org/10.1016/j.jse.2014.05.029>

TRIDIMENSIONAL GEOMETRY OF THE NORMAL SHOULDER: A SOFTWARE ANALYSIS

Identification of Threshold Pathoanatomic Metrics in Primary Glenohumeral Osteoarthritis



ELSEVIER

**JOURNAL OF
SHOULDER AND
ELBOW
SURGERY**

www.elsevier.com/locate/ymse

ORIGINAL ARTICLE

The reverse shoulder arthroplasty angle: a new measurement of glenoid inclination for reverse shoulder arthroplasty

Pascal Boileau, MD, PhD^{a,*}, Marc-Olivier Gauci, MD^a, Eric R. Wagner, MD^b, Gilles Clowez, MD^a, Jean Chaoui, PhD^c, Mikaël Chelli, MD^a, Gilles Walch, MD^d

^aUniversity Institute of Locomotion & Sport (iULS), Pasteur 2 Hospital, University of Nice-Sophia Antipolis, Nice, France

^bDivision of Upper Extremity Surgery, Department of Orthopaedic Surgery, Emory University, Atlanta, GA, USA

^cImascap, Plouzané, France

^dCentre Médical Santy, Lyon, France

Background: Avoiding superior inclination of the glenoid component in reverse shoulder arthroplasty (RSA) is crucial. We hypothesized that superior inclination was underestimated in RSA. Our purpose was to describe and assess a new measurement of inclination for the inferior portion of the glenoid (where the baseplate rests).

Methods: The study included 47 shoulders with rotator cuff tear arthropathy (mean age, 76 years). The reverse shoulder arthroplasty angle (RSA angle), defined as the angle between the inferior part of the glenoid fossa and the perpendicular to the floor of the supraspinatus, was compared with the global glenoid inclination (β angle or total shoulder arthroplasty [TSA] angle). Measurements were made on plain anteroposterior radiographs and reformatted 2-dimensional (2D) computed tomography (CT) scans by 3 independent observers and compared with 3-dimensional (3D) software (Glenosys) measurements.

Results: The mean RSA angle was $25^\circ \pm 8^\circ$ on plain radiographs, $20^\circ \pm 6^\circ$ on reformatted 2D CT scans, and $21^\circ \pm 5^\circ$ via 3D reconstruction software. The mean TSA angle was on average $10^\circ \pm 5^\circ$ lower than the mean RSA angle ($P < .001$); this difference was observed regardless of the method of measurement (radiographs, 2D CT, or 3D CT) and type of glenoid erosion according to Favard. In Favard type E1 glenoids with central concentric erosion, the difference between the 2 angles was $12^\circ \pm 4^\circ$ ($P < .001$).

Conclusion: The same angle cannot be used to measure glenoid inclination in anatomic and reverse prostheses. The TSA (or β) angle underestimates the superior orientation of the reverse baseplate in RSA. The RSA angle ($20^\circ \pm 5^\circ$) needs to be corrected to achieve neutral inclination of the baseplate (RSA angle = 0°). Surgeons should be aware that E1 glenoids (with central erosion) are at risk for baseplate superior tilt if the RSA angle is not corrected.

The Ethical Committee of the University Institute of Locomotion & Sports (iULS), Pasteur 2 Hospital, Nice, France, approved this study (No. 2017-04).

*Reprint requests: Pascal Boileau, MD, PhD, University Institute of Locomotion & Sports (iULS), Pasteur 2 Hospital, 30, voie Romaine, Nice 06000, France.

E-mail address: boileau.p@chu-nice.fr (P. Boileau).

1058-2746/© 2018 Published by Elsevier Inc. on behalf of Journal of Shoulder and Elbow Surgery Board of Trustees. This is an open access article under the CC BY-NC-ND license (<http://creativecommons.org/licenses/by-nc-nd/4.0/>).
<https://doi.org/10.1016/j.jse.2018.11.074>

Level of evidence: Anatomy Study; Imaging

© 2018 Published by Elsevier Inc. on behalf of Journal of Shoulder and Elbow Surgery Board of Trustees. This is an open access article under the CC BY-NC-ND license (<http://creativecommons.org/licenses/by-nc-nd/4.0/>).

Keywords: Glenoid inclination; superior tilt; reverse shoulder arthroplasty; β angle; RSA angle; BIO-RSA; augmented baseplate

Implantation of a reverse shoulder arthroplasty (RSA) with superior tilt of the baseplate is associated with an increased rate of complications.^{13,16,19,25,29,36} Superior inclination of the baseplate increases the stresses at the implant-bone interface while leading to impingement between the inferior humeral polyethylene insert and scapula pillar,¹³ causing medial polyethylene wear, scapular notching, and eventual glenoid implant loosening.^{16,19,25,29,36} In addition, superior inclination of the baseplate has been shown to be associated with decreased shoulder range of motion.^{23,24} Although there is much debate about the best way to correct this superior glenoid inclination, it is critical to implant the baseplate in at least neutral inclination.^{11,12,25} The optimal position of the reverse baseplate is inferior on the glenoid and without superior tilt, in an attempt to optimize impingement-free range of motion while avoiding scapular notching and glenoid loosening.^{5,6,13,26,31,32,35}

Glenoid inclination, as described by Hughes et al²⁰ and Maurer et al,²⁷ is commonly thought to be the angle between the floor of the supraspinatus fossa and the glenoid fossa line: the β angle. From a surgical standpoint, the β angle is useful when planning the implantation of a total shoulder arthroplasty (TSA), as it represents the global glenoid inclination.^{7,20,27} However, although a TSA glenoid component occupies the entire glenoid, most reverse baseplates are implanted on the lower part of the glenoid surface to provide optimal deltoid tension and avoid inferior scapular impingement.³² Furthermore, although the β angle is appropriate to measure glenoid component inclination in TSA, it is not relevant to the RSA baseplate. In other words, given that each prosthesis (TSA and RSA) has a different position on the glenoid, the assessment of glenoid inclination for each prosthesis should be considered separately (Fig. 1).

Therefore, the purpose of this study was to describe and validate a new method for measuring the inclination relevant to the reverse prosthesis in the inferior half of the glenoid for use in both plain radiography and computed tomography (CT) to avoid superior tilt in RSA. The RSA angle was defined as the angle between a line along the inferior part of the glenoid fossa and a line perpendicular to the floor of the supraspinatus fossa, whereas the TSA angle (or β angle) was defined as the angle between the global glenoid fossa and the perpendicular to the floor of the supraspinatus fossa (Fig. 2). We hypothesized that (1) the RSA angle would reliably and accurately measure the inclination relevant to the reverse prosthesis on plain radiographs and CT scans and (2) preoperative measurement

of glenoid inclination over the entire glenoid surface (TSA angle or β angle) would underestimate the potential superior inclination of the RSA baseplate and, therefore, the amount of correction required for implantation in neutral inclination.

Materials and methods

Patient population

The study included 47 shoulders (47 patients) with a diagnosis of rotator cuff tear arthropathy (CTA). Informed consent was obtained from all patients. The exclusion criteria included CT scans that did not contain the entire scapula before surgery and lack of preoperative radiographs. The mean age was 76 years (range, 50-93 years), with 28 male and 19 female patients. The study included 31 right and 16 left shoulders. The Favard classification,²⁶ as agreed on by 4 shoulder surgeons, included 12 type E0, 12 type E1, 6 type E2, and 17 type E3 glenoids. No patients had type E4 glenoids.

Radiographic parameters

Similarly to the β angle proposed by Maurer et al,²⁷ the supraspinatus fossa line was used as the reference.²⁰ The landmark used for the measurements was based on the sclerotic line of the supraspinatus fossa, visible on plain radiographs and CT scans.²⁷ Positive values of angles represent superior glenoid inclination, whereas negative values represent inferior glenoid inclination.

The TSA angle is relevant to TSA and uses the entire glenoid fossa line,² from the superior aspect of the fossa (T) to the inferior aspect of the fossa (S). This measurement is a modification of the β angle²⁰ designed to obtain a more accurate description of superior inclination. The TSA angle is calculated by the angle between the line from T to S and the line from S to A (Fig. 2, A).

The RSA angle was developed to measure the inclination of the inferior portion of the glenoid, which corresponds to the area in which the glenoid component of an RSA is implanted. On a true anteroposterior (AP) radiograph of the shoulder and on a 2-dimensional (2D) CT scan, the line on the supraspinatus fossa and 3 points were drawn: Point S represents the inferior border of the glenoid, point R represents the intersection of the supraspinatus fossa line with the glenoid surface, and point A represents the vertex of the right triangle created by the line of the supraspinatus fossa and a perpendicular line passing through point S; line RS (inferior surface of the glenoid) is the hypotenuse of the right triangle (Figs. 2, B, 2 C).

Plain radiographs with multiple views were obtained in all the included patients, and the measurements were performed on the true AP image with the beam perpendicular to the

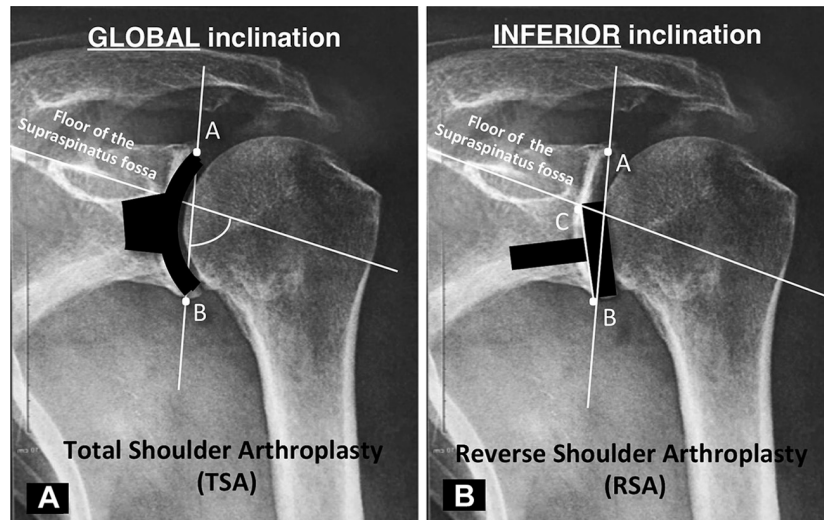


Figure 1 (A) Traditional measurement of glenoid inclination (β angle) considers the entire glenoid fossa and is relevant when planning a total shoulder arthroplasty (TSA). (B) However, because most reverse baseplates are in contact with only the inferior aspect of the glenoid, measurement of the inclination in the inferior half of the glenoid is needed when planning a reverse shoulder arthroplasty (RSA).

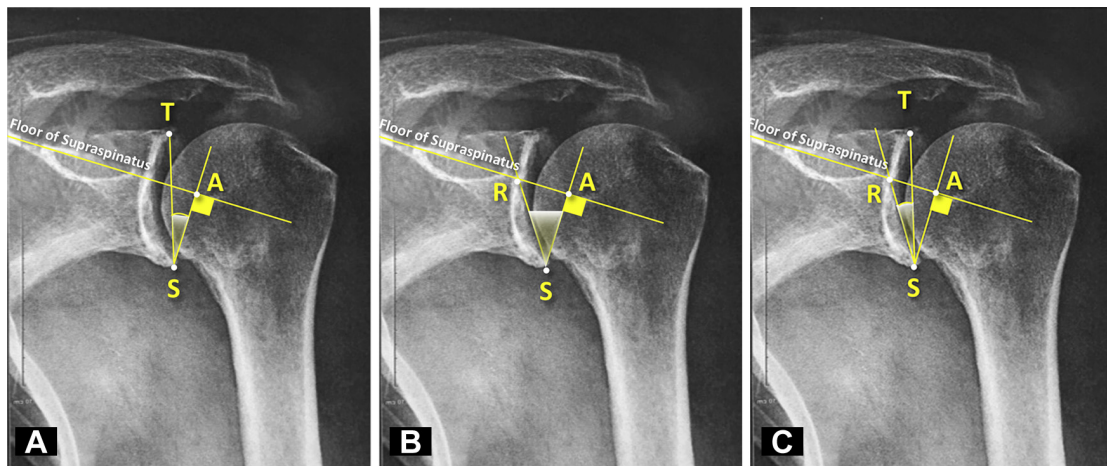


Figure 2 Measurements of total shoulder arthroplasty (TSA) angle (A) and reverse shoulder arthroplasty (RSA) angle (B) on plain anteroposterior radiographs. The RSA angle was defined as the angle between the inferior part of the glenoid fossa and the perpendicular to the floor of the supraspinatus fossa. The TSA angle is a variation of the β angle. The difference between the TSA and RSA angles is represented by the RST angle (C).

glenoid fossa. Two-dimensional CT scans were obtained that included the entire body of the scapula, with coronal views aligned in the plane of the scapula. All native CT scan DICOM (Digital Imaging and Communications in Medicine) series were loaded into 3-dimensional (3D) validated analysis software (Glenosys; Imascap, Plouzané, France). The software provided a fully automatic complete 3D reconstruction of the scapula with automatic measurements of the TSA and RSA angles.^{2,17,38}

Radiographic and CT analysis

The measurement of the RSA and TSA angles on the plain radiographs was performed with a specialized goniometry software

program (OsiriX, version 5.6, 32-bit format; Pixmeo, Bernex, Switzerland). On the 2D CT scans, the angles were measured using this same software in the multiplanar reconstructions in the plane of the scapula on coronal images. Finally, a 3D CT reconstruction software program (Glenosys) was used to automatically detect the plane of the scapular body; it then uses an algorithm to calculate the glenoid inclination according to set parameters.^{2,17,38} To determine this angle, the best-fit sphere model is adjusted to the glenoid surface; then, the angle between the glenoid sphere centerline and the scapular plane is determined and projected onto the scapular body plane.²⁸ The supraspinatus fossa line, defined in 3D as the best-fit line in the deepest part of this fossa, was used as a reference line.³⁷

Three independent observers measured these angles on plain AP radiographs and CT scans. Inter-rater reliability was assessed

by performing the measurements within an interval of 4 weeks. The differences between RSA and TSA angles were then calculated for each glenoid type. These measurements were compared with 3D measurements obtained from previously validated software (Glenosys).

Statistical analysis

The reproducibility of the RSA and TSA angles, measured on radiographs and on 2D CT scans, was analyzed by calculating the intraclass correlation coefficient (ICC) and 95% confidence interval (CI) of the mean difference among 3 observers (M.-O.G., G.C., and M.C.). The ICC and 95% CI were calculated between the 2 analyses performed at 2-week intervals by a single observer (M.-O.G.) to assess the intraobserver reliability. Descriptive statistics were used for the remainder of the analyses. Comparisons between different measurements had a normal distribution and therefore were analyzed for significance using the unpaired Student *t* test. The accuracy of the RSA and TSA angles on radiographs and on 2D CT scans was assessed by comparing these measurements with the automatic 3D measurements, which were considered the gold standard. Statistical significance was set at $P < .05$. All statistical analysis was performed with MedCalc Statistical Software (version 12.0; MedCalc Software, Ostend, Belgium).

Results

Glenoid inclination: TSA angle versus RSA angle

Measurements of glenoid inclination for the TSA angle and RSA angle are presented in Table I. By use of the 2D and 3D measurements, the mean RSA angle was $20^\circ \pm 5^\circ$ (Fig. 3). Regardless of whether the measurements were obtained on plain radiographs, on 2D CT scans, or via 3D CT software reconstruction, the RSA angle was approximately 10° more than the TSA angle ($P < .001$). For both the RSA and TSA angles, plain radiographs estimated approximately 5° higher inclinations than CT scans.

Glenoid inclination: Favard classification

The shoulders were grouped according to the Favard classification.²⁶ The Favard classification describes the most common patterns of glenoid erosion attributed to CTA, with varying degrees of erosion from absent (E0) to central concentric (E1), eccentric superior (E2 and E3), and inferior (E4) erosion. As demonstrated in Tables I and II, TSA angles were on average $10^\circ \pm 5^\circ$ lower than RSA angles ($P < .001$), regardless of the type of glenoid erosion according to the Favard classification. In particular, in Favard type E1 glenoids with central concentric erosion, the difference was $12^\circ \pm 4^\circ$ ($P < .001$). Figure 4 shows 3D measurements of RSA and TSA angles according to glenoid type, whereas Figure 5 demonstrates how a Favard type E1 glenoid (with concentric erosion) is at risk of superior baseplate tilt. The Favard types were similar when

Table I Glenoid inclination measurements for each method (N = 47)

	Radiographs	2D CT	3D CT
TSA angle, °	16 ± 6	11 ± 5	12 ± 6
RSA angle, °	25 ± 8	20 ± 6	20 ± 5
RSA angle – TSA angle, °	9 ± 7	10 ± 3	8 ± 4

2D, 2-dimensional; 3D, 3-dimensional; CT, computed tomography; TSA, total shoulder arthroplasty; RSA, reverse shoulder arthroplasty.

the differences in the angles were compared between plain radiographs and 2D CT scans.

Reproducibility

The interobserver reliability between the various measurements is presented in Table III. Concordance of measurements made by the different observers showed substantial agreement between the plain radiographs and the 2D CT scans for the measures of TSA and RSA angles. The 3D reconstruction software was fully automated. Concordance of measurements made for the intraobserver reliability showed almost perfect agreement, with ICCs of 0.78 (95% CI, 0.75-0.81) for radiographs and 0.86 (95% CI, 0.84-0.86) for 2D CT scans. We found no significant difference in intraobserver or interobserver reliability according to different Favard glenoid types.

Accuracy

The accuracy (compared with the 3D CT reconstructions) of plain radiographs in measuring TSA and RSA angles was 70% and 67%, respectively, whereas the accuracy of 2D CT scans in measuring TSA and RSA angles was 73% and 82%, respectively. We found no significant difference in accuracy according to different Favard glenoid types.

Discussion

Avoiding superior inclination of the glenoid component in RSA is crucial, given its association with the increased risk of component loosening, scapular notching, and decreased range of motion.^{3,26,29,35,40} Whereas traditional measurements of glenoid inclination (β angle or TSA angle) consider the entire glenoid fossa,^{7-9,27} most RSA baseplates are in contact with only the inferior aspect of the glenoid. In this study, we describe and address a new measurement of the inferior portion of the glenoid: the RSA angle (Fig. 2). Our study findings confirm our first hypothesis that this angle provides a reliable and reproducible measure of the inclination of the inferior portion of the native glenoid. By use of 2D and 3D reconstruction software (Glenosys), the average RSA angle was measured to

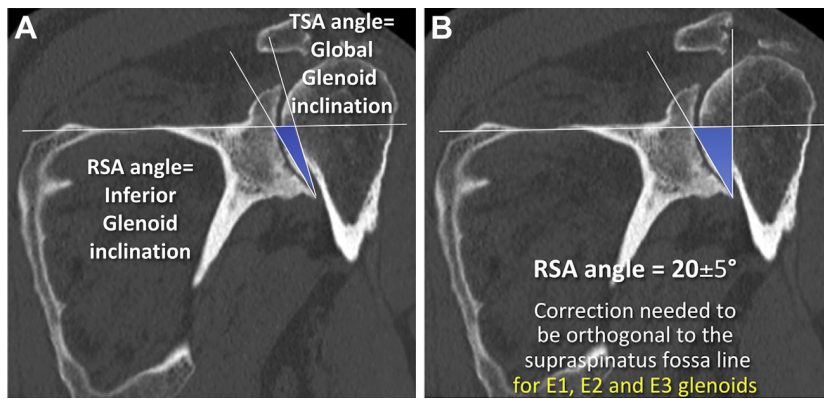


Figure 3 (A) Two-dimensional computed tomography scan cut showing the difference (about 10° on average) between the total shoulder arthroplasty (TSA) and reverse shoulder arthroplasty (RSA) angles. (B) The mean RSA angle, measured on 2- and 3-dimensional computed tomography scans, was $21^\circ \pm 5^\circ$, which represents the angle that needs to be corrected to place the baseplate orthogonal to the supraspinatus fossa line.

Table II Measurements of glenoid TSA and RSA angles by glenoid Favard type: radiographs, CT scans, and 3D CT analysis (N = 47)

Favard type	Radiographs		CT scans		3D CT analysis	
	TSA angle, °	RSA angle, °	TSA angle, °	RSA angle, °	TSA angle, °	RSA angle, °
E0 (n = 12)	11 ± 4 (4 to 18)	20 ± 6 (14 to 28)	8 ± 4 (3 to 15)	16 ± 4 (11 to 25)	8 ± 3 (3 to 14)	16 ± 3 (12 to 20)
E1 (n = 12)	17 ± 4 (11 to 24)	25 ± 11 (-2 to 38)	9 ± 4 (3 to 17)	19 ± 5 (12 to 28)	9 ± 3 (4 to 14)	21 ± 5 (15 to 30)
E2 (n = 6)	23 ± 6 (16 to 33)	27 ± 5 (5 to 20)	19 ± 6 (12 to 29)	28 ± 4 (24 to 36)	22 ± 5 (16 to 27)	26 ± 8 (14 to 39)
E3 (n = 17)	17 ± 6 (11 to 29)	29 ± 7 (21 to 41)	12 ± 5 (4 to 20)	23 ± 4 (12 to 31)	14 ± 3 (9 to 20)	22 ± 4 (14 to 30)

TSA, total shoulder arthroplasty; RSA, reverse shoulder arthroplasty; CT, computed tomography; 3D, 3-dimensional.

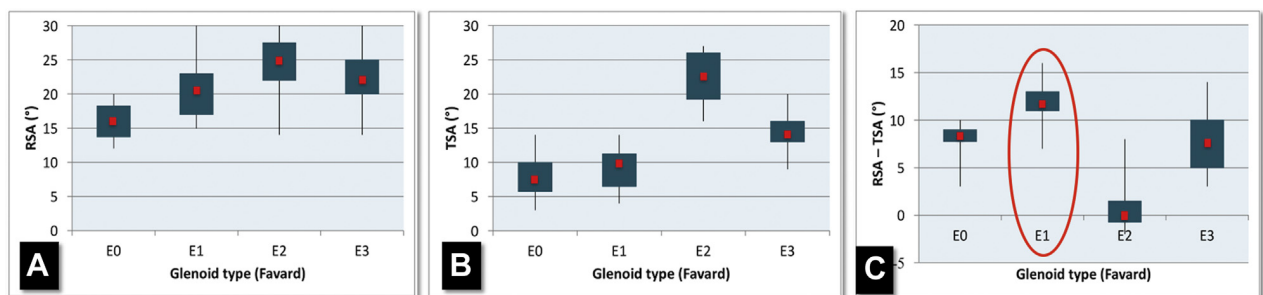


Figure 4 Three-dimensional measurements of RSA angles according to glenoid type (A). Three-dimensional measurements of TSA angles according to glenoid type (B). Three-dimensional measurements of the difference between RSA and TSA angles according to glenoid type (C). Notice the large difference between TSA and RSA angles in E1 glenoids.

be $21^\circ \pm 5^\circ$ in a series of 47 patients with CTA. This implies that when planning preoperatively to perform an RSA procedure in a patient with CTA, between 15° and 25° of superior inclination will need to be corrected to achieve neutral inclination of the baseplate and sphere.

The TSA angle is a modification of the β angle, which provides a measure of the global inclination of the glenoid surface and is useful for planning in TSA. Comparing the RSA and TSA angles, we found that, regardless of the methodology used for measurements (radiographs or 2D or 3D CT scans), the RSA angle consistently measured on average $10^\circ \pm 5^\circ$ more than the TSA angle. In other words, the inclination of the inferior half of the glenoid (where the

reverse prosthesis is optimally implanted) in a patient with CTA is on average 10° superior to the inclination of the entire glenoid fossa. These results confirm our second hypothesis: Preoperative measurement of glenoid inclination over the entire glenoid surface (TSA angle or β angle) underestimates the superior orientation of the reverse baseplate and the amount of correction required in RSA.

The Favard classification describes the most common patterns of glenoid erosion attributed to CTA in the coronal or superior-inferior plane,²⁶ with no erosion (E0) or varying degrees of concentric central (E1), eccentric superior (E2 and E3), and inferior (E4) erosion. We did not find significant differences between different glenoid types

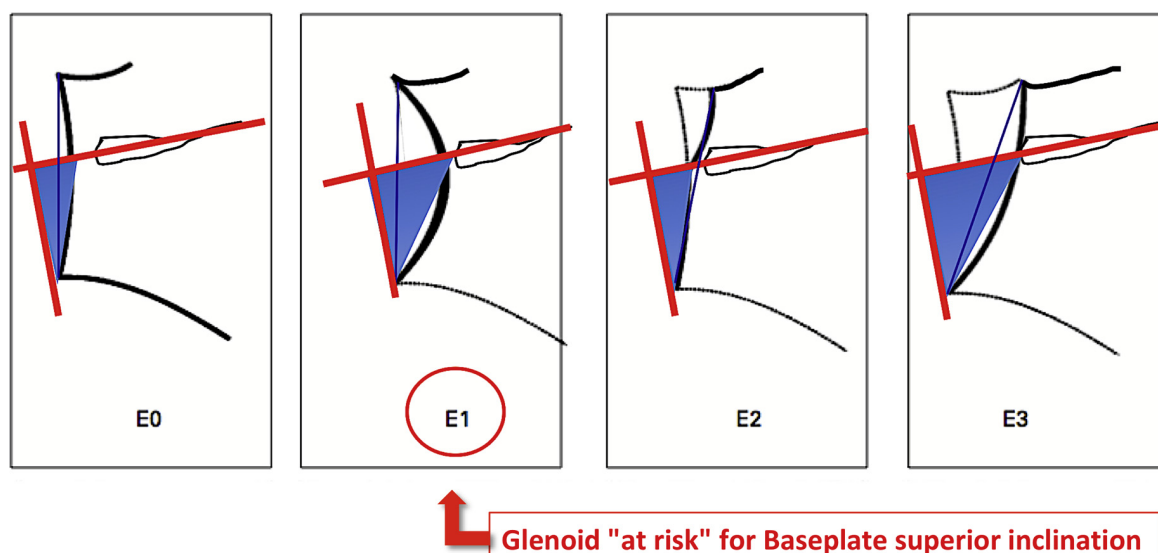


Figure 5 Correction of reverse shoulder arthroplasty angle according to Favard classification. The Favard type E1 glenoid (with concentric erosion) is at risk of superior baseplate tilt and is a trap for the surgeon.

Table III TSA and RSA interobserver analysis from radiographs and CT scan series (N = 47)

	Radiographs		CT scans	
	TSA angle, °	RSA angle, °	TSA angle, °	RSA angle, °
Observer 1				
Mean ± SD	16 ± 6	25 ± 8	11 ± 6	21 ± 6
Range	4 to 33	-2 to 41	3 to 29	11 to 36
Observer 2				
Mean ± SD	13 ± 5	24 ± 7	11 ± 4	23 ± 6
Range	3 to 23	10 to 38	2 to 23	14 to 35
Observer 3				
Mean ± SD	14 ± 5	22 ± 7	11 ± 5	20 ± 7
Range	-3 to 26	2 to 38	0 to 19	1 to 33
ICC (95% CI)	0.59 (0.54 to 0.63)	0.62 (0.58 to 0.65)	0.71 (0.68 to 0.74)	0.75 (0.72 to 0.77)

TSA, total shoulder arthroplasty; RSA, reverse shoulder arthroplasty; CT, computed tomography; SD, standard deviation; ICC, intraclass correlation coefficient; CI, confidence interval.

regarding the RSA angle's measurement on 3D CT scans (Fig. 4). One important note is that even in the absence of glenoid erosion (E0) or presence of central erosion of the glenoid (E1), correction of the RSA angle is required to be able to implant the baseplate in a neutral position. From a surgical standpoint, surgeons should pay particular attention to a central concentric glenoid erosion (Favard type E1), in which the "RSA angle" measures around 20° to 25° and the risk of baseplate implantation with a superior tilt is underestimated when using the TSA (or β) angle.

Although the optimal method to correct superior inclination of the glenoid in RSA is controversial, it is critical to correct it back to neutral and avoid superior tilt of the baseplate.^{11,14,25} The supraspinatus fossa line is a consistent reference line to measure glenoid inclination because the sclerotic line of the supraspinatus fossa line is visible on

true AP radiographs and 2D CT scans. Moreover, from a biomechanical point of view, the supraspinatus fossa line indicates the line of action of the rotator cuff muscles.³⁷ Therefore, the goal of preoperative planning in RSA should be to obtain an RSA angle measurement close to 0° (ie, to implant the baseplate in neutral inclination): In such a configuration, the vectors of the remaining cuff muscles are orthogonal and potentially more efficient.^{15,21,22,37}

Many techniques have been described to correct the superior glenoid inclination when performing an RSA.^{25,31} One of the more common techniques involves eccentric reaming inferiorly (to obtain the subchondral "smiley face"), with an inferiorly angled guide pin. However, correction of a large amount of superior inclination may require reaming of a large amount of native

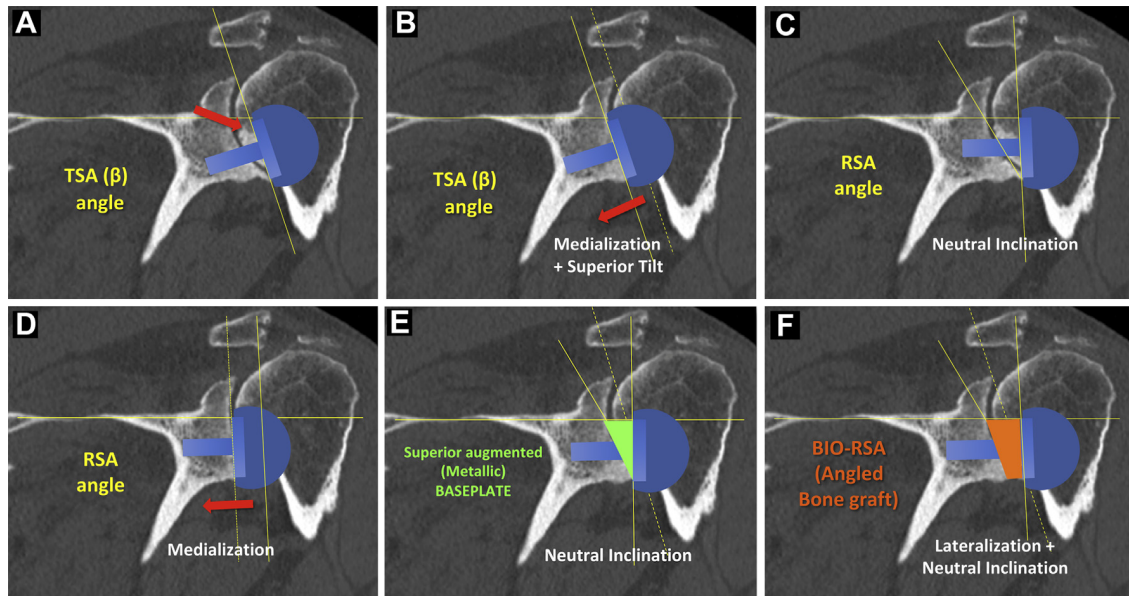


Figure 6 Preoperative 2-dimensional computed tomography templating in a patient with rotator cuff tear arthritis and Favard type E1 glenoid erosion: (A, B) Implantation of the baseplate according to the TSA (β) angle leads to superior tilt of the glenosphere. (C, D) To ensure neutral tilt of the glenoid component (ie, to correct the RSA angle), eccentric inferior reaming of the native glenoid is needed, but this leads to compromise of the bone stock and medialization of the glenosphere. (E, F) Compensating for the superior inclination of the inferior portion of the glenoid with metal (superior augmented metal baseplate) or bone graft allows correction of the RSA angle while avoiding medialization of the glenosphere. TSA, total shoulder arthroplasty; BIO-RSA, bony increased offset-reverse shoulder arthroplasty.

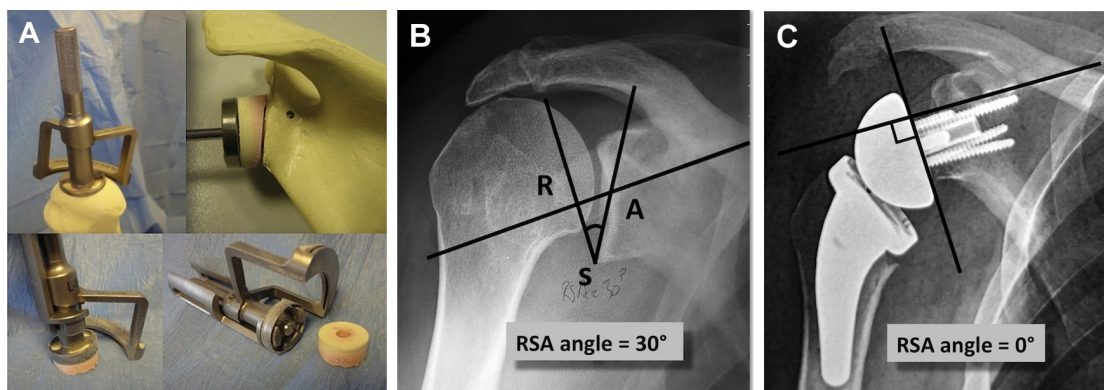


Figure 7 Use of BIO-RSA to lateralize and correct superior glenoid inclination: (A) Asymmetrical inferior reaming combined with an inferiorly angled bone graft, harvested from the humerus with an angled cutting guide, is used to achieve neutral inclination of the baseplate and glenosphere (ie, to correct the RSA angle). (B, C) Preoperative and postoperative radiographs demonstrate correction of the reverse shoulder arthroplasty (RSA) angle with neutral tilt of the baseplate and sphere after angled BIO-RSA.

bone that potentially compromises the bone stock and will medialize the glenoid component. Dilisio et al¹¹ demonstrated that when correcting glenoid superior inclination, the subchondral smile reaming technique or the use of a 10° cannulated guide pin does not correct glenoid inclination reliably. Excessive medialization of the center of rotation (from excessive inferior glenoid reaming) can lead to prosthetic instability, scapular notching, glenoid loosening, and decreased mobility.^{4,5,11} Instead, we suggest the need for component augmentation, including either a superior augmented baseplate^{33,39} or an inferiorly inclined bone

graft.^{4,5,30} In fact, 3 surgical options can be used to correct the superior inclination of the inferior part of the glenoid and obtain neutral inclination of the baseplate (RSA angle, 0°) without medialization of the baseplate: (1) metallic superior augmented baseplate, (2) inferiorly inclined bone graft, or (3) patient-specific baseplate.

In our surgical practice, our preference is to use an angled bone graft harvested from the proximal humerus (BIO-RSA technique) for all cases except when the proximal humerus is not available (humeral head necrosis) or in revision cases in which we use an augmented baseplate or

allograft.^{1,5,6,18,10} Advantages of the BIO-RSA technique include the flexibility to reconstruct multiplanar deformity (inclination and retroversion) and the low morbidity of the “in situ” bone graft harvesting^{4,6,8,34} (Figs. 6 and 7). This technique requires the use of a longer central peg or screw (25-30 mm) to provide full purchase in the glenoid vault and compression of the graft.⁴

Preoperative planning is essential for proper assessment of glenoid erosion and placement of the reverse baseplate tilt. From a surgical standpoint, the RSA angle is useful to ensure a neutral tilt of the glenoid component. By use of 2D or 3D planning, this allows measurement of the thickness and the angle of the bone graft or augmented baseplate needed. One example includes the Blueprint TM (Wright-Tornier) 3D software program, which enables a thorough assessment of glenoid inclination by showing both the global inclination (TSA angle) and the inferior glenoid inclination (RSA angle). This type of preoperative planning software allows the surgeon to anticipate the angulation, dimensions, and shape of the bone graft or metallic augmentation to correct the glenoid inclination and avoid superior tilt of the glenoid component (Fig. 8).

This study’s findings should only be considered in light of its limitations. Although measurements using AP radiographs slightly overestimated glenoid inclination, this was likely secondary to incomplete visualization of the supraspinatus fossa line on some of the radiographs that were cut medially. The small number of patients with each specific Favard subtype limits the ability to perform any subgroup analyses within specific types. Furthermore, although rotator cuff arthropathy is the most common pathology of glenoid erosion, another limitation is that our study was limited to these patients. Future investigations into other pathologies associated with superior inclination are warranted to broaden the clinical translation of these findings. Nonetheless, the results of this study indicate that the RSA angle can be reproducibly used to assess baseplate inclination on both preoperative radiographs and reformatted 2D CT scans or with the help of 3D software. Further prospective clinical investigations will be necessary to determine whether correction of the RSA angle translates into improved outcomes, as well as to determine its role in patient-specific guides or components.

Conclusion

This study demonstrates that (1) preoperative measurement of glenoid inclination over the entire glenoid surface (TSA angle or β angle) underestimates the superior orientation of the reverse baseplate and the amount of correction required and (2) the RSA angle provides a reliable measure of the inclination of the inferior portion of the native glenoid, where the glenoid component is optimally implanted. This angle, which on average is

$20^\circ \pm 5^\circ$ in CTA, needs to be corrected to obtain neutral inclination of the baseplate (RSA angle = 0°). This can be done through inferior glenoid reaming (but at the risk of implant medialization) and/or superior augmentation with bone graft or metal augment. Surgeons should pay particular attention to central concentric glenoid erosion (Favard type E1), as the risk of baseplate implantation with a superior tilt is underestimated with the TSA (or β) angle in these patients.

Acknowledgment

We thank Gregory Gasbarro and Brian Seeto for their help in correcting the manuscript.

Disclaimer

Pascal Boileau and Gilles Walch are paid consultants and receive royalties from Wright-Tornier. Jean Chaoui is an employee of Wright-Tornier. The other authors, their immediate families, and any research foundations with which they are affiliated have not received any financial payments or other benefits from any commercial entity related to the subject of this article.

References

1. Athwal GS, MacDermid JC, Reddy KM, Marsh JP, Faber KJ, Drosdowech D. Does bony increased-offset reverse shoulder arthroplasty decrease scapular notching? *J Shoulder Elbow Surg* 2015;24:468-73. <http://doi.org/10.1016/j.jse.2014.08.015>
2. Boileau P, Cheval D, Gauci M-O, Holzer N, Chaoui J, Walch G. Automated three-dimensional measurement of glenoid version and inclination in arthritic shoulders. *J Bone Joint Surg Am* 2018;100:57-65. <http://doi.org/10.2106/JBJS.16.01122>
3. Boileau P, Melis B, Duperron D, Moineau G, Rumian AP, Han Y. Revision surgery of reverse shoulder arthroplasty. *J Shoulder Elbow Surg* 2013;22:1359-70. <http://doi.org/10.1016/j.jse.2013.02.004>
4. Boileau P, Moineau G, Roussanne Y, O’Shea K. Bony increased-offset reversed shoulder arthroplasty: minimizing scapular impingement while maximizing glenoid fixation. *Clin Orthop Relat Res* 2011;469:2558-67. <http://doi.org/10.1007/s11999-011-1775-4>
5. Boileau P, Morin-Salvo N, Gauci M-O, Seeto BL, Chalmers PN, Holzer N, et al. Angled BIO-RSA (bony-increased offset-reverse shoulder arthroplasty): a solution for the management of glenoid bone loss and erosion. *J Shoulder Elbow Surg* 2017;26:2133-42. <http://doi.org/10.1016/j.jse.2017.05.024>
6. Boileau P, O’Shea K, Moineau G, Roussane Y. Bony increased-offset reverse shoulder arthroplasty (BIO-RSA) for cuff tear arthropathy. *Oper Tech Orthop* 2011;21:69-78. <http://doi.org/10.1053/j.oto.2010.11.003>
7. Churchill RS, Brems JJ, Kotschi H. Glenoid size, inclination, and version: an anatomic study. *J Shoulder Elbow Surg* 2001;10:327-32.
8. Daggett M, Werner B, Collin P, Gauci M-O, Chaoui J, Walch G. Correlation between glenoid inclination and critical shoulder angle: a

- radiographic and computed tomography study. *J Shoulder Elbow Surg* 2015;24:1948-53. <http://doi.org/10.1016/j.jse.2015.07.013>
9. Daggett M, Werner B, Gauci MO, Chaoui J, Walch G. Comparison of glenoid inclination angle using different clinical imaging modalities. *J Shoulder Elbow Surg* 2016;25:180-5. <http://doi.org/10.1016/j.jse.2015.07.001>
 10. de Wilde LF, Poncet D, Middernacht B, Ekelund A. Prosthetic overhang is the most effective way to prevent scapular conflict in a reverse total shoulder prosthesis. *Acta Orthop* 2010;81:719-26. <http://doi.org/10.3109/17453674.2010.538354>
 11. Dilisio MF, Warner JJP, Walch G. Accuracy of the subchondral smile and surface referencing techniques in reverse shoulder arthroplasty. *Orthopedics* 2016;39:e615-20. <http://doi.org/10.3928/01477447-20160610-04>
 12. Edwards TB, Trappey GJ, Riley C, O'Connor DP, Elkousy HA, Gartsman GM. Inferior tilt of the glenoid component does not decrease scapular notching in reverse shoulder arthroplasty: results of a prospective randomized study. *J Shoulder Elbow Surg* 2012;21:641-6. <http://doi.org/10.1016/j.jse.2011.08.057>
 13. Falaise V, Levigne C, Favard L, SOFEC. Scapular notching in reverse shoulder arthroplasties: the influence of glenometaphyseal angle. *Orthop Traumatol Surg Res* 2011;97(Suppl):S131-7. <http://doi.org/10.1016/j.otsr.2011.06.007>
 14. Favard L, Berhouet J, Walch G, Chaoui J, Lévine C. Superior glenoid inclination and glenoid bone loss: definition, assessment, biomechanical consequences, and surgical options. *Orthopade* 2017;46:1015-21. <http://doi.org/10.1007/s00132-017-3496-1>
 15. Flieg NG, Gatti CJ, Doro LC, Langenderfer JE, Carpenter JE, Hughes RE. A stochastic analysis of glenoid inclination angle and superior migration of the humeral head. *Clin Biomech (Bristol, Avon)* 2008;23:554-61. <http://doi.org/10.1016/j.clinbiomech.2008.01.001>
 16. Frankle MA, Teramoto A, Luo Z-P, Levy JC, Pupello D. Glenoid morphology in reverse shoulder arthroplasty: classification and surgical implications. *J Shoulder Elbow Surg* 2009;18:874-85. <http://doi.org/10.1016/j.jse.2009.02.013>
 17. Gauci MO, Boileau P, Baba M, Chaoui J, Walch G. Patient-specific glenoid guides provide accuracy and reproducibility in total shoulder arthroplasty. *Bone Joint J* 2016;98-B:1080-5. <http://doi.org/10.1302/0301-620X.98B8.37257>
 18. Greiner S, Schmidt C, König C, Perka C, Herrmann S. Lateralized reverse shoulder arthroplasty maintains rotational function of the remaining rotator cuff. *Clin Orthop Relat Res* 2013;471:940-6. <http://doi.org/10.1007/s11999-012-2692-x>
 19. Gutiérrez S, Walker M, Willis M, Pupello DR, Frankle MA. Effects of tilt and glenosphere eccentricity on baseplate/bone interface forces in a computational model, validated by a mechanical model, of reverse shoulder arthroplasty. *J Shoulder Elbow Surg* 2011;20:732-9. <http://doi.org/10.1016/j.jse.2010.10.035>
 20. Hughes RE, Bryant CR, Hall JM, Wening J, Huston LJ, Kuhn JE, et al. Glenoid inclination is associated with full-thickness rotator cuff tears. *Clin Orthop Relat Res* 2003;407:86-91.
 21. Kandemir U, Allaire RB, Jolly JT, Debski RE, McMahon PJ. The relationship between the orientation of the glenoid and tears of the rotator cuff. *J Bone Joint Surg Br* 2006;88:1105-9. <http://doi.org/10.1302/0301-620X.88B8.17732>
 22. Konrad GG, Markmiller M, Jolly JT, Ruter AE, Sudkamp NP, McMahon PJ, et al. Decreasing glenoid inclination improves function in shoulders with simulated massive rotator cuff tears. *Clin Biomech (Bristol, Avon)* 2006;21:942-9. <http://doi.org/10.1016/j.clinbiomech.2006.04.013>
 23. Lädermann A, Denard PJ, Boileau P, Farron A, Deransart P, Walch G. What is the best glenoid configuration in onlay reverse shoulder arthroplasty? *Int Orthop* 2018;42:1339-46. <http://doi.org/10.1007/s00264-018-3850-x>
 24. Lädermann A, Gueorguiev B, Charbonnier C, Stimec BV, Fasel JHD, Zderic I, et al. Scapular notching on kinematic simulated range of motion after reverse shoulder arthroplasty is not the result of impingement in adduction. *Medicine (Baltimore)* 2015;94:e1615. <http://doi.org/10.1097/MD.0000000000001615>
 25. Laver L, Garrigues GE. Avoiding superior tilt in reverse shoulder arthroplasty: a review of the literature and technical recommendations. *J Shoulder Elbow Surg* 2014;23:1582-90. <http://doi.org/10.1016/j.jse.2014.06.029>
 26. Lévine C, Boileau P, Favard L, Garaud P, Molé D, Sirveaux F, et al. Scapular notching in reverse shoulder arthroplasty. *J Shoulder Elbow Surg* 2008;17:925-35. <http://doi.org/10.1016/j.jse.2008.02.010>
 27. Maurer A, Fucentese SF, Pfirrmann CWA, Wirth SH, Djahangiri A, Jost B, et al. Assessment of glenoid inclination on routine clinical radiographs and computed tomography examinations of the shoulder. *J Shoulder Elbow Surg* 2012;21:1096-103. <http://doi.org/10.1016/j.jse.2011.07.010>
 28. Moineau G, Levigne C, Boileau P, Young A, Walch G. Three-dimensional measurement method of arthritic glenoid cavity morphology: feasibility and reproducibility. *Orthop Traumatol Surg Res* 2012;98(Suppl):S139-45. <http://doi.org/10.1016/j.otsr.2012.06.007>
 29. Molé D, Wein F, Dézaly C, Valenti P, Sirveaux F. Surgical technique: the anterosuperior approach for reverse shoulder arthroplasty. *Clin Orthop Relat Res* 2011;469:2461-8. <http://doi.org/10.1007/s11999-011-1861-7>
 30. Neyton L, Boileau P, Nové-Josserand L, Edwards TB, Walch G. Glenoid bone grafting with a reverse design prosthesis. *J Shoulder Elbow Surg* 2007;16(3 Suppl):S71-8. <http://doi.org/10.1016/j.jse.2006.02.002>
 31. Nicholson GP, Strauss EJ, Sherman SL. Scapular notching: recognition and strategies to minimize clinical impact. *Clin Orthop Relat Res* 2011;469:2521-30. <http://doi.org/10.1007/s11999-010-1720-y>
 32. Nyffeler RW, Werner CML, Gerber C. Biomechanical relevance of glenoid component positioning in the reverse Delta III total shoulder prosthesis. *J Shoulder Elbow Surg* 2005;14:524-8. <http://doi.org/10.1016/j.jse.2004.09.010>
 33. Roche CP, Stroud NJ, Martin BL, Steiler CA, Flurin P-H, Wright TW, et al. Achieving fixation in glenoids with superior wear using reverse shoulder arthroplasty. *J Shoulder Elbow Surg* 2013;22:1695-701. <http://doi.org/10.1016/j.jse.2013.03.008>
 34. Seidl AJ, Williams GR, Boileau P. Challenges in reverse shoulder arthroplasty: addressing glenoid bone loss. *Orthopedics* 2016;39:14-23. <http://doi.org/10.3928/01477447-20160111-01>
 35. Simovitch RW, Zumstein MA, Lohri E, Helmy N, Gerber C. Predictors of scapular notching in patients managed with the Delta III reverse total shoulder replacement. *J Bone Joint Surg Am* 2007;89:588-600. <http://doi.org/10.2106/JBJS.F.00226>
 36. Sirveaux F, Favard L, Oudet D, Huquet D, Walch G, Molé D. Grammont inverted total shoulder arthroplasty in the treatment of glenohumeral osteoarthritis with massive rupture of the cuff. Results of a multicentre study of 80 shoulders. *J Bone Joint Surg Br* 2004;86:388-95.
 37. Van Haver A, Heylen S, Vuylsteke K, Declercq G, Verborgt O. Reliability analysis of glenoid component inclination measurements on postoperative radiographs and computed tomography-based 3D models in total and reversed shoulder arthroplasty patients. *J Shoulder Elbow Surg* 2016;25:632-40. <http://doi.org/10.1016/j.jse.2015.09.003>
 38. Walch G, Vezeridis PS, Boileau P, Deransart P, Chaoui J. Three-dimensional planning and use of patient-specific guides improve glenoid component position: an in vitro study. *J Shoulder Elbow Surg* 2015;24:302-9. <http://doi.org/10.1016/j.jse.2014.05.029>
 39. Wright TW, Roche CP, Wright L, Flurin P-H, Crosby LA, Zuckerman JD. Reverse shoulder arthroplasty augments for glenoid wear: comparison of posterior augments to superior augments. *Bull Hosp Jt Dis (2013)* 2015;73 Suppl 1:S124-8.
 40. Zumstein MA, Pinedo M, Old J, Boileau P. Problems, complications, reoperations, and revisions in reverse total shoulder arthroplasty: a systematic review. *J Shoulder Elbow Surg* 2011;20:146-57. <http://doi.org/10.1016/j.jse.2010.08.001>

**Can Surgeons Optimize Range Of Motion And Reduce Scapulohumeral Impingements In
Reverse Shoulder Arthroplasty: a Computational Study**



■ SHOULDER AND ELBOW

Patient-specific glenoid guides provide accuracy and reproducibility in total shoulder arthroplasty

M. O. Gauci,
P. Boileau,
M. Baba,
J. Chaoui,
G. Walch

From Centre
Hospitalier
Universitaire de Nice,
Nice, France

■ M. O. Gauci, MD, MSc,
Orthopaedic Surgeon, Institut
Universitaire Locomoteur et du
Sport

■ P. Boileau, MD, Professor,
Institut Universitaire
Locomoteur et du Sport
Hôpital Pasteur 2, 30 Voie
Romaine, Nice, 06000, France.

■ M. Baba, MBBS MSpMed
FRACS(Orth), Orthopaedic
Surgeon
Specialty Orthopaedics,
Sydney, Australia.

■ J. Chaoui, PhD, Associate
Researcher Engineer
Telecom Brittany, 655 Avenue
du Technopole, 29200
Plouzané, France.

■ G. Walch, MD, Orthopaedic
Surgeon
Centre Orthopédique Santy,
Unité EpauLe, 24 Avenue Paul
Santy, 69008 Lyon, France.

Correspondence should be sent
to Dr M. O. Gauci; e-mail:
marc-olivier.gauci@wanadoo.fr

©2016 The British Editorial
Society of Bone & Joint
Surgery
doi:10.1302/0301-620X.98B8.
37257 \$2.00

Bone Joint J
2016;98-B:1080–5.
Received 14 September 2015;
Accepted after revision 8 March
2016

Aims

Patient-specific glenoid guides (PSGs) claim an improvement in accuracy and reproducibility of the positioning of components in total shoulder arthroplasty (TSA). The results have not yet been confirmed in a prospective clinical trial. Our aim was to assess whether the use of PSGs in patients with osteoarthritis of the shoulder would allow accurate and reliable implantation of the glenoid component.

Patients and Methods

A total of 17 patients (three men and 14 women) with a mean age of 71 years (53 to 81) awaiting TSA were enrolled in the study. Pre- and post-operative version and inclination of the glenoid were measured on CT scans, using 3D planning automatic software. During surgery, a congruent 3D-printed PSG was applied onto the glenoid surface, thus determining the entry point and orientation of the central guide wire used for reaming the glenoid and the introduction of the component. Manual segmentation was performed on post-operative CT scans to compare the planned and the actual position of the entry point (mm) and orientation of the component (°).

Results

The mean error in the accuracy of the entry point was -0.1 mm (standard deviation (SD) 1.4) in the horizontal plane, and 0.8 mm (SD 1.3) in the vertical plane. The mean error in the orientation of the glenoid component was 3.4° (SD 5.1°) for version and 1.8° (SD 5.3°) for inclination.

Conclusion

Pre-operative planning with automatic software and the use of PSGs provides accurate and reproducible positioning and orientation of the glenoid component in anatomical TSA.

Cite this article: *Bone Joint J* 2016;98-B:1080–5.

Appropriate positioning of the glenoid component in total shoulder arthroplasty (TSA) is crucial to avoid early loosening. Finite element analyses have shown that there are biomechanical changes that could significantly increase the risk of loosening if it is introduced in > 10° of retroversion.¹

Intra-operatively, no definite reliable landmarks are available to suggest an entry point for the guidewire or appropriate orientation. The accuracy of a surgeon making a visual judgement is to within about 7.5°² and the largest errors in version are seen during drilling and reaming. Moreover, entry point precision accuracy is about 3 mm (standard deviation (SD) 2) in laboratory conditions and this is dependent on the experience of the surgeon.³ This is particularly relevant as retroversion of the glenoid is commonly seen in osteoarthritis.

It has been shown that the surgeon's precision decreases with increasing retroversion.⁴

Low reliability is associated with the use of axillary radiographs, with glenoid retroversion being over-estimated in > 85% of cases.⁵ The measurement of glenoid version using CT scans is inaccurate in the presence of as little as 1° of malalignment of the scapula in the coronal or sagittal plane.⁶ Moreover, minor rotation of the scapula can alter the accuracy of the measurement of glenoid version by up to 10°.⁷

Surgeons can use 3D planning to help determine the correct scapular plane. Manual determination of the anatomical plane of the scapula is time consuming and not suitable for use in clinical practice. The techniques which have been described to assess it use few manually definable landmarks on the scapula.^{8–10} It is also difficult to assess the shape of the

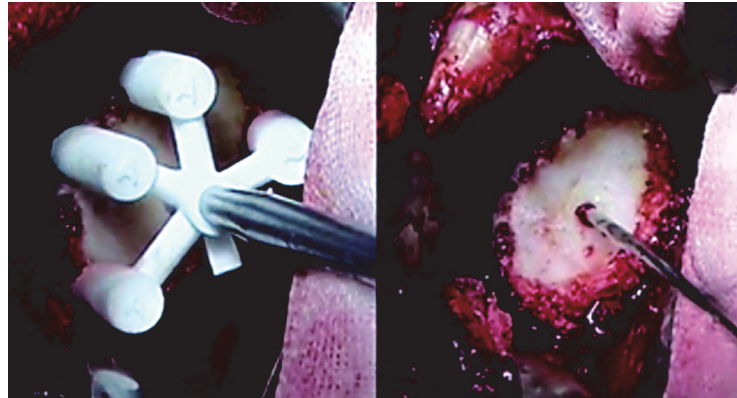


Fig. 1

Intra-operative use of the patient specific instrumentation. All soft tissues and cartilage have been removed from the edge of the glenoid to provide good stability and congruity for placement of the guide.

glenoid intra-operatively in patients with significant loss of glenohumeral joint space, as in osteoarthritis.

The new fully automated pre-operative planning software Glenosys (Imascap, Brest, France) gives reproducible accurate results in the assessment of the shape of the glenoid.^{11,12} There is no need to send Digital Imaging and Communications in Medicine (DICOM) images to a company to be processed. The software provides a complete 3D reconstruction of the scapula and allows measurements of version and inclination of the glenoid, virtual implantation of the glenoid component and generation of a patient-specific guide (PSG) allowing the introduction of a guide wire in the correct position.

In this study, we used 3D CT imaging with novel computer-modelling software in patients awaiting TSA to measure the pre-operative, planned and post-operative version and inclination of the glenoid component. The objectives were to determine the mean error in version and inclination and mean deviation of the position of the entry point of the guide wire in relation to the planned parameters.

Patients and Methods

A total of 17 patients from two centres with osteoarthritis who were awaiting TSA were enrolled into the study. Their demographic details are reported in Table I. CT scans (Siemens Healthcare, Malvern, Pennsylvania) were undertaken with the patient supine and the arm at the side in neutral rotation. The acquisition parameters were 140 kV, bone algorithm, 512 × 512 matrix, slice thickness (Z) < 1.5 mm, resolution (X, Y) < 0.5 mm, 200 mm to 300 mm field of view to visualise the entire scapula, particularly the most inferomedial aspect.

Glenosys software was used for pre-operative planning. The different steps of its segmentation have been previously described.^{12,13} The glenoid Walch type¹⁴ and the automatically measured native glenoid version and inclination were noticed by one of the authors (MOG). The two senior

surgeons (GW: centre 1; PB: centre 2) planned the type and position of the keeled glenoid component which was to be used from the native DICOM series. The PSG for preparation of the glenoid was then ordered. The virtual models of the glenoid and the guide were transmitted to Tornier (SAS, Montbonnot, France) as a Standard Tessellation Language (STL) file for 3D printing. The planning had to be undertaken ten working days before the day of surgery.

In total, two 3D-printed components (Tornier SAS, Montbonnot, France) with natural polyamide PA2200 resin (EOSINT P380 selective laser sintering machine; EOS GmbH, Krailling, Germany) were received and sterilised prior to surgery.

The PSG has a four-pin peripheral support, allowing the surgeon to introduce it onto the glenoid with stability. It has a central hole, through which a 2.5 mm titanium guide wire is introduced.

The model of the glenoid is indented in four locations on the periphery of the glenoid where the feet of the PSG sit, and at another site for the entry point of the guide wire on the native glenoid.

The deltopectoral approach was used in all patients. The glenoid was exposed after the resection of the humeral head and posterior displacement of the humerus. The labrum and synovium were excised and any residual cartilage was removed. Osteophytes were retained to match the 3D model and thus allow precise seating of the PSG. The guide wire was introduced and the PSG removed (Fig. 1). The glenoid was reamed with a powered reamer according to the size and radius of the planned component. The depth was not controlled.

The keeled glenoid component was introduced using the technique developed by Gazielly¹⁵ and reported by Molé et al.¹⁶

A specific artifact reduction protocol was used for the post-operative CT scans. Metallic artifacts did not allow the software to make a correct automatic segmentation of the scapula as its algorithm is based on the density of each pixel of the CT scan DICOM data. Consequently, all

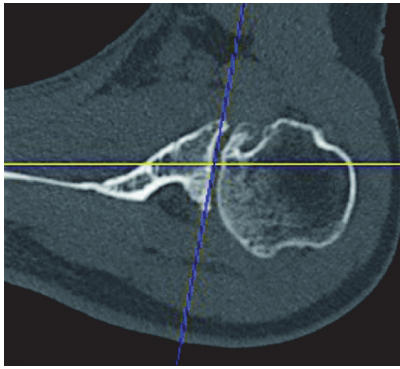


Fig. 2a

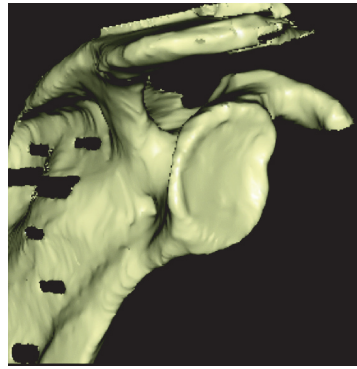


Fig. 2b

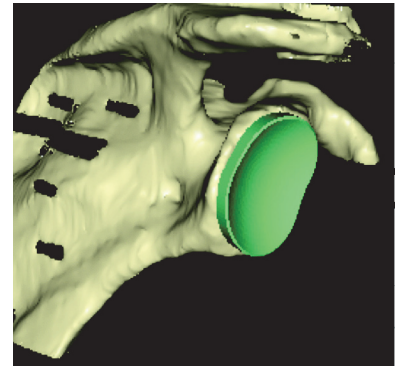


Fig. 2c

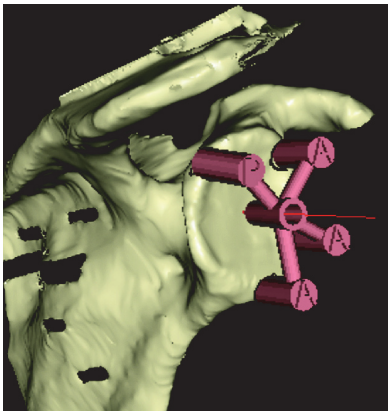


Fig. 2d

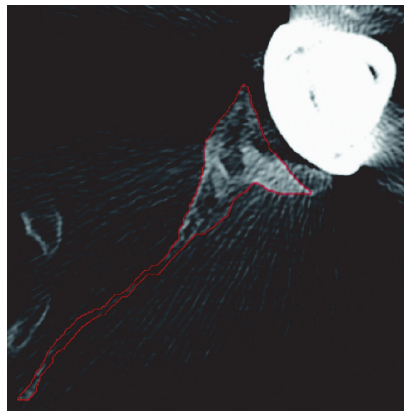


Fig. 2e

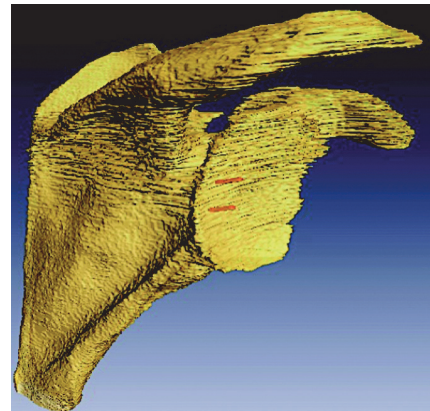


Fig. 2f

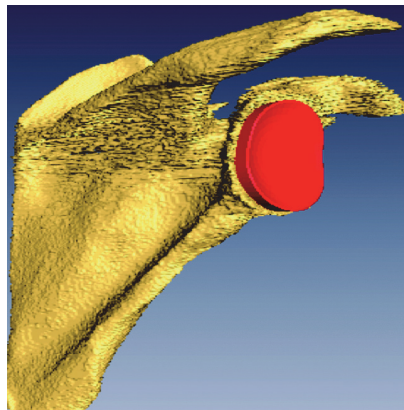


Fig. 2g

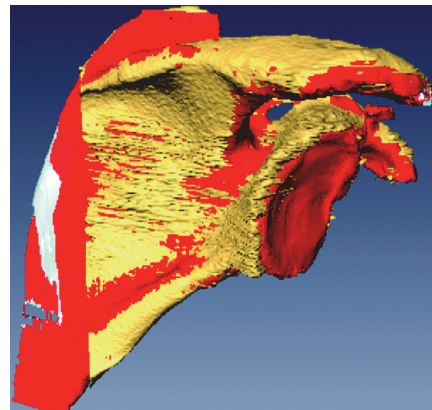


Fig. 2h

Steps to calculate the error between the planned and actual position of the glenoid: a) Glenosys' automatic determination of the plane of the scapula (yellow line) and glenoid (blue line) to calculate the native version and inclination from the pre-operative CT scans; b) Glenosys' automatic segmentation of the scapula (pre-op scapula); c) the surgeon's planning of the position of the glenoid pre-operatively; d) design of the Patient Specific Guide; e) manual segmentation of the scapula post-operatively including segmentation of the markers from the two metallic cylinders in the glenoid component; f) result of the manual segmentation: 'post-op scapula' and 'markers' (in red); g) determination of the post-operative position of the glenoid by applying the virtual glenoid component on the segmented markers; h) matching between the pre-operative (red) and the post-operative (yellow) scapulae. As the two scapulae are strictly superimposed, the difference between the positions of the two glenoids (planned and implanted) is the positioning error of the glenoid.

post-operative scans were loaded into the image processing software Amira (Visualisation Sciences Group, Burlington, Massachusetts) to allow manual segmentation. This was done blindly (without knowledge of the pre-operative planning), slice by slice by an author (MOG) to

create a 3D representation of two distinct objects (STL files): the object 'post-op scapula' and the object 'markers' were retrieved having been made possible by the use of two cylindrical metallic markers in the keel of the component.

Table I. Pre-operative demographic and glenoid data

Patient	Centre	Gender	Age (yrs)	Diagnosis	Glenoid Walch Type	Native glenoid (°)	
						Version	Inclination
1	1	M	81	PGHOA	B2	-13.0	-1.0
2	2	F	64	PGHOA	B2	-11.0	0.0
3	2	M	75	PGHOA	B2	-14.0	1.0
4	2	F	53	PGHOA	B2	-12.0	1.0
5	2	F	66	PGHOA	B2	-11.0	-4.0
6	1	F	73	PGHOA	B2	-7.0	0.0
7	1	F	71	PGHOA	A1	-6.0	0.0
8	1	F	73	PGHOA	B2	-15.0	4.0
9	1	F	66	PGHOA	A2	0.0	-3.0
10	1	F	65	RA	None	-12.0	-1.6
11	2	F	69	PGHOA	A1	-5.0	7.0
12	2	F	64	PGHOA	B2	-18.0	-1.0
13	2	M	79	PGHOA	A1	-8.0	0.0
14	1	F	78	PTA	None	-16.0	0.0
15	2	M	77	PGHOA	B2	-12.0	20.0
16	1	F	66	PGHOA	B2	-25.0	6.0
17	2	F	81	PGHOA	A1	-8.0	13.0

PGHOA, primary glenohumeral osteoarthritis; RA, rheumatoid arthritis; PTA, post traumatic osteoarthritis

Table II. The differences in the orientation and position of the glenoid component

	Version error (°)	Inclination error (°)	Entry point lateral offset (mm)	Entry point anterior offset (mm)	Entry point superior offset (mm)
Mean error	3.4	1.8	0.4	-0.1	-0.8
sd	5.1	5.3	0.9	1.4	1.3
Min	-6.9	-7.3	-1.0	-2.1	-3.6
Max	14.1	11.8	1.7	3.2	1.8

SD, standard deviation

The final aim of this step was to compare the post-operative position of the glenoid component with the pre-operative planned position. The following objects were loaded on to the software:

- the automatically segmented ‘pre-op scapula’ from the Glenosys STL file;
- the manually segmented ‘post-op scapula’, and;
- the manually segmented ‘markers’.

Firstly, the ‘post-op scapula’ was manually superimposed in a best-fit fashion onto the ‘pre-op scapula’. The landmarks used were the coracoid, the acromion, the spine, and the most inferomedial aspects of the scapula. The same rotation matrix was then applied on the ‘markers’ object to position it automatically. Finally, the glenoid component was introduced in its actual position. The registration and repeated measurements during this study had a mean error in 3D of 0.54mm (SD 0.19 mm).

The steps involved in the calculation of the difference in position between the planned and the implanted glenoid component are shown in Figure 2.

A custom application was used to measure the differences between the planned and implanted positions. The total offset was derived from the superoinferior and anteroposterior components, representing the coronal and sagittal planes, respectively. The depth of the entry point on the mediolateral axis was also measured even though it was not controlled. Differences in inclination and version were

measured reflecting differences in the angle of axis of the component (the keeled axis) between the planned and implanted orientation of the keel, projected onto the coronal and transverse planes, respectively. Differences in anteroposterior, superoinferior and lateral-medial offset were expressed in millimetres, and those in inclination and version were expressed in degrees.

Statistical analysis. All statistical analysis was performed with MedCalc StatisticalSoftware version 12.0 (MedCalc Software bvba, Ostend, Belgium). The absolute difference between the measurements of the planned and the implanted position of the component were compared using Student’s *t*-test. The results were considered to be significant at a *p*-value < 0.05.

The study had ethical approval and all patients gave informed consent for the procedure.

Results

The pre-operative planning data of the 17 patients are shown in Table I.

The mean error in 3D orientation of the glenoid component was 0.9 mm (SD 2.1). The mean error in the angles of version and inclination were 3.4° (SD 5.1°) and 1.8° (SD 5.3°), respectively (Table II).

Quantitative analysis showed good agreement between the pre-operative planning and the implanted position of the component. A graphic representation of the planned

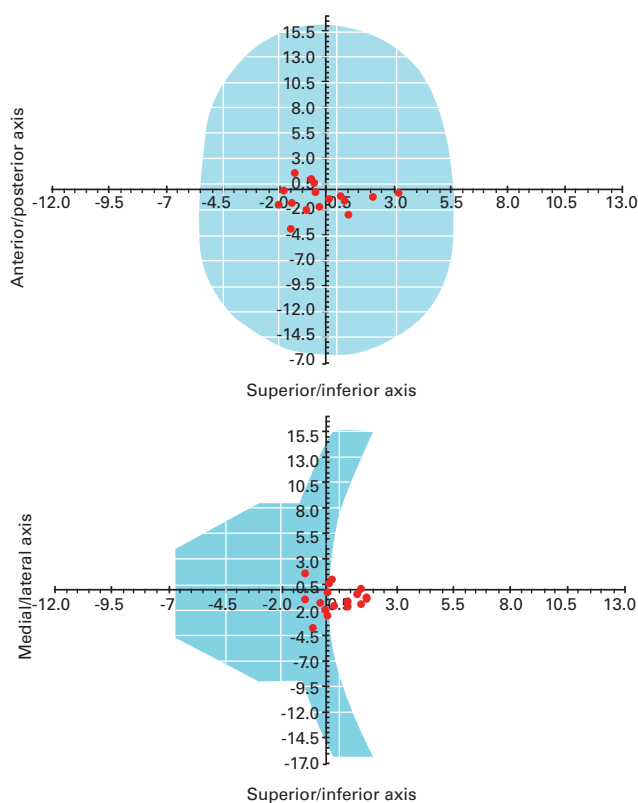


Fig. 3

Graphic representation (error distribution) of the planned and achieved entry point of the guide wire on the surface of the glenoid.

versus the actual placement of the guide wire on the surface of the glenoid is illustrated in Figure 3.

There was no relationship between the Walch type of glenoid and the accuracy of the positioning, and there were no complications related to the use of the PSG during surgery.

Discussion

Precise and reliable implantation of the glenoid component is a predictor of a good long-term outcome of anatomical TSA in patients with glenohumeral osteoarthritis.^{1,17} The amount of erosion of the glenoid varies between patients, and the positioning and orientation of the component can be difficult. It may partly be determined by the experience of the surgeon. However, it has been reported that 80% of TSAs are undertaken by surgeons who perform less than ten a year.^{18,19} The technical difficulties may also be increased by two factors. Firstly, the intra-operative understanding and visualisation of the deformed glenoid is much more difficult than that of normal anatomy; and secondly, there are no reliable intra-operative landmarks.

Our study confirms our hypothesis. Pre-operative planning with computer-3D modelling software and the use of PSGs provides greater accuracy and reproducibility of the

positioning and orientation of the glenoid component in anatomical TSA. The mean deviation of the position of the entry point of the guide wire was < 1 mm in both the vertical and the horizontal planes. The mean errors in inclination and version were about 2° and 3°, respectively.

This was a prospective study to test the accuracy of a PSG which was 3D-printed from the Glensys software in daily clinical practice.

Although the results showed that the entry point in the sagittal and coronal axis, and the direction in version and inclination were accurate, they are worse, as expected, than those obtained during *in vitro* experimentation.¹² The use of the pre-operative planning system and the PSG should provide better correction of version and inclination than the surgeon can achieve without the guide, but a specific study has yet to be performed to test this hypothesis.

The shape of the glenoid has no significant influence on the accuracy of the guide. Optimal positioning of the guide wire requires the humerus and deltoid to be retracted posteriorly, and if this is not achieved, appropriate positioning may not occur, particularly in patients with significant pathological retroversion of the glenoid. Hendel et al²⁰ made this observation and described several contributing factors. The segmentation produced by the Glensys software has been shown to be reliable and reproducible.¹¹ It is a fully automatic method and does not require a third component. Good exposure of the glenoid and removal of all soft tissues are important steps in allowing stable positioning of the four legs of the PSG. Osteophytes have to be conserved in this technique, as they are not differentiated from the native bone. Lastly, reaming was undertaken carefully with respect to the direction of the guide wire despite the constraints provided by the posteriorly retracted deltoid. It is important to note that this step was facilitated by pre-operatively obtained knowledge of the shape of the glenoid and the optimal size and radius of curvature of the glenoid component which is to be used.²¹

This study has limitations. Post-operative measurements were based on CT scans after manual segmentation of the scapula. Artifacts, even with the specific protocols, interfered with the tedious manual segmentation of these images. The matching procedure²⁰ could also generate errors, but we have previous unpublished data relating to > 44 scapulae using three observers that provided perfect agreement between the observers (interclass correlation coefficient = 0.9750). However, in this study, the repeated process gave a very small mean error and standard deviation.

Hendel et al²⁰ achieved the registration and repeated measurements in 3D with accuracy and reproducibility of < 3° and < 1 mm.

It is difficult to evaluate the accuracy of individual components of the process. That is whether it is the planning and the use of a PSG or whether it is the planning itself which determines the accuracy. The accuracy for the whole procedure was much better than surgeons can achieve by 'eye-balling', for which Nguyen et al² reported errors as

high as 7.5°. Further studies are needed which look specifically at implantation of the glenoid component with an isolated pre-operative plan.

Another limitation is that we did not control for rotation of the glenoid component or the depth of the component. An improved PSG should also allow us to control these parameters.

Despite these limitations, it is evident that the fully automatic segmentation achieved by Glenosys and the associated process of pre-operative planning leads to a better understanding of intra-operative difficulties when introducing the glenoid component at TSA.



Take home message:

Patient specific glenoid guides can be used in a daily total shoulder arthroplasty activity with faithful reproduction of the glenoid pre-operative planning.

Author contributions:

M. O. Gauci: Data collection, Data analysis, Writing the paper.

P. Boileau: Performed surgeries.

M. Baba: Proof read.

J. Chaoui: Data analysis.

G. Walch: Performed surgeries.

No benefits in any form have been received or will be received from a commercial party related directly or indirectly to the subject of this article.

This article was primary edited by J. Scott and first proof edited by G. Scott.

References

- Farron A, Terrier A, Büchler P.** Risks of loosening of a prosthetic glenoid implanted in retroversion. *J Shoulder Elbow Surg* 2006;15:521–526.
- Nguyen D, Ferreira LM, Brownhill JR, et al.** Improved accuracy of computer assisted glenoid implantation in total shoulder arthroplasty: an in-vitro randomized controlled trial. *J Shoulder Elbow Surg* 2009;18:907–914.
- Throckmorton TW, Gulotta LV, Bonnarens FO, et al.** Patient-specific targeting guides compared with traditional instrumentation for glenoid component placement in shoulder arthroplasty: a multi-surgeon study in 70 arthritic cadaver specimens. *J Shoulder Elbow Surg* 2015;24:965–971.
- Iannotti JP, Greeson C, Downing D, Sabesan V, Bryan JA.** Effect of glenoid deformity on glenoid component placement in primary shoulder arthroplasty. *J Shoulder Elbow Surg* 2012;21:48–55.
- Nyffeler RW, Jost B, Pfirrmann CWA, Gerber C.** Measurement of glenoid version: conventional radiographs versus computed tomography scans. *J Shoulder Elbow Surg* 2003;12:493–496.
- Bryce CD, Davison AC, Lewis GS, et al.** Two-dimensional glenoid version measurements vary with coronal and sagittal scapular rotation. *J Bone Joint Surg [Am]* 2010;92-A:692–699.
- Bokor DJ, O'Sullivan MD, Hazan GJ.** Variability of measurement of glenoid version on computed tomography scan. *J Shoulder Elbow Surg* 1999;8:595–598.
- Lewis GS, Armstrong AD.** Glenoid spherical orientation and version. *J Shoulder Elbow Surg* 2011;20:3–11.
- Budge MD, Lewis GS, Schaefer E, et al.** Comparison of standard two-dimensional and three-dimensional corrected glenoid version measurements. *J Shoulder Elbow Surg* 2011;20:577–583.
- Ganapathi A, McCarron JA, Chen X, Iannotti JP.** Predicting normal glenoid version from the pathologic scapula: a comparison of 4 methods in 2- and 3-dimensional models. *J Shoulder Elbow Surg* 2011;20:234–244.
- Moineau G, Lévine C, Boileau P, et al.** Three-dimensional measurement method of arthritic glenoid cavity morphology: feasibility and reproducibility. *Orthop Traumatol Surg Res* 2012;98(6 Suppl):S139–S145.
- Walch G, Vezeridis PS, Boileau P, Deransart P, Chaoui J.** Three-dimensional planning and use of patient-specific guides improve glenoid component position: an in vitro study. *J Shoulder Elbow Surg* 2015;24:302–309.
- Chaoui J, Moineau G, Stindel E, Hamitouche C.** Evaluation of recognition-based segmentation method for shoulder augmented surgery: CAOS symposium. *International Society for Computer Assisted Orthopaedic Surgery* 2010;98–102.
- Walch G, Badet R, Boulahia A, Khoury A.** Morphologic study of the glenoid in primary glenohumeral osteoarthritis. *J Arthroplasty* 1999;14:756–760.
- Gazielly DF.** Comment je scelle un implant glénoïdien en polyéthylène convexe à quille avec ma technique de compaction d'os spongieux. *Maîtrise Orthopédique* 2007;162:6–11. (In French)
- Molé D, Roche O, Riand N, Lévine C, Walch G.** Cemented Glenoid Component: Results in Osteoarthritis and Rheumatoid Arthritis. In: Walch G, Boileau P, eds. *Shoulder Arthroplasty*. Berlin, Heidelberg: Springer-Verlag, 1999:163–172.
- Ho JC, Sabesan VJ, Iannotti JP.** Glenoid component retroversion is associated with osteolysis. *J Bone Joint Surg [Am]* 2013;95-A:82.
- Padegimas EM, Maltenfort M, Lazarus MD, et al.** Future patient demand for shoulder arthroplasty by younger patients: national projections. *Clin Orthop Relat Res* 2015;473:1860–1867.
- Jain N, Pietrobon R, Hocker S, et al.** The relationship between surgeon and hospital volume and outcomes for shoulder arthroplasty. *J Bone Joint Surg [Am]* 2004;86-A:496–505.
- Hendel MD, Bryan JA, Barsoum WK, et al.** Comparison of patient-specific instruments with standard surgical instruments in determining glenoid component position: a randomized prospective clinical trial. *J Bone Joint Surg [Am]* 2012;94-A:2167–2175.
- Walch G, Mesiha M, Boileau P, et al.** Three-dimensional assessment of the dimensions of the osteoarthritic glenoid. *Bone Joint J* 2013;95-B:1377–1382.



Proper benefit of a three dimensional pre-operative planning software for glenoid component positioning in total shoulder arthroplasty

Adrien Jacquot^{1,2} · Marc-Olivier Gauci³ · Jean Chaoui^{4,5} · Mohammed Baba⁶ · Pierric Deransart⁴ · Pascal Boileau³ · Daniel Mole^{1,2} · Gilles Walch⁷

Received: 3 April 2018 / Accepted: 12 June 2018
© SICOT aisbl 2018

Abstract

Purpose Glenoid loosening after total shoulder arthroplasty (TSA) is influenced by the position of the glenoid component. 3D planning software and patient-specific guides seem to improve positioning accuracy, but their respective individual application and role are yet to be defined. The aim of this study was to evaluate the accuracy of freehand implantation after 3D pre-operative planning and to compare its accuracy to that of a targeting guide.

Method Seventeen patients scheduled for TSA for primary glenohumeral arthritis were enrolled in this prospective study. Every patient had pre-operative planning, based on a CT scan. Glenoid component implantation was performed freehand, guided by 3D views displayed in the operating room. The position of the glenoid component was determined by manual segmentation of post-operative CT scans and compared to the planned position. The results were compared to those obtained in a previous work with the use of a patient-specific guide.

Results The mean error for the central point was 2.89 mm (SD ± 1.36) with the freehand method versus 2.1 mm (SD ± 0.86) with use of a targeting guide ($p = 0.05$). The observed difference was more significant ($p = 0.03$) for more severely retroverted glenoids ($> 10^\circ$). The mean errors for version and inclination were respectively 4.82° (SD ± 3.12) and 4.2° (SD ± 2.14) with freehand method, compared to 4.87° (SD ± 3.61) and 4.39° (SD ± 3.36) with a targeting guide ($p = 0.97$ and 0.85 , respectively).

Conclusion 3D pre-operative planning allowed accurate glenoid component positioning with a freehand method. Compared to the freehand method, patient-specific guides slightly improved the position of the central point, especially for severely retroverted glenoids, but not the orientation of the component.

Keywords Patient-specific guides · 3D planning · Total shoulder arthroplasty · Positioning · Accuracy · Glenoid component

Introduction

Total shoulder arthroplasty is the preferred treatment for glenohumeral primary osteoarthritis, with good short- and

long-term functional results [1, 2]. Despite these reliable outcomes, glenoid loosening has been reported to be a serious concern. Though exceptional prior five years post-operative, radiographic loosening approximates 50% at ten years follow-

Electronic supplementary material The online version of this article (<https://doi.org/10.1007/s00264-018-4037-1>) contains supplementary material, which is available to authorized users.

✉ Adrien Jacquot
dr.jacquot@chirurgie-artics.fr

¹ SAS Clinique Louis Pasteu, 7 rue Parmentier, 54270 Essey-lès-Nancy, France

² Chirurgie des Articulations et du Sport, Centre ARTICS, 24 rue du XXI^e regiment d'Aviation, 54000 Nancy, France

³ Institut Universitaire Locomoteur et du Sport, Hôpital Pasteur 2, 30 Voie Romaine, 06000 Nice, France

⁴ Société IMASCAP, 65 place Copernic, 29280 Plouzané, France

⁵ Institut Mine Telecom Atlantique, 655 Avenue du Technopole, 29280 Plouzané, France

⁶ Sydney Adventist Hospital, 185 Fox Valley Road, Wahroonga 2076, Australia

⁷ Centre Orthopédique Santy, Unité Epaulé, 24 Avenue Paul Santy, 69008 Lyon, France

up [2, 3]. Improving glenoid implant survivorship over time is one of the more crucial elements of research relating to shoulder arthroplasty [4]. Over the past ten years, much attention has been paid to improve the accuracy of glenoid implant positioning. The shoulder is a highly mobile joint, and stability of this joint is a delicate combination of multiple factors, including bone orientation, ligamentous restrains, and peri-articular muscle balance. With respect to shoulder arthroplasty, malpositioning of the implant, defined by excessive retroversion or inclination (over 10°), may be responsible for increased shear forces and higher loosening rate after years [4–9]. Moreover, reported surgeon's accuracy for glenoid implant positioning is relatively poor, mostly because of lack of pre-operative planning and difficulty with intra-operative landmarks [10–15].

Ideal component positioning requires determining precisely the optimal position of the implant for each patient. This equates to minimal retroversion and inclination, as well as minimal bone reaming in order to preserve subchondral bone and provide sufficient implant-on-bone seating [4–9]. Glensys planning software (Imascap, Plouzané, France) allows fast automatic 3D modeling of the scapula, reliable 3D measurements of scapular parameters, and virtual implantation of the glenoid component prior to surgery, compatible with the surgeon's routine practice [16, 17]. Recently, patient-specific guides (PSG) have been proposed to aim and recreate the planned position intra-operatively. Several of these systems, based on 3D imaging and 3D printing, are currently utilized with promising results, but what is not clear are the respective benefits of each component of this process, that is, the pre-operative planning and then the utility of the specific targeting guides [10, 11, 13, 15–19].

Our hypothesis was that pre-operative planning, even without PSG, could optimize glenoid component positioning. The aim of this study was to evaluate the accuracy of glenoid implant position after isolated 3D pre-operative planning with Glensys Software (Imascap, Plouzané, France) using a free-hand implantation method. Secondly, we compared our results to those obtained in another published series, using the same software, but with the use of a PSG for glenoid implantation and thus evaluated the proper role of this device in improving the surgeon's accuracy.

Patient and method

Population

Seventeen patients, scheduled for a total shoulder arthroplasty (TSA) for primary glenohumeral osteoarthritis, were enrolled in this prospective, single centre study between April 2014 and October 2015. All the patients had a pre-operative CT scan of the entire shoulder (including medial border and

inferior angle of the scapula), performed in the supine position, with the arm at side and with the shoulder in neutral rotation, with specific acquisition parameters (Fig. 1). The native DICOM axial views were used for pre-operative planning with Glensys Software (Imascap, Plouzané, France). There were 14 women and three men, with mean age of 68 ± 12 years (range 48–87). All the subjects were provided clear information and gave written consent for a post-operative CT scan, before inclusion. This study received an Institutional Review Board agreement (Centre Orthopédique Santy, IRB 20.1611).

Pre-operative planning

Using specific validated algorithms, Glensys Software performs automatic 3D reconstruction of the scapula and precisely determines glenoid version, inclination, and humeral head subluxation, with respect to the scapular plane [20, 21]. This software was used by the surgeons to analyze glenoid deformity and to virtually implant the glenoid component for each patient before surgery. All the pre-operative shoulder parameters (version, inclination, humeral head subluxation, and glenoid type according to Walch classification [22]) were recorded for analysis (Table 1). The surgeon had to choose component size and radius of curvature, as well as the optimal position with respect to orientation ($< 10^\circ$ superior inclination, $< 15^\circ$ retroversion), implant-on-bone seating (min. 80%), subchondral bone preservation, and avoiding glenoid vault perforation, based on previously published data [4–9]. The virtual component parameters (type, position, orientation) were created by 3D models saved in a Standard Tessellation Language (.STL) file format, as well as the 3D pre-operative scapula. These two .STL files (“pre-op scapula” and “pre-op implant”) were subsequently used for comparison with post-operative real position of the implant.

Surgical technique

All the procedures were performed in one centre, by two surgeons with significant experience level in shoulder arthroplasty (AJ, DM). Planning parameters and 3D views of the scapula, the implant, and the virtual guidewire were printed and displayed in the operating room (Fig. 2). For all the patients, the humeral implant was an ASCEND FLEX short uncemented stem (Tornier SAS, Montbonnot Saint Martin, France) and glenoid component was a PerFORM polyethylene keeled cemented component (Tornier SAS, Montbonnot Saint Martin, France). After residual cartilage removal, guidewire positioning and reaming were performed freehand, based on planning parameters and displayed 3D views, without any specific guide. Then, glenoid preparation was performed using a standard compacted autograft technique [23] and low viscosity cement.

Recommended parameters

Parameter	Recommended	Min	Max
Modality	CT		
Kernel / Algorithm	Bone or Bone+		
kVp	120 Kvp	120 Kvp	140 Kvp
mA	Manual 240 mA	Manual 200 mA	Manual 300 mA
	Do NOT use auto-mA setting <i>Not doing so will produce images that are incompatible with Glenosys</i>		
Slice Increment	1.2 mm	0.312 mm	1.2 mm
Image Thickness	- Detector Coverage should be maximum - Helical Thickness 0.625 mm or 1.25 mm - Pitch 0.9 or less - Rotation time 1 sec or less		
Exposure time	1000 ms	1000 ms	1500 ms

Display Field of View (DFOV)

Parameter	Recommended	Min	Max
DFOV (Axial plane)	20 to 30 cm to cover full scapula and the elbow level	15 cm	No more than 32 cm
DFOV (Frontal plane)	> 10 cm	8 cm	45 cm
Matrix size	512 x 512	512 x 512	1024 x 1024

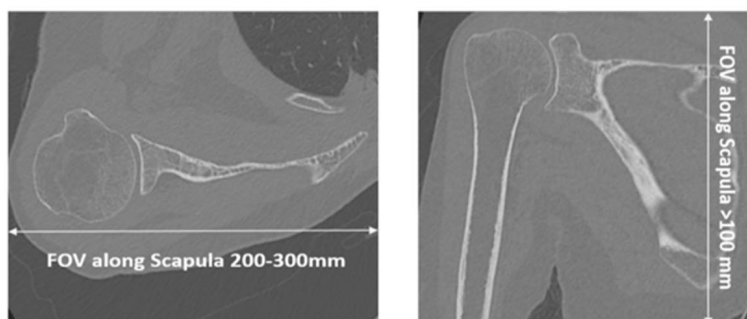


Fig. 1 CT scan parameters for Glenosys Software

Table 1 Native glenoid characteristics in the two compared series

	Freehand series	PSG series (Gauci et al. [17])	p
Version	-14.5° ± 7.8 (-2; -32)	-11.4 ± 5.7° (0; -25)	0.21
Inclination	5.6 ± 5.4° (-4; 15)	2.4 ± 6.1° (-4; 20)	0.13
Glenoid type (Walch classification)			
Type A	7 (4 × A1, 3 × A2)	6 (5 × A1, 1 × A2)	0.72
Type B	10 (3 × B1, 7 × B2)	11 (only B2)	
Type C	0	0	

Version: negative values are for retroversion. Inclination: negative values are for inferior inclination

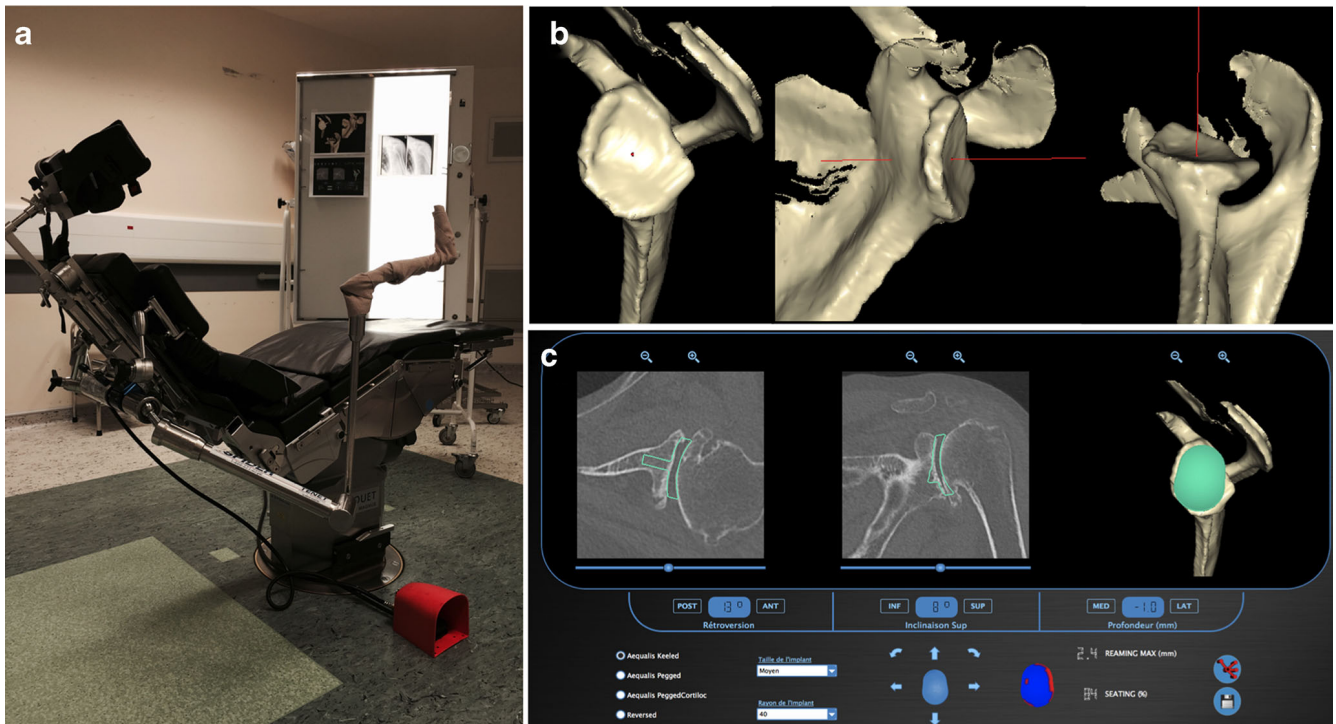


Fig. 2 Planning data and 3D views displayed in the operating room (OR). **a** Overview of the OR before surgery. **b** 3D views showing the planned position of the entry point, the inclination, and the version of the guidewire. **c** Pre-operative planning data (software view)

3D segmentation

A CT scan was performed within two months after surgery, with a specific metallic artifact reduction protocol (Fig. 3). Because of metallic components, automatic segmentation was not possible at this step. Axial views were used for manual 3D segmentation of the scapula (Fig. 3) using Amira Software (Visage Imaging, Inc), according to a previously validated technique (Thesis, Jean Chaoui PhD, unpublished work). The two metallic markers inside the glenoid component were also segmented in a different file (Fig. 3). Thus, 2 .STL files (“post-op scapula” and “metallic markers”) were obtained for each patient, recreating the post-operative scapula and the position of the implanted glenoid component.

Matching and comparison

As the “pre-op scapula” and the “post-op scapula” were not in the same position within the 3D space, manual 3D matching between them had to be performed (Fig. 4). The matching procedure was done with Amira software, by moving “post-op scapula” 3D model onto the “pre-op scapula.” The precision of this overlapping was evaluated by the mean distance between each corresponding points of the two scapulae, which was on average 0.4 ± 0.1 mm (range 0.3–0.6) for the entire series. The same translation matrix was then applied to the “metallic markers” 3D model. Then, a standard 3D model of Perform glenoid component (“post-op implant”) was matched

on these metallic markers. The two 3D components (“pre-op implant” and “post-op implant”) were then in the same 3D referential and could be compared, regarding position and orientation.

For each patient, implanted component (“post-op implant”) was compared to planned component (“pre-op implant”) using specific software (Imascap, Plouzané, France), delivering absolute errors for 3D position of the central point of the implant (“3D offset”, expressed in millimeters), version (degrees), inclination (degrees), and rotation/rolling (degrees). Offsets represented the distance (millimeters) between the theoretical planned position and the real position of the implanted component. The “3D offset” was derived from anteroposterior offset and superoinferior offset in the sagittal plane, and mediolateral offset in the axial plane, which were analyzed separately. Malposition criteria, according to Throckmorton et al. [15], corresponded to a 3D offset > 4 mm or a > 10° error for version or inclination.

Comparison with a published series using PSG

Finally, all the values of the freehand study were compared to those obtained in a previous published series of 17 patients, using the same protocol but with the use of a polyamide 3D-printed patient-specific guide, for glenoid component implantation [17]. The two series were comparable for the demographic data (age and sex) and for the characteristics of the pre-operative glenoids (Table 1).

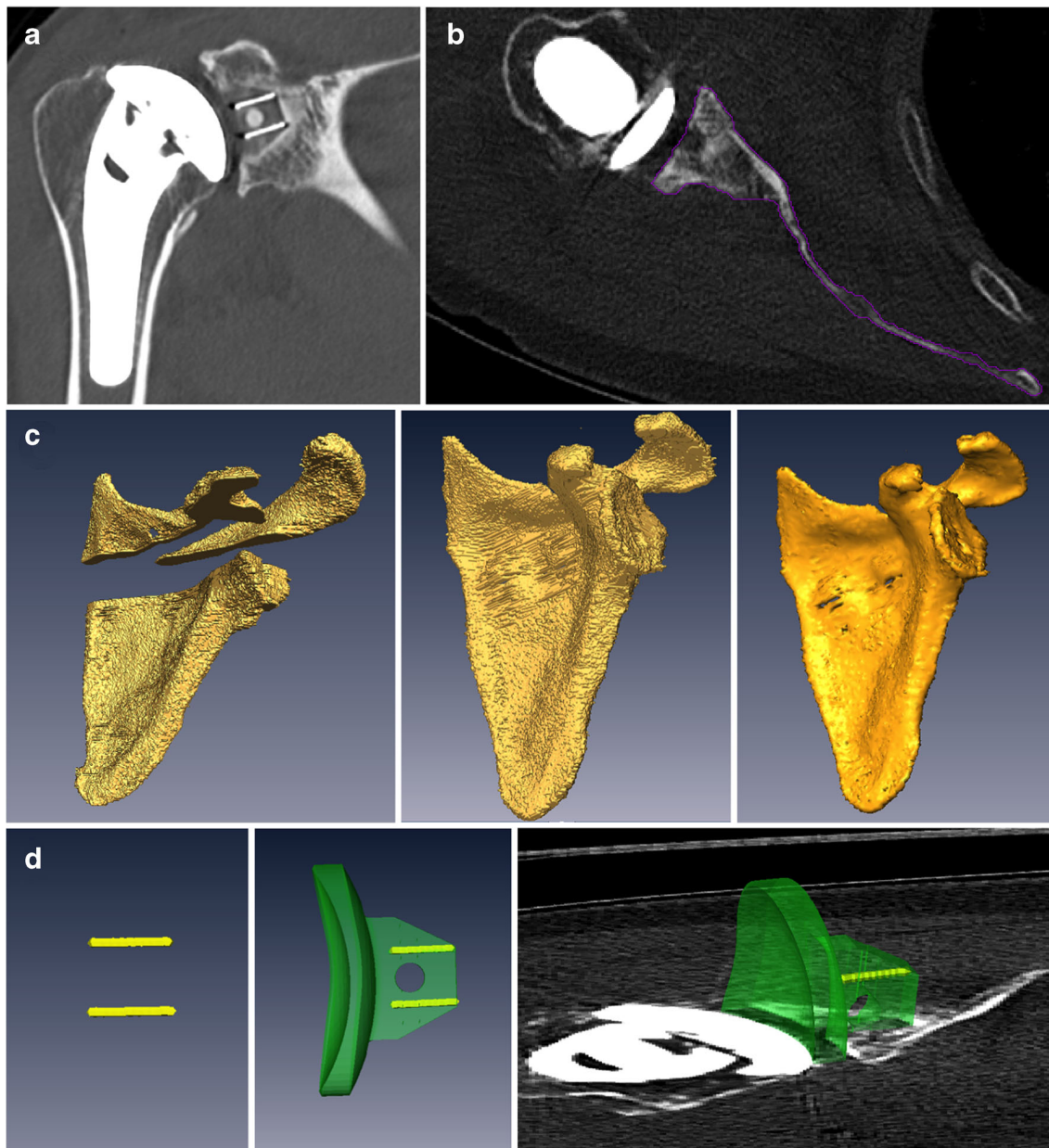


Fig. 3 Manual 3D segmentation steps. **a** Standard post-operative CT scan with metallic artifact reduction protocol. **b** Manual contouring of the scapular body on every slice. **c** 3D segmentation. **d** Segmentation of the

metallic markers/superposition of a 3D implant model/control of the position of the markers on 2D CT scan slices

Statistical analysis

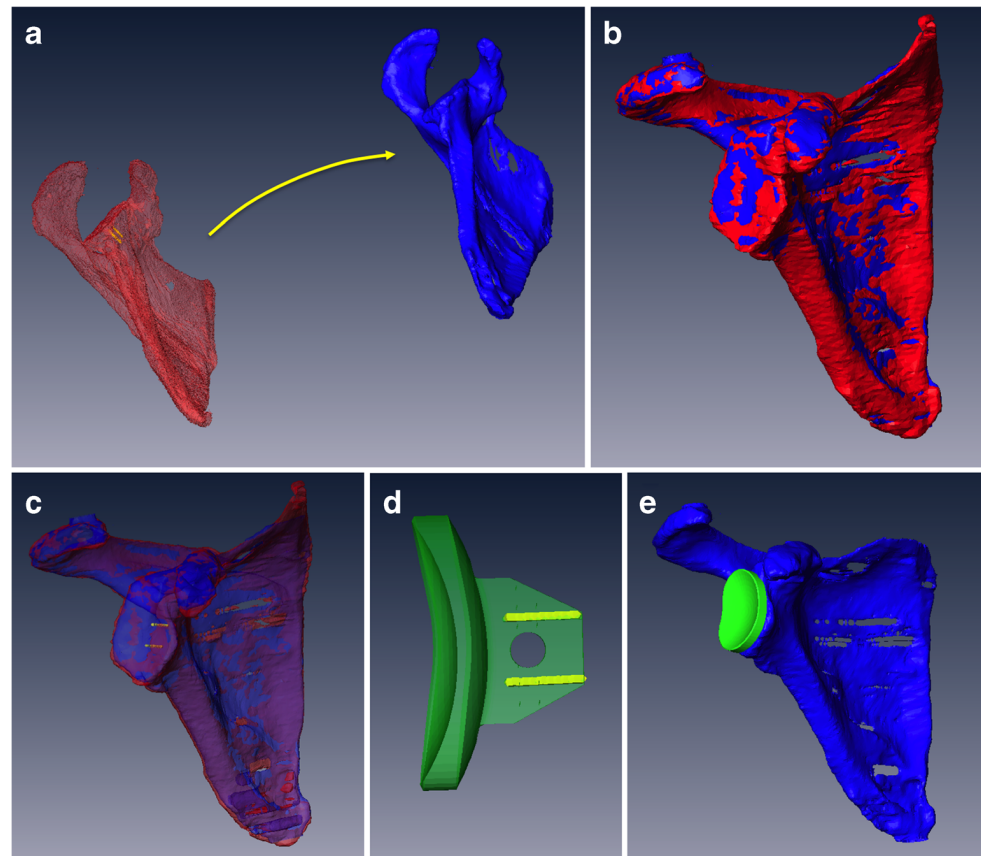
Statistical analysis was performed with MedCalc Statistical Software (MedCalc Software bvba, Ostend, Belgium). A Student's *t* test was used to compare the quantitative data (3D offset, version, inclination) between our “freehand” series and the series of Gauci et al. with PSG [17]. A chi-square test was used for qualitative values or a Fisher exact test utilized when the population of the subgroups was < 5 . A *p* value < 0.05 was considered significant.

Results

All the pre-operative measurements are shown in Table 1. In our series, there were seven type A and ten type B glenoids (Walch classification).

In our series (Table 2), the mean error for 3D position of the central point of the glenoid component was 2.9 ± 1.4 mm (1.2–4.8). The mean errors for version and inclination were respectively $4.8^\circ \pm 3.1^\circ$ (0.4–13.3) and $4.2^\circ \pm 2.1^\circ$ (0.7–7.8). Rolling mean error was $8.8^\circ \pm 5.8$ (1.7–20.1). Seven cases (41%) in our series met the criteria for malposition, according

Fig. 4 Matching protocol. **a** “Pre-op scapula” (blue) and “post-op scapula”/“markers” (red and yellow) were not natively in the same 3D referential. **b** Superimposition of “post-op scapula” (red) onto “pre-op scapula” (blue). **c** The same translation matrix was applied to the metallic markers (yellow). **d** Superimposition of the 3D implant model onto the metallic markers in the new referential. **e** Final view of “post-op implant” (green) in the new referential, which can be compared to the planned “pre-op implant”



to Throckmorton et al. [15] (>4 mm or $>10^\circ$ error), largely because of a 3D offset >4 mm (six cases).

In the PSG series [17] (Table 2), the accuracy was significantly higher for the 3D position of the central point (2.1 ± 0.9 mm, $p = 0.05$) but not for version or inclination. Rolling was not reported. Only two cases (12%) were malpositioned ($p = 0.11$), but no case had a 3D offset greater than 4 mm ($p < 0.01$). Sagittal and frontal 2D offset for the two series are represented in Fig. 5.

We focused on the influence of pre-operative glenoid deformity on the final position of the glenoid component.

Results of this comparative analysis are shown in Table 3. In our series with the freehand technique, the position of the central point was significantly less accurate when pre-operative glenoid version was $\geq 10^\circ$ ($p = 0.04$), whereas there was no influence of glenoid deformity in the PSG series. Thus, 3D offset was significantly higher for high deformities ($\geq 10^\circ$) with freehand technique than with PSG ($p = 0.02$), whereas there were no differences between the two techniques when pre-operative version was $< 10^\circ$. Pre-operative glenoid deformity did not influence the mean error of version or inclination in the two series.

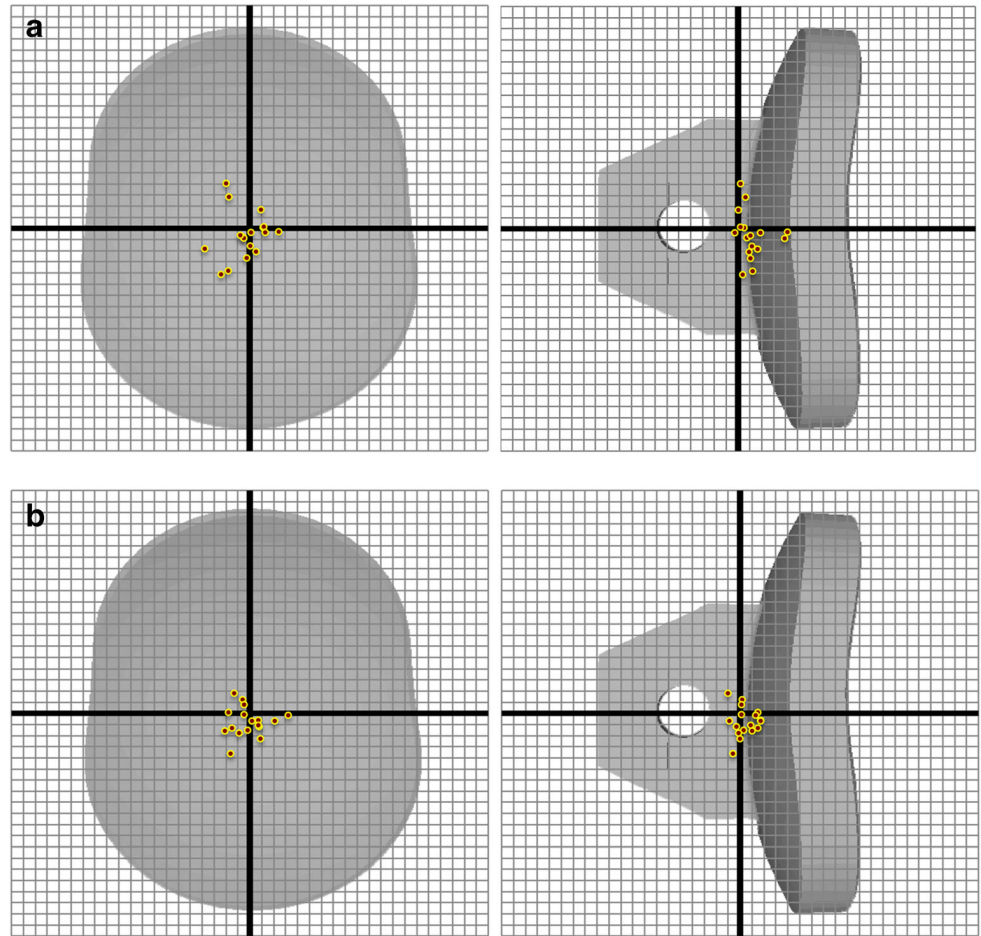
Table 2 Glenoid component positioning errors with freehand method and PSG method (Gauci et al. [17])

	3D offset		Anteroposterior offset		Superoinferior offset		Mediolateral offset		Version		Inclination		Rolling	
	FH	PSG	FH	PSG	FH	PSG	FH	PSG	FH	PSG	FH	PSG	FH	PSG
Mean	2.9	2.1	1.3	1.2	1.7	1.21	1.2	0.8	4.8	4.9	4.2	4.4	8.8	–
SD	1.4	0.9	1	0.8	1.4	0.88	1.2	0.6	3.1	3.6	2.1	3.4	5.8	–
Minimum	1.2	0.5	0	0.2	0.1	0.1	0	0	0.4	0.5	0.7	0.2	1.7	–
Maximum	4.8	4	3.8	3.2	4.1	3.6	4.2	1.7	13.3	14.1	7.8	11.8	20.1	–
<i>p</i>	0.05		0.73		0.27		0.23		0.97		0.85		–	

Offsets are expressed in millimeters (mm). Version, inclination, and rolling are expressed in degrees ($^\circ$)

FH freehand series (current paper), *PSG* patient-specific guide series (Gauci et al. [17])

Fig. 5 2D offsets (position of the central point) with the two compared methods. **a** 2D offsets with the freehand method (our series) in the sagittal plane and in the frontal plane. **b** 2D offsets with the PSG method (Gauci et al. [17]) in the sagittal plane and in the frontal plane



Discussion

Pre-operative 3D planning allowed determination of the ideal glenoid component position for each patient and provided 3D landmarks to the surgeon for accurate freehand implant positioning, close to that obtained with patient-specific guides, underlining the importance of 3D planning before any shoulder replacement. The benefit of PSG was clear for complex and severely retroverted glenoids but not for simpler cases (type A, < 10° retroversion).

In our series, the freehand accuracy of the surgeon was ± 2.9 mm for the position of the central point of the implant and between 4° and 5° for version and inclination. Previous published in vitro and in vivo series reported similar results after

3D planning and freehand technique [11, 13, 18]. Similarly to us, in an in vivo study, Iannotti et al. reported a mean deviation of 1.5 to 1.7 mm for 2D offsets (3D offset not reported), 4.1° for inclination, and 4.3° for version [18], using 3D planning and freehand implantation. Some authors evaluated the mean errors committed by surgeons with a standard technique without planning [10, 11, 13–15, 18] and reported mean deviations were 3 mm for the central point and 7–11° for version and inclination. But in these studies, the mean errors have been calculated by reference to a constant and theoretical objective of 0° version and 0° inclination, which is not necessarily the ideal position for each patient. To correctly assess the ability of a surgeon to precisely reach freehand the ideal position without 3D planning, a study should include shoulders with TSA

Table 3 Accuracy of glenoid component positioning according to glenoid pre-operative deformity

	3D offset (mm)			Version (°)			Inclination (°)		
	FH	PSG	<i>p</i>	FH	PSG	<i>p</i>	FH	PSG	<i>p</i>
Pre-operative glenoid version < 10°	1.9	2.1	0.74	3.7	3.6	0.95	5.6	5.5	0.94
Pre-operative glenoid version ≥ 10°	3.3	2.1	0.02	5.3	5.6	0.86	3.6	3.8	0.86
<i>p</i>	0.04	0.94		0.33	0.25		0.1	0.4	

FH freehand series (current paper), *PSG* patient-specific guide series (Gauci et al. [17])

implanted freehand without any planning and compare the position of the implanted component to the virtual position obtained in a 3D planning performed after the surgery. But there is no such study published in the literature, and benefit of 3D planning cannot be proven. Our results being close to those obtained with a PSG and visually better than those published without 3D planning (at least for orientation), we may hypothesize that 3D planning is useful for glenoid implantation, especially since the software could be used by the surgeon himself in routine practice, thanks to a validated automatic algorithm for 3D segmentation and measurements [20, 21].

With a mean error of 2.1 mm for the central point, 4.9° for version, and 4.4° for inclination, the use of a PSG showed a significant (but slight) improvement only for the position of the central point, compared to our freehand method. Moreover, this difference was only significant for severely retroverted glenoids (> 10°) but not for simpler cases (< 10°). To our knowledge, only three studies [11, 13, 18] reported comparative accuracy between PSG method and planning/freehand method. Lewis et al. [13], in a study based on polymer models, found a significant improvement with a PSG, with a mean error of 3° for version and 3° for inclination (compared to 8° and 9°, respectively, with a planning/freehand method). Iannotti et al. [11], in a sawbone study, reported similar results with 3.1° mean error for version, 2.8° for inclination, and 1.2 mm for central point (compared to 6.7°, 9.3°, and 2.4 mm, respectively, with a planning/freehand method) and a strongly minimized risk of having a > 5° or > 3 mm error. These studies were not in vivo studies. Iannotti et al. [18] published recently a similar study, involving patients, and their conclusions were different. In their study, PSG did not significantly improve accuracy for version, inclination, or central point, compared to a planning/freehand method (3.1° vs 4.1° mean error for inclination, 4° vs 4.3° for version, 0.9 to 1.1 vs 1.5 to 1.7 mm for 2D offsets). In fact, in vivo conditions imply soft tissue contractures and difficulty of exposure and guide positioning, secondary to humeral head obstruction and glenoid retroversion, that do not exist in sawbone studies and that probably explain the observed differences between these studies.

One possible explanation for the errors could be related to imprecise and/or unstable positioning of the guide on the glenoid. One hypothesis could be that polyamide guides are too smooth and not stable enough on the glenoid rim. A decision has been already undertaken to move towards use of metallic guides, with the expectation of being more stable. Another possible explanation is that PSG only control the position of the guidewire, and slight errors could also be related to the next steps, such as reaming, determining rotation, or cementing the implant, as reported by Nguyen et al. [14]. Walch et al. reported much better accuracy with the same planning software and a PSG, in a sawbone study considering only the position of the guidewire, not the implant, and thus

negating all the subsequent steps of implantation and the potential related errors [16]. In order to demonstrate a real superiority of the PSG method over planning/freehand method, optimization of these PSG should be made to improve stability on the glenoid and include control of reaming (orientation and depth) and rotation.

Nevertheless, PSG method was much more reliable than the freehand method, with only 12% glenoid component considered malpositioned (compared to 44% with freehand method). This point is important and can be considered a real potential benefit of the PSG in routine daily practice, as surgeons may not always be as focused on positioning accuracy as we were in the context of a scientific study. Moreover, it has been reported that more than 70% of shoulder prostheses in the USA are performed by low-volume surgeons (< 10 arthroplasty per year) [24], and it is known that the lack of experience strongly influences the quality of implantation and the outcomes of shoulder arthroplasty [11, 24, 25]. In our series, prostheses were only implanted by high-volume surgeons (> 50 arthroplasties per year). This could explain the lack of strong differences between our series and the PSG series. Patient-specific guides may be of real interest for low-volume surgeons, who are not familiar with glenoid implant positioning, but this would also imply a learning curve for 3D pre-operative planning, as well as for the use of the PSG intra-operatively. Finally, the benefit of using a PSG may be clearer for complex and severely retroverted glenoids, regardless of the surgeon's experience.

Our work has some limitations. The first is the small number of patients that could affect the statistical comparison. Moreover, our series involved consecutive cases of shoulder arthroplasty, and there were 41% of type A non-retroverted glenoids, for which the use of a PSG was not clearly beneficial. Accuracy of our freehand method could have been lower in a series with a higher number of retroverted glenoids.

Determination of the mean errors of positioning was based on a manual process, with successive steps such as scapula segmentation, metallic markers segmentation, and scapula matching, as previously described. Although all these steps have been previously validated, and the precision controlled at each step of the process, slight errors could have affected the final measurements.

Finally, we had no control group with a standard method without pre-operative planning, to prove the superiority of 3D pre-operative planning over a standard method. Another study with standard implantation without 3D planning, followed by a "post-operative" planning as a reference, could be of interest.

Conclusion

3D pre-operative planning seemed to be useful before total shoulder replacement, to determine the optimal position of

glenoid component and give 3D views and landmarks to the surgeon to correctly perform the surgery, with a good expected accuracy. The use of a PSG made the positioning a little more precise, and more reliable, especially for complex and severely retroverted glenoids. Our results could limit the actual enthusiasm towards PSG under this current preliminary form, and should lead to optimizations, so that their benefits become clearer. Additionally, long-term studies would be needed to show if a gain of a very few millimeters or degrees is relevant and could seriously affect long-term outcomes of total shoulder arthroplasty.

Compliance with ethical standards

Conflict of interest Dr. Adrien Jacquot is a consultant for Tornier-Wright Medical and for Smith and Nephew Company.

M. Jean Chaoui is an employee of Imascap and owns stock equity in Imascap.

M. Pierric Deransart is an employee of Imascap.

Pr. Daniel Mole receives royalties from Tornier-Wright Medical and is a consultant for Tornier-Wright Medical.

Pr. Pascal Boileau and Dr. Gilles Walch receive royalties from Tornier/Wright Company and equity from Imascap.

Dr. Marc-Olivier Gauci and Dr. Mohammed Baba have no conflict of interest.

Disclaimer None

Ethics approval The Institutional Review Board of the ethical committee of the Hôpital Privé Jean Mermoz and the Centre Orthopédique Santy approved this project (Study 20.1611).

References

- Carter MJ, Mikuls TR, Nayak S et al (2012) Impact of total shoulder arthroplasty on generic and shoulder-specific health-related quality-of-life measures: a systematic literature review and meta-analysis. *J Bone Joint Surg Am* 94:e127. <https://doi.org/10.2106/JBJS.K.00204>
- Walch G, Young AA, Melis B et al (2011) Results of a convex-back cemented keeled glenoid component in primary osteoarthritis: multicenter study with a follow-up greater than 5 years. *J Shoulder Elb Surg* 20:385–394. <https://doi.org/10.1016/j.jse.2010.07.011>
- Torchia ME, Cofield RH, Settergren CR (1997) Total shoulder arthroplasty with the Neer prosthesis: long-term results. *J Shoulder Elb Surg* 6:495–505. [https://doi.org/10.1016/S1058-2746\(97\)90081-1](https://doi.org/10.1016/S1058-2746(97)90081-1)
- Walch G, Young AA, Boileau P et al (2012) Patterns of loosening of polyethylene keeled glenoid components after shoulder arthroplasty for primary osteoarthritis: results of a multicenter study with more than five years of follow-up. *J Bone Jt Surg Am* 94. <https://doi.org/10.2106/JBJS.J.00699>
- Farron A, Terrier A, Büchler P (2006) Risks of loosening of a prosthetic glenoid implanted in retroversion. *J Shoulder Elb Surg* 15:521–526. <https://doi.org/10.1016/j.jse.2005.10.003>
- Hopkins AR, Hansen UN, Amis AA, Emery R (2004) The effects of glenoid component alignment variations on cement mantle stresses in total shoulder arthroplasty. *J Shoulder Elb Surg* 13: 668–675. <https://doi.org/10.1016/j.jse.2004.04.008>
- Iannotti JP, Spencer EE, Winter U et al (2005) Prosthetic positioning in total shoulder arthroplasty. *J Shoulder Elb Surg Am Shoulder Elb Surg* 14:111S–121S. <https://doi.org/10.1016/j.jse.2004.09.026>
- Nyffeler RW, Sheikh R, Atkinson TS et al (2006) Effects of glenoid component version on humeral head displacement and joint reaction forces: an experimental study. *J Shoulder Elb Surg Am Shoulder Elb Surg* 15:625–629. <https://doi.org/10.1016/j.jse.2005.09.016>
- Shapiro TA, McGarry MH, Gupta R et al (2007) Biomechanical effects of glenoid retroversion in total shoulder arthroplasty. *J Shoulder Elb Surg* 16:S90–S95. <https://doi.org/10.1016/j.jse.2006.07.010>
- Hendel MD, Bryan JA, Barsoum WK et al (2012) Comparison of patient-specific instruments with standard surgical instruments in determining glenoid component position: a randomized prospective clinical trial. *J Bone Joint Surg Am* 94:2167–2175. <https://doi.org/10.2106/JBJS.K.01209>
- Iannotti J, Baker J, Rodriguez E et al (2014) Three-dimensional preoperative planning software and a novel information transfer technology improve glenoid component positioning. *J Bone Joint Surg Am* 96:e71. <https://doi.org/10.2106/JBJS.L.01346>
- Iannotti JP, Greeson C, Downing D et al (2012) Effect of glenoid deformity on glenoid component placement in primary shoulder arthroplasty. *J Shoulder Elb Surg Am Shoulder Elb Surg* 21: 48–55. <https://doi.org/10.1016/j.jse.2011.02.011>
- Lewis GS, Stevens NM, Armstrong AD (2015) Testing of a novel pin array guide for accurate three-dimensional glenoid component positioning. *J Shoulder Elb Surg Am Shoulder Elb Surg* 24: 1939–1947. <https://doi.org/10.1016/j.jse.2015.06.022>
- Nguyen D, Ferreira LM, Brownhill JR et al (2009) Improved accuracy of computer assisted glenoid implantation in total shoulder arthroplasty: an in-vitro randomized controlled trial. *J Shoulder Elb Surg Am Shoulder Elb Surg* 18:907–914. <https://doi.org/10.1016/j.jse.2009.02.022>
- Throckmorton TW, Gulotta LV, Bonnarens FO et al (2015) Patient-specific targeting guides compared with traditional instrumentation for glenoid component placement in shoulder arthroplasty: a multi-surgeon study in 70 arthritic cadaver specimens. *J Shoulder Elb Surg Am Shoulder Elb Surg* 24:965–971. <https://doi.org/10.1016/j.jse.2014.10.013>
- Walch G, Vezeridis PS, Boileau P et al (2015) Three-dimensional planning and use of patient-specific guides improve glenoid component position: an in vitro study. *J Shoulder Elb Surg Am Shoulder Elb Surg* 24:302–309. <https://doi.org/10.1016/j.jse.2014.05.029>
- Gauci MO, Boileau P, Baba M et al (2016) Patient-specific glenoid guides provide accuracy and reproducibility in total shoulder arthroplasty. *Bone Jt J* 98-B:1080–1085. <https://doi.org/10.1302/0301-620X.98B8.37257>
- Iannotti JP, Weiner S, Rodriguez E et al (2015) Three-dimensional imaging and templating improve glenoid implant positioning. *J Bone Joint Surg Am* 97:651–658. <https://doi.org/10.2106/JBJS.N.00493>
- Suero EM, Citak M, Lo D et al (2013) Use of a custom alignment guide to improve glenoid component position in total shoulder arthroplasty. *Knee Surg Sports Traumatol Arthrosc Off J ESSKA* 21:2860–2866. <https://doi.org/10.1007/s00167-012-2177-1>
- Chaoui J, Hamitouche C, Stindel E, Roux C (2011) Recognition-based segmentation and registration method for image guided shoulder surgery. *Conf Proc Annu Int Conf IEEE Eng Med Biol Soc IEEE Eng Med Biol Soc Annu Conf* 2011:6212–6215. <https://doi.org/10.1109/IEMBS.2011.6091534>
- Moineau G, Levigne C, Boileau P et al (2012) Three-dimensional measurement method of arthritic glenoid cavity morphology: feasibility and reproducibility. *Orthop Traumatol Surg Res OTSR* 98: S139–S145. <https://doi.org/10.1016/j.otrsr.2012.06.007>

22. Walch G, Badet R, Boulahia A, Khoury A (1999) Morphologic study of the glenoid in primary glenohumeral osteoarthritis. *J Arthroplast* 14:756–760
23. Molé D, Roche O, Riand N, et al (1999) Cemented glenoid component: results in osteoarthritis and rheumatoid arthritis. In: Walch G, Boileau P (eds) *Shoulder arthroplasty*. Springer, Berlin, Heidelberg, pp 163–171
24. Jain N, Pietrobon R, Hocker S et al (2004) The relationship between surgeon and hospital volume and outcomes for shoulder arthroplasty. *J Bone Joint Surg Am* 86-A:496–505
25. Singh A, Yian EH, Dillon MT et al (2014) The effect of surgeon and hospital volume on shoulder arthroplasty perioperative quality metrics. *J Shoulder Elb Surg Am Shoulder Elb Surg AI* 23:1187–1194. <https://doi.org/10.1016/j.jse.2013.11.017>

Liste des articles connexes issus de la base de données

Mahaffy, MD, Knowles NK, Berkmortel C, Abdic S, Walch G, Johnson JA, Athwal GS. "Density Distribution of the Type E2 Glenoid in Cuff Tear Arthropathy." *Journal of Shoulder and Elbow Surgery*, August 28, 2019. <https://doi.org/10.1016/j.jse.2019.05.046>.

Neyton L, **Gauci MO**, Deransart P, Collotte P, Walch G, Athwal GS. "Three-Dimensional Characterization of the Anteverted Glenoid (Type D) in Primary Glenohumeral Osteoarthritis." *Journal of Shoulder and Elbow Surgery*, January 23, 2019. <https://doi.org/10.1016/j.jse.2018.09.015>.

Paul R, Knowles N, Chaoui J, **Gauci MO**, Ferreira LM, Walch G, Athwal GS. "Characterization of the Dysplastic Walch Type C Glenoid." *The Bone & Joint Journal* 100-B, no. 8 (2018): 1074–79. <https://doi.org/10.1302/0301-620X.100B8.BJJ-2018-0116.R1>.

Chan K, Knowles NK, Chaoui J, **Gauci MO**, Ferreira LM, Walch G, Athwal GS. "Characterization of the Walch B3 Glenoid in Primary Osteoarthritis." *Journal of Shoulder and Elbow Surgery*, January 11, 2017. <https://doi.org/10.1016/j.jse.2016.10.003>.

Bouacida, S, **Gauci MO**, Coulet B, Lazerges C, Cyteval C, Boileau P, Chammas M. "Interest in the Glenoid Hull Method for Analyzing Humeral Subluxation in Primary Glenohumeral Osteoarthritis." *Journal of Shoulder and Elbow Surgery*, March 31, 2017. <https://doi.org/10.1016/j.jse.2017.01.027>.

Daggett M, Werner B, Collin P, **Gauci MO**, Chaoui J, Walch G. "Correlation between Glenoid Inclination and Critical Shoulder Angle: A Radiographic and Computed Tomography Study." *Journal of Shoulder and Elbow Surgery* 24, no. 12 (December 2015): 1948–53. <https://doi.org/10.1016/j.jse.2015.07.013>.

Daggett M, Werner B, **Gauci MO**, Chaoui J, Walch G. "Comparison of Glenoid Inclination Angle Using Different Clinical Imaging Modalities." *Journal of Shoulder and Elbow Surgery* 25, no. 2 (February 2016): 180–85. <https://doi.org/10.1016/j.jse.2015.07.001>.

Conclusion et Perspectives pour les recherches à venir

Ce travail de Thèse a permis de valider les performances et l'utilisation d'un logiciel de segmentation tridimensionnel et de planification préopératoire. Nous avons démontré que l'utilisation d'un tel logiciel trouve son application dans plusieurs étapes de la prise en charge d'un patient atteint d'arthrose de l'épaule.

CONCLUSION

1/ **Diagnostic** : la segmentation effectuée par le logiciel est fiable, s'affranchit des problématiques de reproductibilité inter- et intra-observateur et permet d'obtenir des mesures (version, inclinaison) valides et indispensables à la démarche diagnostique.

2/ **Classification**: la décision thérapeutique dans l'omarthrose primaire repose sur les classifications chirurgicales. L'utilisation du logiciel et le reformatage systématique des coupes dans le plan du corps de la scapula a permis d'identifier et de décrire de nouveaux types de glènes (B3, D) qui oriente vers une prise en charge chirurgicale spécifique.

3/ **Connaissances de l'anatomie normale et pathologique** : l'uniformisation et la reproductibilité des plans de références, l'automatisation du processus de segmentation et de mesure ainsi que l'analyse tridimensionnelle (orientation, direction glénohumérales) ont permis de décrire pour la première fois l'anatomie tridimensionnelle de l'épaule normale et pathologique à partir de larges séries de scanners d'épaule (*big data*). Ces données issues de la base de données serviront de base à l'élaboration de nouveaux modèles statistiques de forme.

4/ **Décision thérapeutique** : la décision thérapeutique reposait jusqu'à présent sur l'analyse subjective d'images statiques. Nous avons démontré qu'il est possible de développer à l'aide de l'imagerie tridimensionnelle de nouveaux outils comme le RSA-angle dont la mesure générée automatiquement est désormais validée. D'autres outils de mesures objectifs

pourront permettre d'affiner le diagnostic et entreront dans le panel d'instruments de la décision thérapeutique du chirurgien.

5/ Optimisation de la **pose des implants** : la possibilité de simuler la mobilité géométrique des implants posés (PTEI) a permis de visualiser directement et de quantifier les conflits glénohuméraux dont nous suspicions l'existence. Cette analyse a aussi permis de remettre en question le design de certains implants et d'affiner et valider leurs paramètres de pose (inclinaison humérale, latéralisation et inclinaison glénoïdienne, ...).

6/ Geste technique : **planification et guides patients spécifiques** : le résultat de ce cheminement diagnostic-décision thérapeutique est l'exécution du geste chirurgical. La technologie d'impression 3D permet d'obtenir dans des délais raisonnables un guide patient-spécifique généré uniquement par la planification du chirurgien de façon indépendante. Le process planification + guide fait passer la précision du chirurgien de 15° (« coup d'œil chirurgical ») à moins de 3° pour l'orientation et de 8mm à moins de 1mm pour le point d'entrée. Cette optimisation du geste chirurgical devrait avoir une incidence sur la survie des implants et le résultat fonctionnelle. La planification seule améliore déjà fortement l'orientation des implants quand le guide permet d'ajuster le point d'entrée. Les glènes très déformées sont celles qui bénéficient le plus de l'usage d'un guide.

PROSPECTIVES

Ce travail de Thèse ouvre la voie à d'autres axes de recherche en particulier à partir de l'analyse de l'importante base de données que nous avons rassemblée (cf articles connexes).

Parmi ceci, nous pouvons évoquer :

- L'amélioration des **modèles statistiques** de formes (SSM) pour la glène, l'humérus mais aussi pour l'articulation glénohumérale qui mériterait aussi d'être affinée par des analyses en éléments finis.
- L'extension de la description et de l'analyse tridimensionnelle aux **autres pathologies** arthrosiques (ruptures massives de coiffe, arthropathies post-rupture de coiffe, arthrose post-instabilité, arthrites rhumatoïdes, ...) permettrait d'identifier

d'éventuelles prédispositions au développement de la pathologie arthrosique et de son type.

- Le développement **d'outils de mesures** pour évaluer et prévenir les conflits glénohuméraux devrait permettre au chirurgien de disposer d'un arsenal d'instruments à usage diagnostique et d'obtenir une évaluation exhaustive et objective pour chaque cas à traiter.
- L'utilisation de technologies issues de **l'intelligence artificielle** pour constituer un véritable « ancillaire diagnostique » au service des chirurgiens afin de préciser les diagnostics et d'orienter les choix thérapeutiques.
- L'utilisation de la **réalité augmentée** qui permettrait de s'affranchir du délai d'impression des guides. Cela nécessite de résoudre les problématiques de recalage.
- La validation clinique de la simulation des **mobilités** et l'étude de la **survie** des implants à moyen et long terme : elles permettrait de connaître la valeur ajoutée réelle de la planification et de l'utilisation des guides patient-spécifiques dans les résultats fonctionnels post-opératoires.
- Des développements qui devraient permettre de planification des **révisions** de prothèses d'épaule.
- Ce type de logiciel constitue un véritable **outil pédagogique** pour les chirurgiens en formation avancée à l'heure où la simulation connaît un véritable essor, son apport dans la courbe d'apprentissage mérite d'être évalué.
- Enfin, il est possible et nécessaire de reproduire le modèle de développement utilisé pour l'arthrose à **d'autres pathologies** propres à l'épaule voire aux autres articulations.

Titre : Description et Classification 3D des glènes arthrosiques pour une planification préopératoire 3D assistée par ordinateur

Mots clés : *omarthrose, modélisation 3D, segmentation, simulation, morphométrie, planification, arthroplastie d'épaule.*

Résumé : La modélisation tridimensionnelle est devenue plus accessible et plus rapide en orthopédie et en particulier en chirurgie de l'épaule. L'analyse morphométrique qui en est issue est utilisée pour permettre une meilleure compréhension de l'omarthrose. L'objectif global de cette Thèse était de valider l'application d'un logiciel de segmentation automatisée tridimensionnelle dans les étapes de prise en charge du patient. Huit études ont permis de valider les mesures automatiques calculées par le logiciel, d'améliorer la classification des omarthroses primaires puis de décrire la géométrie 3D normale et pathologique de l'épaule. Des seuils numériques précis ont pu être établis entre les différents types. Le logiciel a permis de développer et valider l'utilisation d'un angle (*RSA-angle*) permettant de mieux positionner l'implant glénoïdien dans les prothèses inversées d'épaule. L'utilisation des mobilités simulées en 3D démontrait l'intérêt du logiciel dans la compréhension des conflits osseux après prothèse et des faiblesses de design d'implant. Enfin, le positionnement de l'implant glénoïdien en peropératoire avec un guide patient-spécifique imprimé en 3D correspondait fidèlement à sa planification préopératoire, cependant, la planification à elle seule améliorait déjà considérablement ce positionnement. Ce travail de Thèse a permis de valider les performances et l'utilisation d'un logiciel de segmentation tridimensionnel et de planification préopératoire. Son application se retrouve dans plusieurs étapes de la prise en charge d'un patient atteint d'omarthrose et devrait

Title : Description and 3D classification of glenoid arthritis for a preoperative computer assisted 3D planning

Keywords: *shoulder arthritis, 3D modeling, segmentation, simulation, morphometry, planning, shoulder arthroplasty.*

Abstract: Three-dimensional modelling has become more accessible and faster in orthopedics and especially in shoulder surgery. The subsequent morphometric analysis is used to provide a better understanding of shoulder arthritis. The overall objective of this Thesis was to validate the use of a 3D-automated segmentation software in the various steps of patients management. Eight studies allowed validating the automatic measurements calculated by the software, improving the classification of primary shoulder arthritis and then describing the normal and pathological 3D geometry of the shoulder. Accurate numerical thresholds could be established between the different types. The software developed and validated the use of an angle (*RSA-angle*) to better position the glenoid implant in reverse shoulder arthroplasty. The use of simulated range of motion in 3D demonstrated the software's interest in understanding bone impingements after prosthesis and implant design weaknesses. Finally, the positioning of the glenoid implant intraoperatively with a patient specific guide printed in 3D corresponded faithfully to its preoperative planning. However, planning alone already greatly improved this positioning. This Thesis made it possible to validate the performance and use of a software of three-dimensional segmentation and pre-operative planning. Its application is found in several steps of the management of a patient with shoulder arthritis and should gradually be integrated into the daily practice of surgeons.